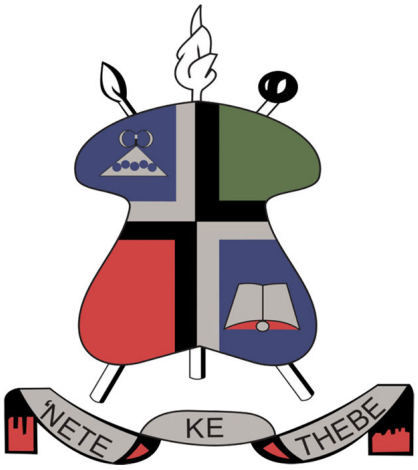

NATIONAL UNIVERSITY
OF LESOTHO

Mathematical modeling of natural killer (NK) cells recruitment in oncolytic virotherapy

by

Senekal Noma Susan

Dissertation presented at the National University of
Lesotho for the degree of

Master of Science in Mathematics (Applied)

Department of Mathematics and Computer Science
National University of Lesotho

Supervisor: Dr. Khaphetsi Joseph Mahasa,
Department of Mathematics and Computer Science,
National University of Lesotho, Roma, Maseru, Lesotho.

Co-supervisor: Prof. Amina Eladdadi,
Department of Mathematics,
The College of Saint Rose, Albany, NY, USA.

December 2020

Declaration

I, the undersigned, hereby declare that the work contained in this thesis is my own original work and has not previously, in its entirety or in part, been submitted at any university for a degree.

---- Senekal -- Noma Susan Senekal Date: February 2021.

Abstract

Natural killer (NK) cells are known to constitute a major part of innate immunity against tumors and viral infections. Upon successfull viral entry into the tumor microenvironment (TME) or tumor, NK cells may however prematurely kill infected tumor cells and oncolytic viruses (OV), which then results in reduced overall efficacy of oncolytic virotherapy. In this thesis, we examine the effects of NK cell recruitment within the TME during tumor treatment with OV. To achieve this, we devised and analyzed a simple mathematical model that describes the dynamic interactions of the tumor cells, OV and NK cells based on currently available preclinical and clinical literature. In particular, a central goal of this work is to investigate and characterize therapeutic conditions under which the synergistic balance between OV-induced NK responses and required viral cytopathicity may or may not result in a successful treatment. Interestingly, we found that NK cell recruitment to the TME must take place neither too early nor too late in the course of OV infection so that treatment will be successful. Notably, we also found that NK cell responses are most influential at either early (partly because of rapid response of NK cells to viral infections or antigens) or later (partly because of antitumoral ability of NK cells) stages of oncolytic virotherapy. The model further predicts that: (a) an NK cell response augments oncolytic virotherapy only if viral cytopathicity is weak; (b) the recruitment of NK cells modulates tumor growth; and (c) the depletion of activated NK cells within the TME enhances the probability of tumor escape in oncolytic virotherapy. Taken together, our findings demonstrate that OV infection is crucial, not just to cytoreduce tumor burden, but also to induce potent NK cell response necessary to achieve complete or at least partial tumor remission. Furthermore, our modeling framework supports combination therapies involving NK cells and OV which are currently used in oncolytic immunovirotherapy to treat several cancer types.

Dedication

This thesis is dedicated to my dearest late mother 'Mak'humalo Sylvia Senekal.

Acknowledgments

I would like to thank my beloved husband Sebaki Francis Leluma for being with me every step of the way. Your patience and understanding exceeded my expectations throughout this tedious journey. Attentively listening to every idea that I bounced to you, was one of the great gifts you can ever give to me. Thank you for fetching me from the office at the most awkward hours without showing a single sign of annoyance. Many thanks for always believing in me, and encouraging me to keep going with my research at the times I felt like quitting. Surely, there were times I was wondering, without seeing any light, in this tunnel of relentless research, but you persistently motivated me to keep moving . I could never thank you enough. Your amicable and endless support throughout this project can never be equalled. Thank you my love!

I would like also to pass my deepest gratitude to my supervisor, Dr Khaphetsi Joseph Mahasa. Thank you Sir for the patience and guidance you gave me. To me your were more than a supervisor. From you, I fortunately and uniquely got both a genuine supervisor and mentor. Thank you for teaching me, with great care and patience, all the skills that have enabled me to reach this far end. Above all, I would like to thank you for introducing me to this wonderful field of mathematical oncology. At each stage of this long journey, you always made my work seem easy even though it really was not. You always told me to relax and take things easily at the times when my anxiety and desolation overwhelmed me. Sir, I wholeheartedly thank you.

Moreover, I would also like to cease this moment to profoundly thank my co-supervisor, Prof. Amina Eladdadi, from The College of Saint Rose, USA. I cannot forget of the first draft of my work that I sent to you which came back with “red” color everywhere. The instructive and constructive comments, suggestions and complementary edits, have immensely aided me to ameliorate my work to this fruitful end. Most importantly, I would

like to thank you for teaching me how to grammatically write and reorganize this thesis. Your professional and commendable co-supervision is greatly appreciated. I, surely, would have not accomplished this project without you.

I would also like to sincerely thank my family for their endless prayers and aspirational words. In particular, I would like to thank my son, Lereko Sylvester Leluma, for always playing with me, asking me many life related questions when I really needed to take my mind away from my troublesome research. That, greatly helped me to fresh and resume my work with more improved focus and curiosity. To my all friends, my colleagues and everyone else who directly or indirectly supported me in this journey, I deeply thank you. I would have never done this without you.

Last but definitely not the least, I would like to thank the National University of Lesotho for fully sponsoring this project, and giving me space and all needed facilities to accomplish this work.

List of Publications

The results in this thesis constituted one publication given below.

1. NS Senekal, KJ Mahasa, A Eladdadi, L De Pillis, R Ouifki, **Natural killer cells recruitment in oncolytic virotherapy: A mathematical model**. Bulletin of Mathematical Biology, 2021; 83(75). https://link.springer.com/article/10.1007/s11538-021-00903-6

Contents

List of Figures

List of Tables

Chapter 1

Introduction

In the past decade, there has been a commendable progress in understanding of manifold mechanisms and pathways that influence tumor growth and progression, and the molecular networks that orchestrate the immune system's response to tumor development [3]. Tumors often develop various mechanisms to evade immune system detection and control [4–7]. As one of the mechanisms to escape adaptive immune system, tumors often abrogate major histocompatibility complex (MHC) class I molecules expressed on their cell surfaces [8–11]. This mechanism, however, renders tumor to natural killer (NK) cells cytotoxicity [12–14]. NK cells always serve as a first line of defense against invading infections or transformed cells in contact-dependent manner via engagement of activating or inhibitory receptors [15]. They can also lyse target cells via the production of cytotoxic granules and cytokines [16]. Hence, NK cells are important cytotoxic lymphocytes of the innate immunity that play a crucial role in immunosurveillance of tumors and viral infections [17]. Without loss of generality, host immune system (both innate and adaptive parts) provides an important surveillance against several tumor cells or viruses, and also contributes positively for many cancer patients [17–21].

While it still remains a major challenge in immunotherapy to design effective therapeutic agents that can consistently work against several cancer types [3], to date, several immunotherapeutic approaches have been developed [1, 3, 22–27]. These include immune checkpoint (IC) inhibitors, combination of immunostimulatory cytokines (e.g., interleukin 12 (IL-12) and granulocyte monocyte stimulating factor (GM-CSF) [28–30]. In the past $10-15$ years, immunotherapy, particularly the use of immune checkpoint inhibitors (ICI),

has triggered a keen interest in preclinical [31], clinical [32, 33] and mathematical researchers [34] that seek to find better ways to improve immune system's ability to combat cancer development and progression. The use of immune checkpoints (IC) (often represented as inhibitory receptors) has been shown to elicit potent immunotherapeutic outcomes in several preclinical and clinical models [35, 36]. Physiologically, IC control the lytic ability of immune effector cells by enabling peripheral tolerance (e.g., via a programmed death-1 (PD-1) receptor, expressed by T and NK cells, which binds to a PDL-1 ligand often upregulated on tumor cells [35] or immune cells [33]). Furthermore, an increasing evidence demonstrates that combining IC with OV can effectively result in more robust and pronounced antitumor effects [32, 37].

Recently, oncolytic virotherapy has become one of promising therapeutic modalities that showed favorable therapeutic outcomes in several clinical studies [38]. Oncolytic virotherapy utilizes naturally-occurring viruses (e.g., reovirus [39, 40], (parvovirus (PV) [41]), myxoma virus [42], Seneca valley virus [43], and Newcastle disease virus (NDV) [43, 44]) or genetically-engineered viruses (e.g., vesicular stomatitis virus (VSV)[45], measles virus (MV) [45, 46], vaccinia virus [47], adenovirus (Ad) [48–50], herpes simplex virus (HSV) [51–53]), that have a natural or genetically-engineered tropism to preferentially replicate in, and kill cancerous cells while having no or limited effects on normal cells [43, 54–56]. Even though multiple oncolytic viruses (OV) have progressed to advanced clinical stages [57], numerous obstacles or limitations still need to be addressed to attain improved therapeutic efficacy [38, 58, 59]. The current challenges in oncolytic virotherapy include, but are not limited to, premature viral clearance by the circulating antibodies and several immune cells [60], modest oncolytic viral amplification [61–63], and physical barriers within the tumor microenvironment (TME) (e.g., extracellular matrix (ECM) components (such as chondroitin sulfate proteoglycans (CSPGs) [64])) [44] or within tumors (e.g., interstitial fluid pressure [65]).

Among many attractive attributes of OV therapy is the direct or indirect recruitment (e.g., via immunogenic cell death (ICD) of infected tumor cells [66–69]) or stimulation of antitumoral and antiviral immune cells, particularly NK cells [69], within the TME. While within the TME, NK cells may act as a "double-edged sword" in the sense that, on the one hand, activated NK cells can mount potent antiviral response that can diminish OV spread and replication [48, 70]; while on the other hand, late antitumoral response by NK

cells can provide robust antitumoral surveillance that may eliminate tumor cells [71–73]. The role of activated NK cells (recruited via ICD) in oncolytic virotherapy is currently not fully explored [69, 74]. It is also, however, still not fully understood what is a relative balance between direct viral oncolysis and indirect NK-mediated responses that can result in improved overall efficacy of OV therapy [70, 75]. Undoubtedly, the determination of such timely balance can immensely enhance our knowledge of OV replication and subsequent viral oncolysis that can optimally result in better prognosis for many cancer patients.

Increasing evidence indicates that one other promising novel therapeutic strategy that can create an effective antitumor response is a combinatorial therapy of replicating oncolytic viruses and NK-based immunotherapy [71, 76]. Accumulating evidence further shows that, in combination, OV and NK cells provide an effective antitumor response in several cancer types [71–73]. Despite these promising therapeutic advances in treatment of various human cancers, only a limited number of patients with life-threating cancers completely or partially benefit from these available therapies. This is due to a complex and highly nonlinear correlation between cancer and the immune system [70, 77–79]. Hence, to date, an effective antitumor treatment against several cancer types still remains a major challenge [3, 70, 80].

1.0.1 Project Motivation

Due to the lack of precise information regarding the dynamic interaction between tumor cells, OV and NK cells within the TME, in this thesis, we consider and investigate the role of NK cells on uninfected and infected tumor cells during the treatment with OV. In particular, we consider the lytic role of NK cells on tumor cells induced by varying recruitment rates of OV infection. It is important to note that an early higher recruitment rate of NK cells will result in increased number of NK cells within the TME, which may ultimately lead to premature killing of infected tumor cells. In contrast, later higher recruitment of NK cells can lead to increased NK-cell-mediated killing of OV-infected and uninfected tumor cells, which will result in greater tumor remission and reduced number of virus particles within the TME, and, thereby, improved antitumor effect of oncolytic immunovirotherapy. With these considerations in mind, we are led to the following aims:

1. To formulate a novel ordinary differential equations (ODE) model that describes how

NK cell recruitment to the TME affects oncolytic virotherapy. The model consists of oncolytic viruses (OV), natural killer (NK) cells and tumor cells.

2. To characterize conditions under which the synergistic balance between OV-induced NK responses and required viral cytopathicity may or may not result in a successful treatment. We derive the basic reproductive number of the model and the steady states solutions, and then use their joined stability analyses to assess the potential success of OV-based therapy in the presence of active NK cells within the TME.
3. To simulate and compare the therapeutic efficacy of OV in the absence of and presence of NK cells. This comparison is important for assessing the possible treatment outcomes of OV in immunocompetent hosts, where NK cells may either limit or augment the therapy.

1.1 Outline of the Thesis

While a complete discussion of the major contributions of this thesis is presented in Chapter 3, we should re-emphasize that the work presented herein highlights the significance of information characterizing virus-induced NK cell response during oncolytic virotherapy. This thesis is structured as follows:

Chapter 2: Background Literature. Here, we present a brief overview of biological aspects of tumor growth and of NK cell response to tumur growth and OV infection. We also present a brief discussion of mathematical models that directly or indirectly motivated our novel mathematical model developed in this thesis.

Chapter 3: Natural killer cells recruitment in oncolytic virotherapy: a mathematical model. We present a novel ordinary differential-equation mathematical model that describes the dynamics of OV-induced NK recruitment to oncolytic viral infection. We perform numerical simulations of the proposed model and discuss the corresponding results. Interestingly, numerical simulations are comparable with previously published models describing local interactions between tumor cells, activated NK cells and OV. In summary, our simulations illustrate that while treating tumor with OV is a promising therapeutic approach for eliminating tumors, it is equally important to recruit NK cells at some stage during oncolytic virotherapy to achieve a complete tumor remission or at least

a low controllable tumor steady state.

Chapter 4: Conclusions. We end this thesis by highlighting the major findings and contributions of our study in the field of mathematical oncology. Finally, we present a conclusion of the present work, and highlight possible future directions that can further improve the results attained in this thesis.

Chapter 2

Background Literature

In this chapter, we present a brief overview of relevant tumor biology and appropriate mathematical models that describe local interactions between tumor cells, natural killer (NK) cells and oncolytic viruses. First, we provide a succinct discussion of appropriate biology relating to tumor growth and innate immune system response mediated by NK cells. In particular, we discuss the biological aspects pertaining to how tumor develops in the presence of active innate immune system. Second, while there is ample literature relating to tumor-immune-oncolytic virus dynamics, mathematical models discussed in this chapter motivate the choice of our modeling techniques used in the subsequent chapter of this thesis.

2.1 Biology of tumor growth and treatment

While tumor growth is a complex biological process that is governed by multiple mechanisms that occur at the molecular, cellular, and tissue scales, in this section we provide a brief review of tumor growth under attack by natural killer (NK) cells and treatment with oncolytic viruses.

2.1.1 Tumor treatment: Oncolytic virotherapy

Tumor growth and progression is a sophisticated biological mechanism that is defined by a complex network of regulatory mechanisms of cellular growth and death. Hence treating tumor requires a thorough understanding of theses biological processes and mechanisms. Of particular interest, in this section we discuss one of the promising tumor treatments, namely oncolytic virotherapy. Oncolytic viruses (OV) are viruses that specifically replicate in, and kill tumor cells without harming (or having limited effect on) normal cells [43, 54, 55, 81–84]. OV is a promising agent to treat cancer because it has a natural tumor tropism or can be genetically engineered to replicate in cancerous cells [41, 56, 66, 85, 86]. OV is usually administered intratumorally (i.e., directly injected into the tumor) or intravenously (i.e., injected into the blood). While the intratumoral administration of OV minimizes virus sequestration within the blood and maximizes viral load within a tumor, intravenous administration is a common treatment protocol often used to treat various cancer types [87, 88]. Despite the promising outcomes of intravenous OV administration in treating various metastatic tumors [89, 90], accumulating evidence indicates that systemic administration of OV has many obstacles [91]. Upon injection into the blood system, OV becomes susceptible to neutralization by circulating anti-bodies and/ or removal by virus-specific immune cells [43, 89, 92]. In particular, NK cells known to rapidly eliminate OV [26, 72, 93, 94]. As part of this thesis, we shall investigate the role of NK cell response that is triggered by OV infection from a qualitative point view.

2.1.2 NK cells in tumor microenvironment

NK cells constitute an important part of effector immune cells of the innate immunity that are able to quickly provide potent antitumor and antiviral responses against invading pathogens or transformed cells in the body. NK cells are primarily known to both directly kill tumor cells or virally infected cells [93, 95]. NK cells are also known to indirectly communicate with other effector cells (such as T cells) within the tumor microenvironment (TME) by releasing cytokines that activate cells of the adaptive immunity or other innate immune cells (such as macrophages, neutrophils and dendritic cells) [95]. In this view, the engagement of NK cells in the battle against tumor growth and development confer NK cells as key innate immune cells that are capable of influencing immune-mediated

cell-mediated cytotoxicity [96].

Usually, NK cells target and destroy cells not expressing self major histocompatibility complex (MHC) class I molecules, through a molecular process known as "missing-self recognition" [12–14, 97]. To carry out their innate immune functions, NK cells use a large range of activating (such as natural cytotoxicity receptors (NCRs) – (e.g., NKp30 and NKp46 [95, 98])) and inhibitory receptors (such as human leukocyte antigen (HLA)-specific inhibitory NK receptors (iNKR) – (e.g., KIRs and CD94/NKG2A [99, 100])) that, upon their interactions with target cells (e.g., tumor cells or virus-infected cells) which express respective cellular ligands, are able to kill or spare the target cell (see Figure 2.1 for examples of receptors and ligands that are used in NK cell-mediated surveillance). NK cells rely on the balance between activating and inhibitory signals to engage with cognate ligands on tumor cells [101].

In particular, NK cells eliminate tumor cells through secretion of cytolytic granules [13, 93, 100], such as perforin/granzyme, which usually bind to a target cell membrane, and form lytic pores that are used to send through cytotoxic cytokines into the target cell [102, 103]. Furthermore, by binding to the appropriate ligand, such as tumor necrosis factor (TNF) family ligands, tumor-necrosis factor-related apoptosis-inducing ligand (TRAIL), Fas ligand (CD178), NK cells are able to induce apoptosis into the target cells. NK cell surveillance in tumor immunology has been demonstrated in various preclinical and clinical models illustrating that a depletion in the number of NK cells within the TME is correlated with poor prognosis [104].

In the context of oncolytic virotherapy, several preclinical and clinical studies have shown that NK cells play two mutually opposite roles. On one hand, activated NK cells are known to rapidly eradicate infected tumor cells, thereby limiting the spread of OV and reduce overall efficacy of oncolytic virotherapy [48, 70, 71]. On the other hand, activated NK cells have been shown to indispensably augment antitumoral activity of oncolytic viruses [71–73]. Thus, NK cells, activated by oncolytic viruses, are important effector immune cells necessary for successful overall therapy [72]. As an example, the antitumoral and antiviral roles of NK cells in mice treated with a combination of oncolytic virus and bortezomib, revealed that either reducing the number of endogenous NK cells or increasing the number of exogenous NK cells leads to enhanced treatment outcomes [71]. More

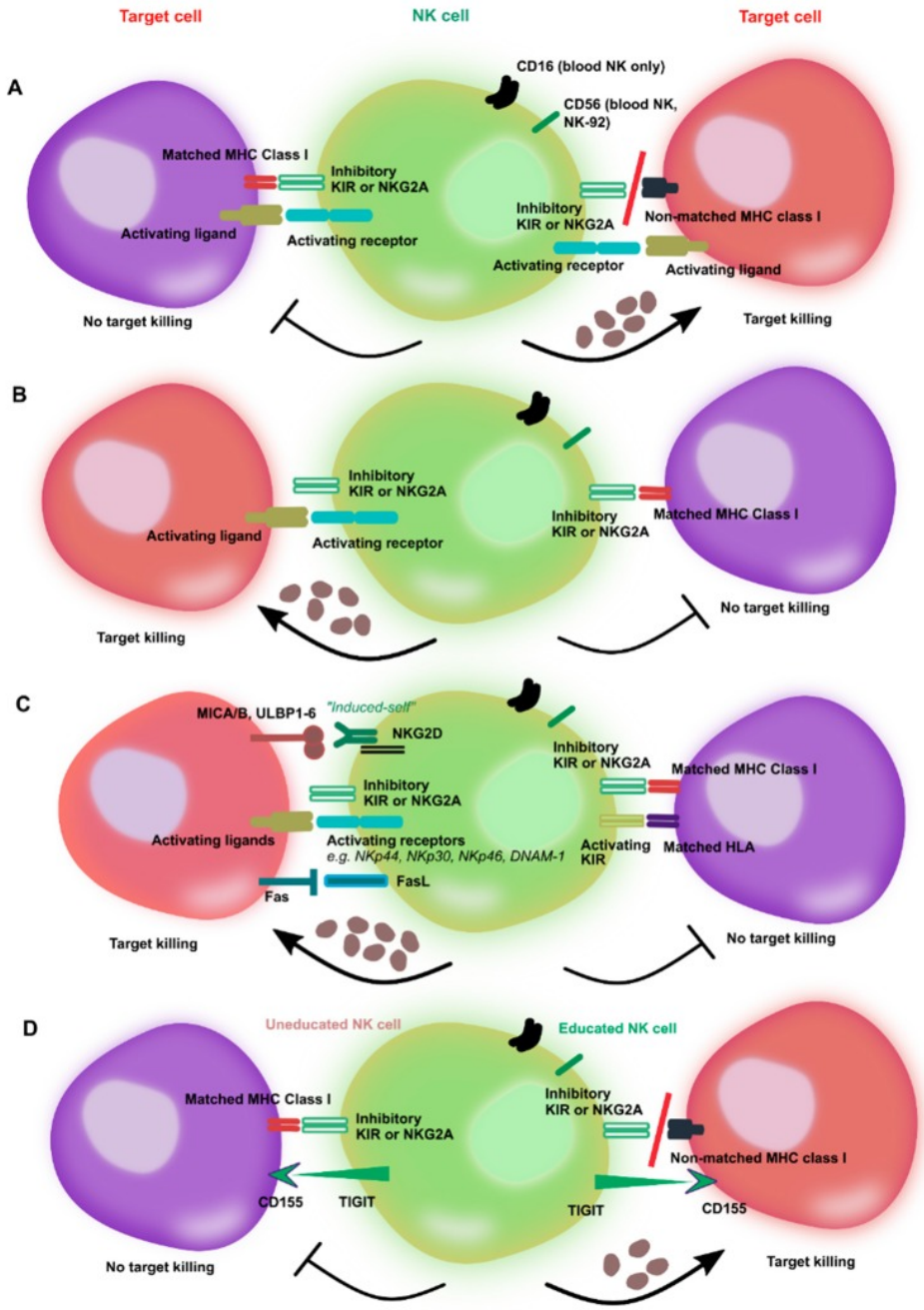

FIG. 2.1. Target killing or sparing by NK cells using activating and inhibitory receptors. Source [1].

recently, Leung et al. [72] showed that ovarian cancer cells, infected with OV, activated NK cells via a contact-dependent manner. It was further illustrated that the activated NK cells provided an addition arm in antitumoral activity of OV against infected cancer cells.

The combinatorial activities of OV and NK cells resulted in more potent killing of infected ovarian cancer cells compared to OV administered as a standalone treatment [72]. Taken together, these studies show that virus oncolysis and NK cell responses work cordially in combat against tumor growth and progression. However, the distinct roles played by activated NK cells in oncolytic virotherapy are still largely unexplored [105].

2.2 Mathematical models of tumor growth and treatment with oncolytic viruses

From basic to advanced modeling approaches, several mathematical models that describe various tumor-immune cell interactions have been developed [5, 106–110]. As an example, numerical results in Mahasa et al. [5] indicate that an increment in the number of activated NK cells within the tumor microenvironment might be essential to enhance NK-mediated immune surveillance. Of note, it was further shown that immune response alone is not sufficient to completely thwart tumor growth, and as such tumors often turn to develop immunoresistance that abrogates immune surveillance. To date, there is a growing need to develop better models (possibly motivated by, and calibrated with, experimental data [111]), despite the existence of rich knowledge of tumor-immune interactions (see [19, 110, 112–114] for reviews of tumor-immune models). In the past decade, mathematical and computational models of tumor growth under treatment with oncolytic viruses have received a significant interest in the development and evaluation of new approaches to battle cancer. In particular, there are several mathematical models that illustrate how to control tumor growth with oncolytic viruses, without immune response [115–119], and with immune response [63, 75, 120–123]. For example, Kim et al. [71] developed and investigated antitumoral and antiviral roles of NK cells in a triple combination therapy with oncolytic virus and bortezomib. Of note, they showed that either reducing the number of endogenous NK cells or increasing the number of exogenous NK cells leads to better treatment outcomes.

2.3 Summary

In this chapter, we provided a brief literature review of both tumor biology and mathematical models of tumor-immune interactions, and those of tumor treatment with oncolytic viruses. Of note, this short literature review provides a basic view of a long journey and continued battle in preclinical, clinical and mathematical oncology research, as well as the need for better comprehension of complex tumor-immune-oncolytic virus interactions. While many of the mathematical models discussed above are mostly deterministic in nature (usually defined by systems of ordinary differential equations (ODEs)), in the present study we adopt and consider similar ODE-based approach to describe various aspects of tumor-immune-virus dynamics. We start off with a relatively complex ODE system, and then deconvolute it to determine the most essential dynamical processes that govern tumor growth in oncolytic immunovirotherapy. While mathematical modeling approaches have enhanced our understanding of the complex dynamics of tumor progression or remission under various treatment modalities, there is still a need for better approaches to precisely define various mechanisms in oncolytic immnunovirothrapy. In the next chapter, we will provide a simple overview of tumor-immune-virus interactions that might help to eliminate or at least control tumor growth. In particular, since NK cells (as part of innate immune system) may be a major obstacle or an enhancer of the success of oncolytic virotherapy, we will devise and analyze our mathematical model to assess the effect of NK cells within the TME during oncolytic virotherapy.

Chapter 3

Mathematical modeling of natural killer cells recruitment in oncolytic virotherapy

Oncolytic virotherapy has shown promising antitumoral effects in variety of preclinical tumor models [62, 63, 72, 82, 124] and recently in clinical studies [57–59, 125]. This treatment approach makes use of an oncolytic virus (OV) that selectively replicates to kill cancer cells while sparing healthy normal cells. In addition, OV stimulates a potent immune response to the virus-infected and uninfected tumors [43, 50, 62, 63, 126, 127]. OV, however, when administered intravenously in immunocompetent hosts, is often prone to immune cell clearance which reduces the likelihood of virotherapeutic success [65, 72, 128]. There are more than ten types of immune cells that are known to play a vital role in oncolytic virotherapy, such as viral-tumor specific T cell (CTL) [129], natural killer (NK) cells [53, 128, 130], and tumor-associated macrophages [131]. Immune cell depletion studies show that both NK and CTL cells are essential to the therapeutic effect of OV [132]. In this study, we only consider the emerging role of NK cells in oncolytic virotherapy because their dual and counter-intuitive contributions require deeper examination [72].

NK cells are a type of cytotoxic lymphocyte critical to the innate immune system that have the ability to rapidly eliminate invading pathogens, such as viruses, or transformed cells, such as cancerous cells, in the body [26, 72, 93]. In the context of oncolytic virotherapy, NK cells are known to mediate both antiviral and antitumoral responses [72, 94]. Nonetheless,

an appropriate balance between rapid viral elimination (or clearance) of OV-infected cells by NK cells and the later antitumoral NK cell response is still not yet fully understood [70, 75]. It should be noted that the efficacy of oncolytic virotherapy in immunocompetent hosts depends heavily on this balance [58, 59, 70, 75, 125, 133]. Upon successful entry into tumor cells, OV replicates within infected cells, which may release pathogen-associated molecular patterns (PAMPs) (e.g., calreticulin (CRT) ecto-expression and adenosine triphosphate (ATP) [134–136]), as well as damage-associated molecular patterns (DAMPs) (e.g., high-mobility group box 1 (HMGB1) protein, heat shock proteins (HSP70,HSP90) [136, 137]). The presence of PAMPs or DAMPs indicates that a cell is undergoing immunogenic cell death (ICD) induced by oncolytic viruses [27, 66]. Moreover, these danger signals released during ICD can be rapidly recognized by the innate immune cells, and can activate the innate immune response, including NK cells [68, 69, 74, 136]. Although NK cells have been shown to play a significant role in the context of ICD [138], the recruitment of NK cells via ICD still requires further investigation, especially in OV-based treatments [69, 74].

The cytolytic activity of NK cells against OV-infected or uninfected tumor cells is regulated by the engagement of either activating or inhibitory NK cell surface receptors, the actions of cytokines, and cross talk with other immune cells [13, 26, 98, 139]. Upon binding with their respective ligands expressed on surfaces of tumor cells, the receptors on NK cells become activated [26, 94, 140, 141]. This activation triggers an intracellular signaling process, through a complex cascade of phosphorylation reactions [141, 142], which leads to NK cell activation and possible NK cell-mediated tumor cell lysis [13, 98, 141].

NK cells play a major role against viral infections, and are known to indiscriminately attack both uninfected and OV-infected tumor cells rapidly [72, 143]. This rapid clearance, however, may limit the spread of OV and hence diminish overall oncolytic virotherapeutic efficacy [48, 70, 71]. While numerous studies have shown that NK cell responses halt OV spread and infection [70, 95], there is ample evidence indicating that virus-induced NK cell responses can lead to indispensable augmentation of oncolytic virotherapy [71–73]. For example, Kim et al. [71] investigated, through an experimental-mathematical modeling approach, the antitumoral and antiviral roles of NK cells in a triple combination therapy with oncolytic virus and bortezomib. They showed that variations in the number of NK cells within the tumor microenvironment (TME) (e.g., either reducing the number of endogenous NK cells, or increasing the number of exogenous NK cells), led to improved

treatment efficacy. Recently, in [72], the synergistic role of NK cells in the activity of two different oncolytic adenoviruses was examined. The study showed that infected ovarian cancer cells activated NK cells in a contact-dependent manner. Moreover, the activated NK cells significantly augmented the killing of infected cancer cells by the OV, where the NK cells were in direct contact with the OV-infected cancer cells. This interaction of NK cells and infected tumor cells resulted in more significant cell killing compared to OV infection alone [72]. Taken together, these studies imply that there is a complex trade-off underlying virus oncolysis and OV-induced NK cell responses. Thus, it is vital to understand the role of NK cell-mediated responses in oncolytic virotherapy [70]. As will be demonstrated by our model, this balance depends on how rapidly the productively infected tumor cells die from OV infection (viral cytopathicity) (i.e., we compare strongly cytopathic vs. weakly cytopathic OV) [2, 80] and the immunostimulatory ability of OV in recruiting NK cells to the TME.

There are several mathematical models of the interactions of the OV, tumor cells and immune responses (see for example [75, 144–146]) and of the effects of the immune response on oncolytic therapy (see [63, 75, 146]). To date, there is a wide variety of mathematical models in virotherapy, ranging from ordinary differential equations (ODEs) [75, 120, 123, 147], partial differential equations (PDEs) [148], multi-scale models [149], to agent-based [150] and stochastic processes models [151]. In the present study, we consider the ODE modeling framework which normally assumes that tumors and OV are perfectly mixed. We follow this approach for two reasons: (i) ODE models are usually analytically tractable, and basic insights gained from such models can easily be validated with experimental data. (ii) when modeling virus dynamics, ODE models often provide a basic understand of tumor-virus dynamics which can easily be extended to more complex spatial scenarios. Although the diverse roles of NK cells regulation have been investigated in several mathematical models (see Watzl et al. [130] for a review), the dynamical interactions of OV-induced NK cell recruitment during oncolytic virotherapy have not been fully explored [105].

Thus, we develop what we believe to be the first simple mathematical model of the dynamical interactions between OV, tumor cells, and activated OV-induced NK cells within the TME. Our aim in this work is to gain insights into the dynamics of the tumor and the OV-induced NK cell responses via a mathematical model employing a system of nonlinear ordinary differential equations.

The chapter is organized as follows. In section 3.1, we formulate the immunocompetent model and describe the underlying assumptions. In section 3.2, we present the linear stability analysis, basic reproductive number and local sensitivity index of endemic equilibrium. Global parameter sensitivity analysis is presented in section 3.5. Results of the numerical simulations are detailed in section 3.6. In section 3.7, we discuss the significance of the results and suggest future directions for OV-NK combination therapies.

3.1 Model formulation

In this section, we formulate a new simple ODE-based mathematical model describing the local interactions between tumor cells, OV and the NK cells. The quantities of interest in the model are the concentration of the uninfected tumor cells, T_u $(cells)$, the infected tumor cells, T_i $(cells)$, NK cells, N $(cells)$, and oncolytic viruses, V $(PFU/cell)$. Here, we use plaque-forming units (PFU) for V. PFU is a generally accepted measurement for infectious OVs, whereby non-infectious (defective) viruses that are not able to form plaques are excluded when counting the plaque-forming units [75]. The non-infectious viruses are not able to infect tumor cells; hence they are excluded when measuring the PFU. The summary of the model parameters, their meaning and base values are given in Table 3.1.

3.1.1 Model equations

We propose the following immunocompetent system of ordinary differential equations (ODEs) based on Fig. 3.1:

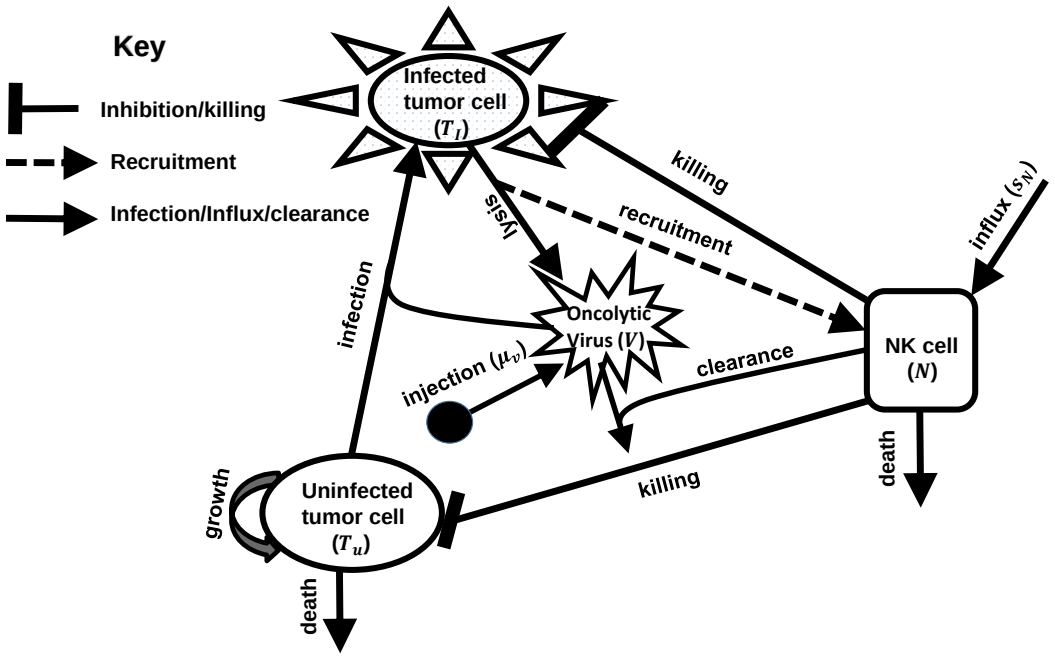

FIG. 3.1. A schematic diagram of the local interactions between tumor cells, OV and NK cells. Uninfected tumor cell (T_u) proliferates and undergoes natural death. Oncolytic viruses (V) are injected into the system at time t from an appropriate injection site according to a function μ_v. Upon infection, uninfected tumor cells become infected cells (T_i) following productive entry of the virus. Infected cells also undergo lysis and release more free infectious viruses. There is a constant influx (s_N) of NK cells (N) into the tumor microenvironment. NK cells become activated due to immunogenic cell death (ICD) of infected tumor cells, leading to additional recruitment of NK cells. Moreover, NK cells kill tumor cells and clear free viruses. Finally, NK cells undergo natural death.

$$\frac{dT_u}{dt} = \underbrace{\alpha T_u\left(1-\frac{T_u+T_i}{\theta_T}\right)}_{\text{tumor proliferation}} - \underbrace{\beta T_u V}_{\text{virus infection}} - \underbrace{c_{T_u} N T_u}_{\text{killed by NK cells}} \tag{3.1}$$

$$\frac{dT_i}{dt} = \underbrace{\beta T_u V}_{\text{virus infection}} - \underbrace{\delta T_i}_{\text{lysis}} - \underbrace{c_{T_i} N T_i}_{\text{killed by NK cells}} \tag{3.2}$$

$$\frac{dV}{dt} = \underbrace{\mu_v(t)}_{\text{virus injection}} + \underbrace{bT_i}_{\text{released by } T_i \text{ death}} - \underbrace{d_V N V}_{\text{killed by NK cells}} \tag{3.3}$$

$$\frac{dN}{dt} = \underbrace{s_N}_{\text{NK cell influx}} + \underbrace{\xi_N N\left(1-\frac{N}{\theta_N}\right)\left(\frac{T_i}{k_N+T_i}\right)}_{\substack{\text{NK cell activation and saturation, and} \\ \text{recruitment after infected cell death}}} - \underbrace{\sigma\left(T_u+T_i\right)N}_{\text{NK cell inactivation}} - \underbrace{dN}_{\text{death}} \tag{3.4}$$

where s_N and k_N are the constant influx of NK cells from the lymph node and the half-maximal constant which supports the NK cell activation and recruitment by immunogenic infected tumor cell death, respectively. NK cells are known to be non-specific and attack "non-self" cells as compared with $CD8^+$ T cells that have to be primed to attack a specific target. It is, however, also important to note that NK cells can rely on similar signaling pathways to those of T cells that enable them to become fully functional [130], and that NK cells can be specific or non-specific during oncolytic virotherapy [128]. We should emphasize that we assume there is a pre-existing NK cell population (s_N) within the tumor vicinity which, within hours post infection [105], is recruited to the TME and mediates initial OV clearance. In this study, "activation of NK cells" means stimulation (e.g., via multiple stimulatory receptors (such as CD16 and NKp46 [152, 153]) often expressed on NK cell surface) and local expansion (proliferation) of NK cell population within the TME [13]. Note also that, for simplicity, our model does not account for subcellular events and stimulatory pathways leading to activation of NK cells as modeled in [141]. We complete the system with the following non-negative initial conditions:

$$T_u(0) = T_{u0} \text{ cells}, \quad T_i(0) = 0 \text{ cells}, \quad V(0) = 0 \text{ virions}, \quad N(0) = N_0 \text{ cells}, \tag{3.5}$$

As in previous models [75, 123], OV injection into the system is modeled using a delta function $\mu_v(t) = \mu_v(0)\Delta(t-\tau)$, which accounts for an amount $\mu_v(0)$ of viruses injected on a specified day (τ), and Δ is the Dirac delta function [75]. Here we follow the experiments in [42], where $\mu_v(0) = 5 \times 10^6$ PFU is injected into the system on day $\tau (e.g., \tau = 19)$. A detailed description of the model is as follows:

In Eq. (3.1), the first term, $\alpha T_u \left(1 - \frac{T_u + T_i}{\theta_T}\right)$, denotes that in the absence of OV infection and NK response, the uninfected tumor cells grow logistically [75, 154], up to the carrying capacity θ_T, with the growth rate α. The second term, $-\beta T_u V$, denotes the productive infection of uninfected tumor cells by OV with the constant rate β. Note that we have used the mass action kinetics to model OV-tumor interactions because we assume that OV interacts with tumor cells at the rate that is proportional to the total number of uninfected tumor cells within the TME. Thus, we implicitly assume that there is no multiple infection of tumor cells (i.e., no tumor cell can be infected several times by an OV). It is, however, conceivable that tumor architecture can obstruct viral replication and propagation [155],

and in such cases other kinetics such as frequency-dependent or Michaelis-Menten kinetics can be considered to model OV-tumor interactions. Moreover, we assume that NK cells are able to recognize tumor antigens as well as viral antigens, not the virus inside of the infected cells; hence NK cells indiscriminately kill tumor cells independent of their infection status [143]. We assume NK cells kill tumor cells at different rates. Indeed, the NK cell killing rates can be tumor-specific or virus-specific due to diverse stimulatory ligands in tumor cells or virus-derived tumor antigens which is recognized by NK cells [142, 156]. Upon their interactions with activated NK cells, denoted by the term $c_{T_u}NT_u$, uninfected tumor cells are killed by NK cells at a constant rate c_{T_u}.

In Eq. (3.2), the proportion of newly infected tumor cells is denoted by the first term $\beta T_u V$. The OV-induced cell death of infected tumor cells is denoted by the second term $-\delta T_i$, where δ is the constant lysis rate. Note that the infected cells are assumed to be lysed by OVs within a short period of time. Thus, we assume no growth law for the infected cell population, a common assumption in models of tumor-virus dynamics [2, 118, 151]. The last term, $-c_{T_i}NT_i$, denotes the killing of infected tumor cells by NK cells with the constant rate c_{T_i}.

In Eq. (3.3), OV injection into the system is administered through the function $\mu_v(t)$ discussed above. When an infected tumor cell dies, it releases new infectious viral progeny which proceed to infect other susceptible tumor cells [48, 70]. The second term, bT_i, denotes that upon successful viral replication, OV are released from infected tumor cells at the constant burst size b. Free viruses within the TME are cleared by circulating immune effector cells [157] such as natural killer (NK) cells and activated cytotoxic T lymphocytes (CTLs), and/or non-specific immune-induced responses [158]. Note also that while there are several antiviral immune cells, in this study, for simplicity we assume that the majority of viral clearance is mediated by NK cells. In addition, we assume that oncolytic virotherapy is only effective when the rate of OV replication is greater than the rate of OV clearance [70, 137]. The last term $-d_V NV$ denotes the viral clearance of free OV within the TME by NK cells at the constant rate d_V.

In Eq. (3.4), the first term, denotes that as part of the innate immunity, NK cells are assumed to be always present within the TME, and are supplied from the lymph node at a constant rate, s_N, into the TME [5, 132, 154, 159]. Although the NK cells can directly be activated by free viruses within the TME, as modeled in [34], in this study we assume that activation of NK cells is dependent on contact with OV-infected tumor cells, as experimentally observed in [72]. The second term, $\xi_N N\left(1-\frac{N}{\theta_N}\right)\left(\frac{T_i}{k_N+T_i}\right)$, represents the stimulation and recruitment of NK cells. Note that we have used a saturated term $\frac{T_i}{k_N+T_i}$ to describe the limited effector effects of NK response on tumor killing, which accounts for reduced lysis of tumor cells by NK cells [160]. We also assume that NK cell response is further enhanced by lysis, which induces immunogenic cell death (ICD) [67, 127, 161, 162], of infected tumor cells at the rate ξ_N until it attains the maximum capacity θ_N (since the body can only support a limited number of activated immune cells; otherwise, a large number of activated immune cells could trigger a cytokine storm [163]). In the present study, for simplicity, we shall not consider a cascade of subcellular interactions or precesses leading to activation and recruitment of NK cells via ICD, but rather assume that there is an additional recruitment of NK cells to the TME due to ICD. While it is also conceivable that local interactions between the immune effector cells and tumor cells ultimately (or at least transiently) lead to immunogenic tumor cell death [111, 119], in this study we are mostly interested in OV-induced immunogenic tumor cell death. Instead of directly modeling the danger signals (such as DAMPs and PAMPs) released during ICD, we use the fact that these signals are over-expressed on the cell surfaces of OV-infected cells or released by the OV-infected cells [70, 134–136]. We therefore use the infected cell population as a proxy for modeling the actions of ICD. Parameter ξ_N is the recruitment/proliferation of NK cells in response to danger signals (such as DAMPs and PAMPs) released during ICD of OV-infected tumor cells. For simplicity, immunogenic infected tumor cell death is embedded into the recruitment rate, ξ_N (i.e., $\xi_N = r_i\delta$, where r_i and δ are the antigenic recruitment and OV-induced cell death rates, respectively). Parameter k_N represents the half-saturation constant of NK cells that supports the maximum killing of tumor cells by NK cells. The interactions of NK cells with tumor cells can lead to inactivation of NK cells at a constant rate, σ, that is proportional to their interactions [5, 154, 164]. Thus, the third term, $-\sigma\left(T_u+T_i\right)N$, denotes the inactivation of NK cells upon their interactions with tumor cells with the rate σ. Finally, the last term, dN, denotes the natural death of NK cells with the constant rate d.

We should emphasize that while CTLs and other immune cells play important antitumoral and antiviral roles in oncolytic virotherapy, by not modeling them in our study does not, in anyway, disregard their vital therapeutic effects against tumors, but simply means that the only tumor death occurring will be as a result of NK cell interactions. The summary of the model parameters, their meaning and base values are given in Table 3.1.

TABLE. 3.1. Summary of parameter definitions, values and their sources. A detailed description of how these parameters were obtained is found in Appendix 3.6.

Parameter	Description	Baseline value or Range	References
α	Proliferation rate of uninfected tumor cells	0.31 day^{-1}	[63]
θ_T	Carrying capacity of tumor cells	1.47×10^8 $(10^7 - 10^9)$ cells	[34]
β	Infection rate of uninfected tumor cells by free viruses	8.9×10^{-4} $(\text{PFU}^{-1})(\text{day}^{-1})$	[63, 144]
c_{T_u}	Killing rate of uninfected tumor cells by NK cells	8.68×10^{-10} $(\text{cells}^{-1})(\text{day}^{-1})$	[63]
c_{T_i}	Killing rate of infected tumor cells by NK cells	8.68×10^{-10} $(\text{cells}^{-1})(\text{day}^{-1})$	[63]
δ	Lysis rate of infected tumor cells	1.5 day^{-1}	[165]
b	Viral burst size of a lysed infected tumor cell	$10^3(10 - 1,350)$ $(\text{PFU})(\text{cells}^{-1})(\text{day}^{-1})$	[166]
ξ_N	Recruitment rate of NK cells via ICD by infected cells	1×10^{-5} day^{-1}	[167]
θ_N	Maximum capacity for NK cell production	6.63×10^{10} cells	[168]
k_N	Half-saturation constant of infected tumor cells	10^4 cells	[34]
σ	Inactivation rate of NK cells by tumor cells	1.0×10^{-7} $(\text{cells}^{-1})(\text{day}^{-1})$	[63, 159]
$\gamma = d_V$	Viral clearance rate	2.3 day^{-1}	[63, 144]
d	Natural death rate of NK cells	4.12×10^{-2} day^{-1}	[5, 159]
s_N	Constant influx of NK cells	$3.2 \times 10^3 - 3.2 \times 10^4$ $(\text{cells})(\text{day}^{-1})$	[5]

3.2 Model analysis

To begin our analysis, we first examine the immune-free submodel, that is, in the absence of the immune response. The objective of this analysis is to investigate conditions and parameters that can impact the attainment of a tumor-free state with oncolytic virotherapy in the absence of NK cells intervention. We use both linear stability analysis and basic reproductive number to get a better understanding of how tumor elimination may depend on OV characteristics.

To assess how model parameters impact tumor progression and their relative significance to the therapeutic outcome, we also carried out a forward local sensitivity index analysis of the virus basic reproductive number, $\mathcal{R}_0$, and the tumor endemic equilibrium with respect to the model key parameters. We first derive the model basic reproductive number, $\mathcal{R}_0$,

and then calculate its elasticity indices with respect to the model parameters to identify which of them are most sensitive during tumor infection.

We later assess the effect of NK cell response in oncolytic virotherapy by exploring the qualitative behavior of the models numerically. The respective findings of the immuno-competent model and immune-free submodel will be crucial for comparative purposes when assessing our model predictions in oncolytic virotherapy treatment.

3.2.1 The immune-free submodel

In the absence of the NK cell intervention, model system 3.1.1 is reduced to:

$$\frac{dT_u}{dt} = \underbrace{\alpha T_u\left(1-\frac{T_u+T_i}{\theta_T}\right)}_{\text{tumor proliferation}} - \underbrace{\beta T_u V}_{\text{virus infection}} \tag{3.6}$$

$$\frac{dT_i}{dt} = \underbrace{\beta T_u V}_{\text{virus infection}} - \underbrace{\delta T_i}_{\text{lysis}} \tag{3.7}$$

$$\frac{dV}{dt} = \underbrace{\mu_v(t)}_{\text{virus injection}} + \underbrace{bT_i}_{\text{released by } T_i \text{ death}} - \underbrace{\gamma V}_{\text{clearance}} . \tag{3.8}$$

3.3 Nondimensionalization

To begin our analysis, we first non-dimensionalize the full model described by Eqs. (3.1)–(3.4), by rescaling time with δ^{-1}, the half-life of the infected tumor cell population (as in [122]), the tumor cell populations with θ_T, the carrying capacity of tumor cells (as in [159, 169]), oncolytic viruses with b, the viral burst size of infected tumor cells (as in [118]), and the NK cells with θ_N, the maximum carrying capacity for the activated NK cells. Let $\hat{T}_u, \hat{T}_i$, $\hat{V}$ and $\hat{N}$ denote dimensionless variables corresponding to the dimensional state variables of our model. Then, $\hat{T}_u = \frac{T_u}{\theta_T}$, $\hat{T}_i = \frac{T_i}{\theta_T}$, $\hat{V} = \frac{V}{\theta_T}$, $\hat{N} = \frac{N}{\theta_N}$, $\hat{t} = \delta t$. Then substituting into Eqs. (3.1)–(3.4), for convenience, we drop all the hats over the state variables and time to obtain the dimensionless system (3.9–3.12) with Eq. (3.13).

$$\frac{dT_u}{dt} = rT_u\left(1 - T_u - T_i\right) - \lambda_v T_u V - c_T T_u N \tag{3.9}$$
$$\frac{dT_i}{dt} = \lambda_v T_u V - T_i - c_{TV} T_i N \tag{3.10}$$
$$\frac{dV}{dt} = I_v(t) + \rho T_i - c_V V N \tag{3.11}$$
$$\frac{dN}{dt} = f_N + a_N N\left(1 - N\right)\left(\frac{T_i}{h_N + T_i}\right) - \eta\left(T_u + T_i\right)N - \kappa_N N, \tag{3.12}$$

with initial conditions

$$T_u(0) = T_{u0}, \quad T_i(0) = 0, \quad V(0) = 0, \quad N(0) = N_0, \tag{3.13}$$

where: $r = \frac{\alpha}{\delta}$, $\lambda_v = \frac{\beta\theta_T}{\delta}$, $c_T = \frac{\theta_N}{\delta}$, $\kappa_N = \frac{d}{\delta}$, $I(t) = \frac{\mu_v(t)}{\delta b}$, $\rho = \frac{\theta_T}{\delta}$, $\omega_v = \frac{\gamma}{\delta}$, $T_{u0} = \frac{T_{u0}}{\theta_T}$, $c_{TV} = \frac{\theta_N}{\delta}$, $a_N = \frac{\xi_N}{\delta}$, $\eta = \frac{\sigma\theta_T}{\delta}$, $h_N = \frac{k_N}{\theta_T}$, $c_V = \frac{\theta_N}{\delta}$, $f_N = \frac{s_N}{\delta b}$, $N_0 = \frac{N_0}{\theta_N}$.

The dimensionless system of the immune-free submodel (Eqs. (3.6)–(3.8)) is given by

$$\frac{dT_u}{dt} = rT_u\left(1 - T_u - T_i\right) - \lambda_v T_u V \tag{3.14}$$
$$\frac{dT_i}{dt} = \lambda_v T_u V - T_i \tag{3.15}$$
$$\frac{dV}{dt} = I_v(t) + \rho T_i - \omega_v V, \tag{3.16}$$

with the initial conditions

$$T_u(0) = T_{u0}, \quad T_i(0) = 0, \quad V(0) = 0. \tag{3.17}$$

3.4 Basic properties of solutions

The proposed model describes the temporal evolution of cells and virus populations, and therefore, the cell concentrations should remain nonnegative and bounded. Here, we only establish the well-posedness of the immune-free submodel (Eqs. (3.6)–(3.8)). The well-posedness theorem is stated below with its corresponding proofs.

Theorem 1 *Well-posedness*

(i) (non-negativity of solutions) Given that the non-negative initial conditions $(T_{u0} > 0, T_{i0} > 0, V_0 > 0)$*, the corresponding solutions* $(T_u(t), T_i(t), V(t))$ *will remain non-negative for all* $t \in [0, \infty)$.

(ii) (boundedness of solutions and invariant region) The model system is bounded and the invariant region is given by

$$\mathbf{\Omega_V} = \{(T_u, T_i, V) \in \mathbb{R}^3_+ \mid \ 0 \leqslant T_u \leqslant \theta_T,\ 0 \leqslant T_i \leqslant \frac{1}{\delta}\beta T_u V,\ 0 \leqslant V \leqslant \frac{1}{\gamma}(\mu_v(t) + bT_i)\} \tag{3.18}$$

Moreover, the domain $\mathbf{\Omega_V}$ is positively invariant for the model and therefore biologically meaningful for the cell concentrations and regarded as a "global" domain. The corresponding dimensionless system, Eqs. (3.14)–(3.16), is valid under the following positively invariant domain:

$$\mathbf{\Omega_{V1}} = \{(T_u, T_i, V) \in \mathbb{R}^3_+ \mid \ T_u \geq 0,\ T_i \geq 0,\ 0 \leqslant T_u + T_i \leqslant 1,\ V \geq 0\}. \tag{3.19}$$

(iii) (existence and uniqueness) For any non-negative initial values of the model state variables, a solution to the model exists and is unique in the positively invariant domain $\mathbf{\Omega_V}$ for all time $t > 0$.

3.4.1 Proof of the well-posedness theorem

Here we provide a detail discussion of the well-posedness of our immune-free submodel (see Eqs. (3.6)–(3.8)), and a brief outline for extending the solutions to our immunocompetent system (see Eqs. (3.1)–(3.4)).

(i) Non-negativity of solutions

Proof. Considering Eq. (3.6), we have a Bernoulli differential equation. We now rewrite Eq. (3.6) as $\frac{dT_u}{dt} = \alpha T_u - \frac{\alpha T_u^2}{\theta_T} - \frac{\alpha T_u T_i}{\theta_T} - \beta T_u V = \left(\alpha - \frac{\alpha T_i}{\theta_T} - \beta V\right) T_u - \frac{\alpha T_u^2}{\theta_T}$. Thus, the Bernoulli standard form of Eq. (3.6) is $\frac{dT_u}{dt} + \left(\beta V + \frac{\alpha T_i}{\theta_T} - \alpha\right) T_u = -\frac{\alpha T_u^2}{\theta_T}$. Here, $n = 2$, $P(t) = \beta V + \frac{\alpha T_i}{\theta_T} - \alpha$, $Q(t) = -\frac{\alpha}{\theta_T}$. The integrating factor is $I(t) = e^{\int (1-2)\left(\beta V + \frac{\alpha T_i}{\theta_T} - \alpha\right) dt} = e^{-\left(\beta V + \frac{\alpha T_i}{\theta_T} - \alpha\right) t}$. The solution is therefore given by: $T_u^{-1} = e^{\left(\beta V + \frac{\alpha T_i}{\theta_T} - \alpha\right) t} \left[\int (-1) \left(-\frac{\alpha}{\theta_T}\right) e^{-\left(\beta V + \frac{\alpha T_i}{\theta_T} - \alpha\right) t} dt + c\right] = e^{\left(\beta V + \frac{\alpha T_i}{\theta_T} - \alpha\right) t} \left[\frac{\alpha}{\theta_T} \int e^{-\left(\beta V + \frac{\alpha T_i}{\theta_T} - \alpha\right) t} dt + c\right] = e^{nt} \left[-\frac{\alpha}{\theta_T n} e^{-nt} + c\right]$, where $n = \beta V + \frac{\alpha T_i}{\theta_T} - \alpha = -\frac{\alpha}{\theta_T n} + ce^{nt}$.

At $t = 0$, $T_u = T_{u0}$, solving for c we obtain $c = T_{u0} + \frac{\alpha}{\theta_T n}$. Now substituting c in the equation for

T_u^-1 above, we get $T_u^-1 = \frac{(\theta_T n T_{u0}+\alpha)e^{nt}-\alpha}{\theta_T n}$., and thus,

$$\begin{aligned} T_u &= \frac{\theta_T n}{(\theta_T n T_{u0}+\alpha)\, e^{nt}-\alpha} \\ &= \frac{\theta_T \left(\beta V + \frac{\alpha T_i}{\theta_T} - \alpha\right)}{\left(\theta_T T_{u0}\left(\beta V + \frac{\alpha T_i}{\theta_T} - \alpha\right)+\alpha\right) e^{\left(\beta V + \frac{\alpha T_i}{\theta_T} - \alpha\right)t} - \alpha} > 0. \end{aligned}$$

Considering Eq. (3.7), we have a first-order ODE which can easily be written as $\frac{dT_i}{dt} + \delta T_i = \beta T_u V$. Using the following integrating factor $I(t) = e^{\int \delta dt} = e^{\delta t}$, and solving we get, $T_i = \frac{1}{\delta}\beta T_u V + ce^{-\delta t}$. At $t = 0$, $T_i(t) = 0$, solving for c we obtain $c = -\frac{1}{\delta}\beta T_u V$. Substituting c in the equation of T_i above we get $T_i = \frac{1}{\delta}\beta T_u V - \frac{1}{\delta}\beta T_u V e^{-\delta t} = \frac{1}{\delta}\beta T_u V\left(1 - e^{-\delta t}\right) > 0$.

Similarly, considering Eq. (3.8), we have a first-order ODE which can be rewritten as $\frac{dV}{dt} + \gamma V = \mu_v(t) + bT_i$. The integrating factor is given by $I(t) = e^{\int \gamma dt} = e^{\gamma t}$, which is used to solve for $V = \frac{1}{\gamma}\left(\mu_v(t) + bT_i\right) + ce^{-\gamma t}$. At $t = 0$, $V(t) = 0$, solving for c we obtain $c = -\frac{1}{\gamma}(\mu_v(t) + bT_i)$. Substituting c in the equation of V above we get $V = \frac{1}{\gamma}(\mu_v(t) + bT_i)(1 - e^{-\gamma t}) > 0$. ■

(ii) Boundedness of solutions and invariant region

In this section, we discuss the boundedness of the solutions of our model.
For the uninfected population, Eq. (3.6) can be rewritten as

$$\frac{dT_u}{dt} = \alpha T_u - \frac{\alpha T_u^2}{\theta_T} - \frac{\alpha T_u T_i}{\theta_T} - \beta T_u V.$$

From which we have

$$\begin{aligned} \frac{dT_u}{dt} &\leqslant \alpha T_u - \frac{\alpha T_u^2}{\theta_T} \\ &= \frac{\theta_T \alpha T_u - \alpha T_u^2}{\theta_T} \\ \implies \frac{\theta_T dT_u}{\theta_T \alpha T_u - \alpha T_u^2} &\leqslant dt \end{aligned}$$

$$\frac{\theta_T dT_u}{\alpha T_u(\theta_T - T_u)} \leqslant dt \tag{3.20}$$

Integrating the left hand side of Eq. (3.20) using partial fractions, we have

$$\frac{1}{T_u(\theta_T - T_u)} = \frac{A}{T_u} + \frac{B}{\theta_T - T_u}$$

Comparing coefficients and solving for A and B, we get $A = \frac{1}{\theta_T}$ and $B = \frac{1}{\theta_T}$. So

$$\frac{1}{T_u(\theta_T - T_u)} = \frac{1}{\theta_T T_u} + \frac{1}{\theta_T(\theta_T - T_u)}.$$

Integrating the above yields

$$\frac{1}{\theta_T}(ln(T_u) - ln(\theta_T - T_u)).$$

So the integral for Eq. (3.20) is

$$\frac{\theta_T}{\alpha}\left(\frac{ln(T_u)}{\theta_T} - \frac{ln(\theta_T - T_u)}{\theta_T}\right) \leqslant t + c.$$

At $t = 0,\ T_u = T_{u0}$

$$c = \frac{\theta_T}{\alpha}\left(\frac{ln(T_{u0})}{\theta_T} - \frac{ln(\theta_T - T_{u0})}{\theta_T}\right),$$

so

$$\begin{aligned}
\frac{\theta_T}{\alpha}\left(\frac{ln(T_u)}{\theta_T} - \frac{ln(\theta_T - T_u)}{\theta_T}\right) &\leqslant t + \frac{\theta_T}{\alpha}\left(\frac{ln(T_{u0})}{\theta_T} - \frac{ln(\theta_T - T_{u0})}{\theta_T}\right) \\
\frac{1}{\alpha}(ln(T_u) - ln(\theta_T - T_u)) &\leqslant t + \frac{1}{\alpha}(ln(T_{u0}) - ln(\theta_T - T_{u0})) \\
ln(T_u) - ln(\theta_T - T_u) &\leqslant \alpha t + ln(T_{u0}) - ln(\theta_T - T_{u0}) \\
ln\left(\frac{T_u}{\theta_T - T_u}\right) &\leqslant \alpha t + ln\left(\frac{T_{u0}}{\theta_T - T_{u0}}\right) \\
ln\left(\frac{T_u}{\theta_T - T_u}\right) - ln\left(\frac{T_{u0}}{\theta_T - T_{u0}}\right) &\leqslant \alpha t \\
ln\left(\frac{T_u(\theta_T - T_{u0})}{T_{u0}(\theta_T - T_u)}\right) &\leqslant \alpha t \\
\frac{T_u(\theta_T - T_{u0})}{T_{u0}(\theta_T - T_u)} &\leqslant e^{\alpha t} \\
T_u(\theta_T - T_{u0}) &\leqslant e^{\alpha t} T_{u0}(\theta_T - T_u) \\
&= e^{\alpha t} T_{u0}\theta_T - e^{\alpha t} T_u T_{u0} \\
T_u(\theta_T - T_{u0}) + e^{\alpha t} T_u T_{u0} &\leqslant e^{\alpha t} T_{u0}\theta_T \\
T_u((\theta_T - T_{u0}) + e^{\alpha t} T_{u0}) &\leqslant e^{\alpha t} T_{u0}\theta_T \\
T_u &\leqslant \frac{e^{\alpha t} T_{u0}\theta_T}{\frac{e^{\alpha t}}{e^{\alpha t}}(\theta_T - T_{u0}) + e^{\alpha t} T_{u0}} \\
&= \frac{T_{u0}\theta_T}{\frac{(\theta_T - T_{u0})}{e^{\alpha t}} + T_{u0}}.
\end{aligned}$$

Taking the limit supremum on both sides, we have

$$\begin{aligned}\limsup_{t\to\infty} T_u &\leqslant \limsup_{t\to\infty} \frac{T_{u0}\theta_T}{\frac{(\theta_T - T_{u0})}{e^{\alpha t}} + T_{u0}} \\ &= \frac{T_{u0}\theta_T}{T_{u0}} \\ &= \theta_T, \text{ which is the upper bound for } T_u.\end{aligned}$$

Now, considering the infected tumor cell population, re-writing Eq. (3.7) leads to

$$\frac{dT_i}{dt} + \delta T_i = \beta T_u V,$$

which is now in first order linear standard form and its solution is given by

$$T_i = \frac{1}{\delta}\beta T_u V\left(1 - e^{-\delta t}\right).$$

Taking limits on both sides of the above equation,

$$\begin{aligned}\limsup_{t\to\infty} T_i &= \lim_{t\to\infty} \frac{1}{\delta}\beta T_u V\left(1 - e^{-\delta t}\right) \\ &\leqslant \lim_{t\to\infty} \frac{1}{\delta}\beta T_u V \\ &= \frac{1}{\delta}\beta T_u V, \text{ Which is the upper bound fot } T_i.\end{aligned}$$

For the virus population, Eq. (3.8) can be rewritten as

$$\frac{dV}{dt} + \gamma V = \mu_v(t) + bT_i,$$

which gives rise to the solution

$$V = \frac{1}{\gamma}(\mu_v(t) + bT_i)\left(1 - e^{-\gamma t}\right).$$

Taking limits on both sides of the above equation,

$$\begin{aligned}\limsup_{t\to\infty} V &= \lim_{t\to\infty} \frac{1}{\gamma}(\mu_v(t) + bT_i)\left(1 - e^{-\gamma t}\right) \\ &\leqslant \lim_{t\to\infty} \frac{1}{\gamma}(\mu_v(t) + bT_i) \\ &= \frac{1}{\gamma}(\mu_v(t) + bT_i), \text{ which is the upper bound for } V.\end{aligned}$$

We can therefore conclude that the system above is bounded and the invariant region is given by

$$\mathbf{\Omega_V} = \left\{(T_u, T_i, V) \in \mathbb{R}^3_+ \mid \ 0 \leqslant T_u \leqslant \theta_T,\ 0 \leqslant T_i \leqslant \frac{1}{\delta}\beta T_u V,\ 0 \leqslant V \leqslant \frac{1}{\gamma}(\mu_v(t) + bT_i)\right\}.$$

Note that $\mathbf{\Omega_V}$ is a positively invariant domain for the system (Eqs. (3.6)–(3.8)). Moreover, notice also that $0 \leq T_u(t) + T_i(t) \leq \theta_T$ for $t > 0$. This shows that the total tumor burden $T_u(t) + T_i(t)$ cannot exceed the carrying capacity θ_T. This proof is analogous to the proof in Appendix A of Dingli et al. [170]. $\mathbf{\Omega_V}$ is also a biologically feasible region for the state variables. Hence, we shall also regard this region as a "global" domain.

(iii) Existence and uniqueness of solutions

Proof. Since the right-hand side of system is $\mathbf{C}^1$ (class of continuously differentiable functions) satisfies the properties of locally Lipschitz functions, then the existence and uniqueness of solutions of the system is ascertained by the Cauchy-Lipschitz theorem [171, 172]. ■

For the immunocompetent model (see Eqs. (3.1)–(3.4)), it is not difficult to establish that the solutions will remain non-negative for $t \geq 0$ since $\frac{dN}{dt} \geq 0$ whenever $N(t) = 0$ and $N(t) \geq 0$, Also it can easily be verified that N is bounded by $0 \leq N \leq \frac{s_N}{d}$. Thus, we define the invariant region for the system (Eqs. (3.1)–(3.4)) as

$$\mathbf{\Omega_{VN}} = \left\{ (T_u, T_i, V, N) \in \mathbb{R}^4_+ \mid \ 0 \leqslant T_u \leqslant \theta_T,\ 0 \leqslant T_i \leqslant \frac{1}{\delta}\beta T_u V,\ 0 \leqslant V \leqslant \frac{1}{\gamma}(\mu_v(t) + bT_i),\ 0 \leq N \leq \frac{s_N}{d} \right\}.$$

Hence, the existence and uniqueness of solutions theorem for our immunocompetent model is preserved. Note that the right hand side of our immunocompetent system is $\mathbf{C}^1$ on $\mathbb{R}^4_+$.

The non-negativity and boundedness of the immunocompetent model directly follow from the same type of logical arguments presented here and hence we omit their proofs.

3.4.2 Steady state analysis

Here we find the equilibria of the non-dimensionalized system, which occur at the intersections of the tumor and OV nullclines, where $\frac{dT_u}{dt} = 0$, $\frac{dT_i}{dt} = 0$, *and* $\frac{dV}{dt} = 0$. To determine the stability of the steady states, we apply linear stability analysis and discuss in detail their clinical implications. The linearized system at point (T_u, T_i, V) is summarized by the variational matrix

$$J = \begin{pmatrix} -V\lambda_v - (T_i + T_u - 1)r - T_u r & -T_u r & -T_u\lambda_v \\ V\lambda_v & -1 & T_u\lambda_v \\ 0 & \rho & -\omega_v \end{pmatrix}$$

There are three steady state solutions namely:

(i) **Tumor Eradication Steady State ($\mathbf{SS_0}$): $\mathbf{SS_0}$** $= (T_u^*, T_i^*, V^*) = (0, 0, 0)$ which represents the situation with a complete tumor eradication. Importantly, this steady state

indicates a successful oncolytic virotherapy, where all state variables are zero. Evaluating the variational matrix at this steady state gives

$$J(\mathbf{SS_0}) = \begin{pmatrix} r & 0 & 0 \\ 0 & -1 & 0 \\ 0 & \rho & -\omega_v \end{pmatrix}. \tag{3.21}$$

The corresponding eigenvalues are $r, -1, -\omega_v$. $\mathbf{SS_0}$ is unstable since $r > 0$. Note that $T_i - V$ plane is the stable invariant subspace of the system defined by Eqs. (3.14)–(3.16), and the T_u-axis is the unstable invariant subspace. We also note that the local stable invariant manifold for our system (Eqs. (3.14)–(3.16)) is in the $T_i - V$ plane, while T_u-axis denotes the unstable invariant manifold. A possible interpretation for $\mathbf{SS_0}$ is that without OV, the uninfected tumor cell population will proliferate from a small initial value in the neighborhood of $\mathbf{SS_0}$. If, on the other hand, the OV manages to successfully and productively infect all tumor cells, then the tumor will shrink, due to oncolysis of infected cells, until no tumor cell exists in the subsystem.

(ii) **Ineffective Virotherapy Steady State ($\mathbf{SS_1}$):** $(T_u^*, T_i^*, V^*) = (r, 0, 0)$ which corresponds to a tumor constituted entirely by susceptible (uninfected) cells. This indicates a failed oncolytic virotherapy since the uninfected tumor cells T_u continues to grow up to the carrying capacity of the system (i.e., here tumor reaches its environmental carrying capacity when $T_u^* = 1$), and no oncolytic virus survives. The variational matrix evaluated at this steady state yields:

$$J(\mathbf{SS_1}) = \begin{pmatrix} -r & -r & -\lambda_v \\ 0 & -1 & \lambda_v \\ 0 & \rho & -\omega_v \end{pmatrix}, \tag{3.22}$$

and the corresponding characteristic polynomial of this matrix is $P(s) = s^3 + (r + \omega_v + 1)\, s^2 + (-\lambda_v\rho + r\omega_v + r + \omega_v)\, s - r\lambda_v\rho + r\omega_v = 0$. The eigenvalues are $s_1 = -r,\ s_{2,3} = \frac{1}{2}(-\omega_v - 1 \pm \sqrt{(\omega_v - 1)^2 + 4\lambda_v\rho})$. Next, we state the stability theorems and their corresponding proofs.

Theorem 2 *(Local Stability)* $\mathbf{SS_1}$ *is locally asymptotically stable when* $\rho < \frac{\omega_v}{\lambda_v}$ *and unstable when* $\rho > \frac{\omega_v}{\lambda_v}$.

Proof. We note that $s_1 = -r < 0$ and $s_2 = \frac{1}{2}(-\omega_v - 1 - \sqrt{(\omega_v - 1)^2 + 4\lambda_v\rho}) < 0$, for all non-negative parameter values, and $s_3 = \frac{1}{2}(-\omega_v - 1 + \sqrt{(\omega_v - 1)^2 + 4\lambda_v\rho})$ can either be negative, positive and zero. If $\sqrt{(\omega_v - 1)^2 + 4\lambda_v\rho} < 1 + \omega_v$, then $s_3 < 0$. Since $1 + \omega_v$ is positive, then it follows that $(\omega_v - 1)^2 + 4\lambda_v\rho < (1 + \omega_v)^2$, which is equivalent to $\rho < \frac{\omega_v}{\lambda_v}$. Thus, when $\rho < \frac{\omega_v}{\lambda_v}$, all three eigenvalues (s_1, s_2 and s_3) are negative. Hence $\mathbf{SS_1}$ is locally asymptotically stable. Equivalently, since $P(s) = s^3 + (r + \omega_v + 1)\, s^2 + (-\lambda_v\rho + r\omega_v + r + \omega_v)\, s - r\lambda_v\rho + r\omega_v = s^3 + a_2 s^2 + a_1 s + a_0 = 0$, where $a_2 = \omega_v + r + 1,\ a_1 = \omega_v r + r + \omega_v - \rho\lambda_v,\ a_0 = \omega_v r - \lambda_v\rho r$, we notice that $a_2 > 0$ and that if $\mathcal{R}_0 < 1$ then $a_1 > 0, a_0 > 0$ and $a_1 a_2 - a_0 > 0$. Hence, by the Routh-Hurwitz criterion [173, 174], we deduce that $\mathbf{SS_1}$ is locally asymptotically stable.

Similarly, whenever $\rho > \frac{\omega_v}{\lambda_v}$, then $\sqrt{(\omega_v - 1)^2 + 4\lambda_v\rho} > 1 + \omega_v$. This implies that $s_3 > 0$. Hence $\mathbf{SS_1}$ is unstable. ■

Given the positively invariant domain $\mathbf{\Omega_{V1}}$ (see Eq. (3.19)), we can actually prove that the steady state solution $\mathbf{SS_1}$ is globally asymptotically stable in the whole domain $\mathbf{\Omega_V}$ (see Eq. (3.18)) using Lyapunov functions. Here, we state the main theorem and provide its full proof.

Theorem 3 *(Global Stability) When* $\rho < \frac{\omega_v}{\lambda_v}$, $\mathbf{SS_1}$ *is globally asymptotically stable.*

Before we provide a detailed proof of this theorem, note that given the positively invariant domain $\mathbf{\Omega_{V1}}$ (see Eq. (3.19)), the steady state solution $\mathbf{SS_1}$ should be globally asymptotically stable in the whole domain $\mathbf{\Omega_V}$ (see Eq. (3.18)). To prove this, we first construct a Lyapunov function based on a specified range of the parameter ρ. We simplify the model by the translating the state variables as follow: $T_u = 1 - \hat{T}_u$, $T_i = \hat{T}_i$, and $V = \hat{V}$. For notation convenience, we drop the hats over the state variables, and have the following system:

$$\frac{dT_u}{dt} = -rT_u + rT_i + rT_u^2 + \lambda_v V - rT_uT_i - \lambda_v T_u V \tag{3.23}$$

$$\frac{dT_i}{dt} = \lambda_v V - \lambda_v T_u V - T_i \tag{3.24}$$

$$\frac{dV}{dt} = \rho T_i - \omega_v V, \tag{3.25}$$

and the invariant domain $\mathbf{\Omega_{V1}}$ (see Eq. (3.19)) is translated to

$$\mathbf{\Omega_{V2}} = \left\{(T_u, T_i, V) \in \mathbb{R}^3_+ \mid \ T_u \geq 0,\ T_i \geq 0,\ 0 \leqslant T_u - T_i \leqslant 1,\ V \geq 0\right\}. \tag{3.26}$$

Now we give the proof of Theorem 3:

Proof. Given the nonnegative initial conditions (T_{u0}, T_{i0}, V_0) in $\mathbf{\Omega_{V2}}$, then by Theorem 3.4.1 and 3.4.1, the corresponding solutions of the dimensionless state variable satisfy $0 \leq T_u(t) \leq 1$, $0 \leq T_i(t) \leq 1$, and $V(t) \geq 0$. It suffices to show that if $T_i(t)$ and $V(t)$ approach zero, then $T_u(t)$ also approaches zero. When $0 < \rho < 1$, we define a Lyapunov function

$$G(T_u, T_i, V) = \frac{1}{2}\lambda_v\rho\omega_v T_i^2 + \lambda_v^2\rho T_i V + \frac{1}{2}\lambda_v^2 V^2$$

Using Theorem 3.4.1, it is easy to check that $G(T_u, T_i, V) > 0$. The orbital derivative is given by

$$\begin{aligned}
\dot{G}(T_u, T_i, V) &= \lambda_v\rho\omega_v T_i\dot{T}_i + \lambda_v^2\rho\dot{T}_i V + \lambda_v^2\rho\dot{V}T_i + \lambda_v^2 V\dot{V} \\
&= \lambda_v\rho\omega_v T_i\left(\lambda_v V - \lambda_v T_u V - T_i\right) + \lambda_v^2\rho\left(\lambda_v V - \lambda_v T_u V - T_i\right)V \\
&\quad + \lambda_v^2\rho\left(\rho T_i - \omega_v V\right)T_i + \lambda_v^2 V\left(\rho T_i - \omega_v V\right) \\
&= \lambda_v\rho\left(\lambda_v\rho - \omega_v\right)T_i^2 - \lambda_v^2\rho\omega_v T_i T_u V + \lambda_v^2\left(\lambda_v\rho - \omega_v\right)V^2 - \lambda_v^3\rho T_u V^2 \\
&\quad + \lambda_v\omega_v\left(\rho - 1\right)T_i V.
\end{aligned}$$

Since $\rho < \frac{\omega_v}{\lambda_v}$, which means, $\lambda_v\rho - \omega_v < 0$, and $0 < \rho < 1$, implies that $\rho - 1 < 0$, then it follows that $\dot{G}(T_u, T_i, V) < 0$. Therefore, using this Lyapunov function, we have $T_i(t) \to 0$ and $V(t) \to 0$ as $t \to +\infty$ when $\rho < \frac{\omega_v}{\lambda_v}$.

Now, we show that $T_u(t) \to 0$ as $t \to +\infty$ too. From Eq. (3.23), we have

$$\begin{aligned}\frac{dT_u}{dt} &= -rT_u + rT_i + rT_u^2 + \lambda_v V - rT_uT_i - \lambda_v T_u V \\ &= -rT_u(1-T_u) + rT_i(1-T_u) + \lambda_v V(1-T_u) \\ &= (1-T_u)\left[rT_i + \lambda_v V - rT_u\right] \\ &\leq rT_i + \lambda_v V - rT_u.\end{aligned}$$

Solving for T_u, we obtain

$$0 \leq T_u(t) \leq T_{u0}e^{-rt} + e^{-rt}\int_0^t \left(rT_i(s) + \lambda_v V(s)\right)e^{rs}ds.$$

Taking the limit on both sides we have

$$\begin{aligned}\lim_{t\to\infty} T_u(t) &\leq T_{u0}e^{-rt} + \lim_{t\to\infty} e^{-rt}\int_0^t \left(rT_i(s) + \lambda_v V(s)\right)e^{rs}ds \\ &\leq 0 + \lim_{t\to\infty}\frac{\int_0^t \left(rT_i(s) + \lambda_v V(s)\right)e^{rs}ds}{e^{rt}} \\ &\leq \lim_{t\to\infty}\frac{1}{r}\frac{\left(rT_i(t) + \lambda_v V(t)\right)e^{rt}}{e^{rt}} \\ &\leq \frac{1}{r}\left[\lim_{t\to\infty} rT_i + \lim_{t\to\infty}\lambda_v V(t)\right] \\ &\leq \frac{1}{r}(0+0) \quad \text{(since both } T_u(t)\to 0 \text{ and } V(t)\to 0 \text{ as } t\to+\infty.\text{)} \\ &\leq 0.\end{aligned}$$

Thus, we notice that $T_u(t) \to 0$ as $t \to +\infty$. Hence, given an initial condition in the domain $\mathbf{\Omega_{V2}}$, then $T_u(t)$, $T_i(t)$ and $V(t)$ all approach the origin as $t \to +\infty$. Therefore, $\mathbf{SS_1}$ is a global attractor for the system (3.14 – 3.16). ■

Clinical implication: Theorem 3 has an important clinical implication. An oncolytic virotherapy fails when the burst size of an oncolytic virus is less than $\frac{\omega_v}{\lambda_v}$, since there will be an insufficient number newly produced viruses to productively infect tumor cells. This means that whenever the number of released viruses from infected cells is less than $\frac{\omega_v}{\lambda_v}$, then the tumor regrows uncontrollably up to a maximum size (i.e., when $T_u = 1$). It is also important to note that this therapeutic failure depends on the number of factors, including the initial tumor size, the replication ability of oncolytic virus, the initial number of infected tumor cells, and the initial virus inoculum (which is often manipulated in orders of magnitude $(10^3 - 10^{10})$ plaque-forming units (PFU) [175]). In other words, when these therapeutic factors are within the domain $\mathbf{\Omega_{V2}}$ (defined in Eq. (3.26)), oncolytic virotherapy will fail whenever $\rho < \frac{\omega_v}{\lambda_v}$. Furthermore, it is also crucial to note that the burst size is independent of the initial conditions.

We shall denote by $\rho_c = \frac{\omega_v}{\lambda_v}$ the threshold upon which virotherapy fails. That is, ρ_c is a threshold value for the burst size. Let $\rho = \rho_c$, then $\rho\lambda_v = \omega_v$. To complete the steady state analysis, we shall investigate the stability of the linearized system (see Eqs. (3.23)–(3.25)) at $\mathbf{SS_1}$ at this critical case $\rho = \rho_c$. In this case, the variational matrix at $\mathbf{SS_1}$ has two

negative eigenvalues and one zero eigenvalue. We use the center manifold theorem to reduce the linearized system, Eqs. (3.23)–(3.25), to its local center manifold, and investigate the qualitative behavior of the reduced system. Here, we state the main theorem and its detailed proof below. We also provide a brief discussion about the general biological significance of this fundamental theorem.

Theorem 4 *(Threshold Local Stability)* $\mathbf{SS_1}$ *is locally asymptotically stable when* $\rho = \rho_c = \frac{\omega_v}{\lambda_v}$.

Proof. We use a center manifold theorem to reduce the system (3.23–3.25) to its local center manifold. First we segregate the system into two parts, the part with zero eigenvalue and the one with negative eigenvalues. Considering the linear part of system (3.23–3.25), then the corresponding matrix is

$$L = \begin{pmatrix} -r & r & \lambda_v \\ 0 & -1 & \lambda_v \\ 0 & \rho & -\rho\lambda_v \end{pmatrix}$$

The eigenvalues and corresponding eigenvectors of L are

$$\begin{aligned} &\lambda_1 = -r, \quad \text{with} \quad V_1 = (1,0,0)^{\mathrm{T}} \\ &\lambda_2 = -\left(1+\rho\lambda_v\right), \quad \text{with} \quad V_2 = (\rho\lambda_v - r, 1+\rho\lambda_v - r, \rho(1+\rho\lambda_v - r))^{\mathrm{T}} \\ &\lambda_3 = 0, \quad \text{with} \quad V_3 = (\lambda_v(r+1), r\lambda_v, r)^{\mathrm{T}}. \end{aligned}$$

Let $T = (V_1, V_2, V_3)$ be the transformation matrix and let $Y = (T_u, T_i, V)^{\mathrm{T}}$, then we can write the system $(3.23 - 3.25)$ into a reduced system

$$\frac{dY}{dt} = LY + N, \tag{3.27}$$

where $N = \left(rT_u^2 - rT_uT_i - \lambda_vT_uV, -\lambda_vT_uV, 0\right)^{\mathrm{T}}$. Now let $Y = TX$, then we have

$$\frac{dX}{dt} = T^{-1}LTX + T^{-1}N, \tag{3.28}$$

where the diagonal matrix $T^{-1}LT$ is define as

$$T^{-1}LT = \begin{pmatrix} -r & 0 & 0 \\ 0 & -(1+r\lambda_v) & 0 \\ 0 & 0 & 0 \end{pmatrix},$$

and $T_u = x_1 + (\rho\lambda_v - r)x_2 + \lambda_v(r+1)x_3$, $T_i = (1+\rho\lambda_v - r)x_2 + r\lambda_v x_3$, and $V = -\rho(1+\rho\lambda_v - r)x_2 + rx_3$. Now considering the last term, $T^{-1}N$, in Eq. (3.28), and let

$T^{-1}N = (n_1, n_2, n_3)^{\mathrm{T}}$, then expressing $n_i,\ i = 1, 2, 3$ in terms of x_i, we have

$$\begin{aligned}
n_1 &= rT_u^2 - rT_iT_u - \lambda_v T_u V \\
&= A_{11}x_1^2 + A_{12}x_1x_2 + A_{13}x_1x_3 + A_{22}x_2^2 + A_{23}x_2x_3 + A_{33}x_3^2. \\
n_2 &= \frac{1}{\lambda_v^2\rho^2 - \lambda_v r\rho + r - 1}\left(\left(\lambda_v T_u V + rT_iT_u - rT_u^2\right)\left(\left(\lambda_v^2 r + \lambda_v^2\right)\rho^2 + r^2\right.\right. \\
&\quad \left.\left. - \left(\lambda_v r^2 + \lambda_v r - \lambda_v\right)\rho\right) + r\lambda_v T_u V\right) \\
&= B_{11}x_1^2 + B_{12}x_1x_2 + B_{13}x_1x_3 + B_{22}x_2^2 + B_{23}x_2x_3 + B_{33}x_3^2. \\
n_3 &= \frac{1}{\lambda_v^2\rho^2 - \lambda_v r\rho + r - 1}\left(\left(\lambda_v T_u V + rT_iT_u - rT_u^2\right)\left(\lambda_v^2\rho + \lambda_v\right) - r\lambda_v^2 T_u V\right) \\
&= C_{11}x_1^2 + C_{12}x_1x_2 + C_{13}x_1x_3 + C_{22}x_2^2 + C_{23}x_2x_3 + C_{33}x_3^2.
\end{aligned}$$

where the coefficients A_{ij}, B_{ij}, and $C_{ij},\ i, j = 1, 2, 3$ can be easily determined. Then the transformed system can now be written as

$$\frac{dZ}{dt} = BZ + \begin{pmatrix} n_1 \\ n_2 \end{pmatrix} \tag{3.29}$$

$$\frac{dx_3}{dt} = Ax_3 + n_3. \tag{3.30}$$

where

$$B = \begin{pmatrix} -r & 0 \\ 0 & -(1 + r\lambda_v) \end{pmatrix}, \qquad \text{and} \qquad A = (0)\,.$$

It is easy to verify that the matrix B has negative eigenvalues and A has zero eigenvalue. It can also be easy checked that each $n_i,\ i = 1, 2, 3$, is a C^2 differentiable function, $n_i(0, 0, 0) = 0$ and $Dn_i(0, 0, 0) = 0$, where Dn_i is the variational matrix of the function n_i. Then, by the Center Manifold Theorem [176], there exits a center manifold given by

$$Z = h(x_3) = \begin{pmatrix} h_1(x_3) \\ h_2(x_3) \end{pmatrix} \tag{3.31}$$

with $h(0) = 0$ and $Dh(0) = 0$, and it satisfies the equation

$$Bh(x_3) + \begin{pmatrix} n_1\left(h(x_3), x_3\right) \\ n_2\left(h(x_3), x_3\right) \end{pmatrix} = Dh(x_3) \cdot \left(Ax_3 + n_3\left(h(x_3), x_3\right)\right) \tag{3.32}$$

$$= Dh(x_3) \cdot n_3\left(h(x_3), x_3\right). \tag{3.33}$$

Let $u = x_3$, then we can approximate $h(u)$ as follows:

$$h(u) = \begin{pmatrix} h_1(u) \\ h_2(u) \end{pmatrix} \tag{3.34}$$

$$= \begin{pmatrix} c_2u^2 + c_3u^3 + c_4u^4 + O\left(u^5\right) \\ d_2u^2 + d_3u^3 + d_4u^4 + O\left(u^5\right) \end{pmatrix}. \tag{3.35}$$

For simplicity, we consider the order up to 5, and we will know later if it is enough. Then we calculate the $n_i,\ i = 1, 2, 3$, as follows:

$$\begin{aligned} n_1(h(u), u) &= n_1\left(h_1(u), h_2(u), u\right) \\ &= A_{33}u^2 + O\left(u^4\right) \\ n_2(h(u), u) &= n_2\left(h_1(u), h_2(u), u\right) \\ &= B_{33}u^2 + O\left(u^4\right) \\ n_3(h(u), u) &= n_3\left(h_1(u), h_2(u), u\right) \\ &= C_{33}u^2 + O\left(u^4\right). \end{aligned}$$

We substituting $n_i,\ i = 1, 2, 3$, into Eq. (3.33), and comparing the coefficients on both sides of the equation, we obtain $C_{33} = \frac{-r\lambda_v^2(r+1)^2(\lambda_v\rho+1)}{\lambda_v^2\rho^2-\lambda_v r\rho+r-1} < 0$. Now reducing the system (3.23–3.25) to its local center manifold, which is a single equation, we have

$$\frac{dx_3}{dt} = n_3(h(x_3), x_3) = C_{33}x_3^2 + O\left(x_3^4\right). \tag{3.36}$$

Eq. (3.36) governs the stability of the zero solution of the system (3.29–3.30). Since $C_{33} < 0$, then the zero solution, $x_3 = 0$, is locally asymptotically stable. Therefore, we conclude that the trivial solution of the system (3.23–3.25) is locally asymptotically stable when $\rho = \rho_c = \frac{\omega_v}{\lambda_v}$. ■

Clinical implication: Theorem 4 implies if the viral burst size is at the limiting value, ρ_c, then OV therapy can control tumor growth (i.e., oncolytic virotherapy has reached a stable state). Below this threshold value, as Theorem 3 indicates, oncolytic virotherapy fails. This is reasonable because when burst sizes are too low, tumor growth cannot be controlled by OV [75, 166, 177]. Interestingly, OV can easily be genetically modified to yield high titers [48], which gives OV therapy more therapeutic benefit over other treatment modalities. If OV burst size is big, there will be more free OV within the TME, thereby increasing the chance of tumor infection.

Note that when $\rho > \rho_c = \frac{\omega_v}{\lambda_v} > 0$, there is a third steady state which we define below. This is a unique positive steady state where tumor and OV coexist within the TME.

(iii) **Coexistence Steady State ($\mathbf{SS_2}$):** $(T_u^*, T_i^*, V^*) = \left(\frac{\omega_v}{\rho\lambda_v}, \frac{\omega_v r(\lambda_v\rho-\omega_v)}{\lambda_v\rho(\omega_v r+\lambda_v\rho)}, \frac{r(\lambda_v\rho-\omega_v)}{\lambda_v(\omega_v r+\lambda_v\rho)}\right)$ which describes a therapeutic situation where both tumor and oncolytic viruses coexist within the TME.

Clinical implication: Since $\mathbf{SS_2}$ is locally asymptotically stable, then one plausible biological interpretation of this state is that OV when used as a monotherapy is still capable of eradicating tumor cells. In agreement with this finding, several preclinical studies have demonstrated that intratumoral administration of OV can induce complete tumor regression [178, 179]. It is important to note, however, that a systemic administration of OV to tumor sites is still limited and has had some varying degree of success in tumor elimination [62, 63, 180].

3.4.3 Basic reproductive number

To get a better understanding of how tumor elimination may depend on OV characteristics, we consider the basic reproductive number of the model, $\mathcal{R}_0$. A basic reproductive number can be defined as the average number of new tumor infections generated by one infected cell, via cell lysis, during virotherapy in a completely susceptible cell population [181]. In general, if $\mathcal{R}_0 > 1$, then, on average, the number of new infections resulting from one infected cell is greater than one. Thus, viral infections will persist in tumor cell populations. If $\mathcal{R}_0 < 1$, then, on average, the number of new infections generated by one infected cell in virotherapy is less than one. This threshold can as well be used to delineate parameters which are most important during tumor infection. We used the next generation method described in [181] to calculate the basic reproductive number, $\mathcal{R}_0$, and obtained $\mathcal{R}_0 = \frac{\rho\lambda_v}{\omega_v}$. Importantly, we can summarize the following result of the non-dimensionalized immune-free submodel (Eqs. (3.14)–(3.16)) as follows:

Theorem 5 *The model defined by Eqs.* (3.14)–(3.16) *always has a trivial steady state (Tumor Eradication Steady State)* $\mathbf{SS_0} = (0, 0, 0)$ *which is unstable. Moreover,*

1. *If* $\mathcal{R}_0 < 1$*, then the system (3.14–3.16) has an additional steady state, namely the Ineffective Virotherapy Steady State (virus-free equilibrium)* $\mathbf{SS_1} = (r, 0, 0)$ *which is locally asymptotically stable.*

2. *If* $\mathcal{R}_0 > 1$*, then* $\mathbf{SS_1}$ *becomes unstable and the system (3.14–3.16) has an additional steady state (Coexistence Steady State (*$\mathbf{SS_2}$*)) given by*

$$\mathbf{SS_2} = \left(\frac{\omega_v}{\rho\lambda_v}, \frac{\omega_v r\left(\lambda_v\rho - \omega_v\right)}{\lambda_v\rho\left(\omega_v r + \lambda_v\rho\right)}, \frac{r\left(\lambda_v\rho - \omega_v\right)}{\lambda_v\left(\omega_v r + \lambda_v\rho\right)} \right).$$

which is locally asymptotically stable.

The proof is as follows:

Proof. If $\mathcal{R}_0 < 1$, it is easy to see that $\mathbf{SS_0} = (T_u^*, T_i^*, V^*) = (0, 0, 0)$ is an equilibrium point of the system (3.14–3.16) and that $\lambda = r$ is an eigenvalue of the Jacobian matrix at $\mathbf{SS_0}$ (see Matrix $J(\mathbf{SS_0})$ 3.21), implying that it is locally asymptotically stable.

If $\mathcal{R}_0 > 1$, then we know that there is an additional steady state (Coexistence Steady State ($\mathbf{SS_2}$)) given by

$$\mathbf{SS_2} = \left(\frac{\omega_v}{\rho\lambda_v}, \frac{\omega_v r\left(\lambda_v\rho - \omega_v\right)}{\lambda_v\rho\left(\omega_v r + \lambda_v\rho\right)}, \frac{r\left(\lambda_v\rho - \omega_v\right)}{\lambda_v\left(\omega_v r + \lambda_v\rho\right)} \right).$$

Furthermore, the characteristic equation at $\mathbf{SS_2}$ is

$$z^3 + b_2 z^2 + b_1 z + b_0 = 0$$

with

$$b_2 = \frac{\lambda_v\rho\omega_v+\omega_v r+\rho\lambda_v}{\rho\lambda_v}$$
$$b_1 = \frac{\omega_v r\left(\lambda_v\rho r+{\omega_v}^2 r+\lambda_v\rho\omega_v+\rho\lambda_v\right)}{\rho\lambda_v(\omega_v r+\rho\lambda_v)}\,\frac{\omega_v r(\rho\lambda_v-\omega_v)}{\rho\lambda_v}$$
$$b_0 = \frac{\omega_v r\left(r\rho\lambda_v{\omega_v}^3-\ \rho^3{\lambda_v}^3+\rho^2{\lambda_v}^2{\omega_v}^2+\lambda_v\omega_v r^2\rho+r^2{\omega_v}^3+{\lambda_v}^2\rho^2 r+3r\rho\lambda_v{\omega_v}^2+3\rho^2{\lambda_v}^2\omega_v+\lambda_v\omega_v r\rho+\ {\lambda_v}^2\rho^2\right)}{\rho^2{\lambda_v}^2(\omega_v r+\rho\lambda_v)}.$$

Moreover, we have $b_2 > 0$ and if $\mathcal{R}_0 > 1$, then $b_1 > 0, b_0 > 0$ and

$$b_1 b_2 - b_0 = \left(\frac{\omega_v r\left(r\rho\lambda_v{\omega_v}^3-\rho^3{\lambda_v}^3+\rho^2{\lambda_v}^2{\omega_v}^2+\lambda_v\omega_v r^2\rho+r^2{\omega_v}^3\right.}{\rho^2{\lambda_v}^2\left(\omega_v r+\rho\lambda_v\right)}\right.$$
$$\left.+\frac{{\lambda_v}^2\rho^2 r+3r\rho\lambda_v{\omega_v}^2+3\rho^2{\lambda_v}^2\omega_v+\lambda_v\omega_v r\rho+\ {\lambda_v}^2\rho^2\right)}{\rho^2{\lambda_v}^2\left(\omega_v r+\rho\lambda_v\right)}\right) > 0$$

Hence, by Routh-Hurwitz criterion [173, 174], we deduce that $\mathbf{SS_2}$ is locally asymptotically stable. ■

3.4.4 Local sensitivity index of endemic equilibria

As a preliminary step and to understand how model parameters impact tumor progression, we carried out a forward local sensitivity index, with respect to total tumor size at equilibrium, and the virus basic reproductive number, $\mathcal{R}_0$. This analysis is important, not only for identifying key parameters affecting total size at tumor endemic equilibrium, but also for determining the relative significance of each parameter change to therapeutic outcome. Thus, we could quantify an appropriate OV inoculum that could cytoreduce tumor burden to tumor equilibrium. The total tumor size at equilibrium of the non-dimensionalized immune-free submodel (see Eqs. (3.14)–(3.16)) is given by

$$Tot = T_u^* + T_i^* = \frac{(r+1)\,\omega_v}{\omega_v r+\rho\lambda_v}. \tag{3.37}$$

With this, we obtain the sensitivity indices of the model to the total tumor endemic equilibria with respect to the dimensionless viral clearance rate (ω_v), proliferation rate (r) and infection rate (λ_v) respectively as

$$\Gamma_{\omega_v}^{Tot} = \frac{\rho\lambda_v}{\omega_v r+\rho\lambda_v} \tag{3.38}$$
$$\Gamma_{r}^{Tot} = \frac{r\left(\rho\lambda_v-\omega_v\right)}{(r+1)\left(\omega_v r+\rho\lambda_v\right)} \tag{3.39}$$
$$\Gamma_{\lambda_v}^{Tot} = -\frac{\rho\lambda_v}{\omega_v r+\rho\lambda_v}. \tag{3.40}$$

To further comprehend therapeutic conditions that are best indicators of tumor control or persistence, we now consider our non-dimensionalized immunocompetent system (see Eqs. (3.9)–(3.12)).

Most importantly, we assess whether NK cells alone can eradicate or at least control tumor growth to a certain low level. Without virotherapy the model reduces to

$$\begin{cases} \frac{dT_u}{dt} = rT_u\left(1-T_u\right) - c_T T_u N \\ \frac{dN}{dt} = f_N - \eta T_u N - \kappa_N N. \end{cases} \tag{3.41}$$

We have the following theorem:

Theorem 6 *1. If $r < \frac{c_T f_N}{\kappa_N}$, then (3.41) has a unique equilibrium point, $E_{00} = \left(0, \frac{f_N}{\kappa_N}\right)$ which is locally asymptotically stable.*

2. If $r > \frac{c_T f_N}{\kappa_N}$, then E_{00} is unstable and (3.41) has an additional equilibrium point given by

$$E_0 = \left(\frac{\eta - \kappa_N + \sqrt{\Delta}}{2\eta}, \frac{r\left(\eta+\kappa_N\right) - r\sqrt{\Delta}}{2\eta c_T}\right), \tag{3.42}$$

where $\Delta = \left(\eta+\kappa_N\right)^2 - 4\frac{\eta c_T f_N}{r}$, which is locally asymptotically stable.

Proof. The equilibrium points of (3.41) are given by the solutions of

$$\begin{cases} \left(r\left(1-T_u\right) - c_T N\right) T_u = 0 \\ f_N - \eta T_u N - \kappa_N N = 0. \end{cases} \tag{3.43}$$

From $(3.43)_1$ we obtain $T_u = 0$ or $T_u = \frac{r - c_T N}{r}$.

1. If $T_u = 0$, then we obtain the equilibrium point, $E_{00} = \left(0, \frac{f_N}{\kappa_N}\right)$. The eigenvalues of the variational matrix at E_{00} are $-\kappa_N$ and $r - \frac{f_N}{\kappa_N} c_T$. Hence E_{00} is locally asymptotically stable if $r < \frac{c_T f_N}{\kappa_N}$.

2. If $T_u = \frac{r - c_T N}{r}$, then $r > \frac{c_T f_N}{\kappa_N}$, then from $(3.43)_2$ we obtain

$$\frac{\eta c_T}{r} N^2 - \left(\eta + \kappa_N\right) N + f_N = 0. \tag{3.44}$$

The discriminant of (3.44) is $\Delta = \left(\eta+\kappa_N\right)^2 - 4\frac{\eta c_T f_N}{r} > \left(\eta - \kappa_N\right)^2$ (since $r > \frac{c_T f_N}{\kappa_N}$). Hence, (3.44) has two real roots $N_\pm = \frac{r\left(\eta + \kappa_N \pm \sqrt{\Delta}\right)}{2\eta c_T}$ which are positive (since their product and sum positive). Moreover, we have $T_{u_\pm} = \frac{r - c_T N_\pm}{r} = \frac{\eta - \kappa_N \mp \sqrt{\Delta}}{2\eta}$ which, by $\Delta > \left(\eta - \kappa_N\right)^2$, implies that $T_{u_+} < 0$ *and* $T_{u_-} > 0$.
This leads to the following virus-free equilibrium point

$$E_0 = \left(T_{u_-}, N_-\right).$$

The eigenvalues of the variational matrix at E_0 are given by the roots of the following characteristic equation

$$z^2 + \left((r+\eta)\,T_{u\_} + \kappa_N\right) z + r\sqrt{\Delta} T_{u\_} = 0. \tag{3.45}$$

Hence, $r > \dfrac{c_T f_N}{\kappa_N}$, then $T_{u\_} > 0$ implying that (3.45) does not have roots with negative real parts.

■

From this theorem, we find that if $r < \dfrac{c_T f_N}{\kappa_N}$, then E_{00} is locally asymptotically stable implying that tumor will be eliminated by NK cells, though it is unclear when NK cells first get evolved in combating tumor growth and progression [140].

Thus, we only focus on the case where $r > \dfrac{c_T f_N}{\kappa_N}$. In this case, tumor growth persists in the presence of actived NK cells. The virus-free model stabilizes at E_0 (see Eq. (3.42)). Based on this analysis, we deduce that (3.41) has a virus-free equilibrium point given by E_0, which is locally asymptotically stable. Furthermore, the virus basic reproductive number of the model at E_0 is given by

$$\mathcal{R}_0 = \frac{\rho\lambda_v\,(r - c_T N_0)}{r\,(c_{TV} N_0 + 1)\,(\omega_v + c_V N_0)}. \tag{3.46}$$

calculated using the next generation method described in [181]. The vector formed by the rates of new infections is given by

$$\mathcal{F} = \begin{bmatrix} \lambda_v T_u V \\ 0 \end{bmatrix}$$

The vector formed by the other transfer rates is

$$\mathcal{W} = \begin{bmatrix} T_i + c_{TV} T_i N \\ -\rho T_i + \omega_v V + c_V V N \end{bmatrix}$$

The next generation matrix is given by $M = FV^{-1}$, where $F = D\mathcal{F}_{E_0} = \begin{bmatrix} 0 & \lambda_v T_{u0} \\ 0 & 0 \end{bmatrix}$ and $W = D\mathcal{W}_{E_0} = \begin{bmatrix} 1 + c_{TV} N_0 & 0 \\ -\rho & \omega_v + c_V N_0 \end{bmatrix}$. We obtain

$$M = \begin{bmatrix} \frac{\rho\lambda_v (r - c_T N_0)}{r(c_{TV} N_0 + 1)(\omega_v + c_V N_0)} & \frac{\lambda_v (r - c_T N_0)}{r(\omega_v + c_V N_0)} \\ 0 & 0 \end{bmatrix}.$$

Thus

$$\mathcal{R}_0 = \frac{\rho\lambda_v\,(r - c_T N_0)}{r\,(c_{TV} N_0 + 1)\,(\omega_v + c_V N_0)}.$$

Due to a complex nature of the local dynamics described by Eq. (3.41), it is not easy to analytically define the total size at equilibrium, as done for the immune-free submodel (see Eqs. (3.14)–(3.16)). Thus, we calculate the sensitivity indices of the virus-free model with respect to the virus basic reproductive number, $\mathcal{R}_0$. We have

$$\Gamma_{N_0}^{\mathcal{R}_0} = -\frac{N_0\left(c_{TV}c_V N_0\left(2r - N_0 c_T\right) + \left(rc_V + \omega_v c_T + r\omega_v c_{TV}\right)\right)}{\left(r - N_0 c_T\right)\left(\omega_v + N_0 c_V\right)\left(N_0 c_{TV} + 1\right)} < 0 \tag{3.47}$$

$$\Gamma_{c_V}^{\mathcal{R}_0} = -\frac{N_0}{N_0 + \omega_v} < 0 \tag{3.48}$$

$$\Gamma_{c_{TV}}^{\mathcal{R}_0} = -\frac{c_{TV}N_0}{1 + c_{TV}N_0} < 0 \tag{3.49}$$

$$\Gamma_{c_T}^{\mathcal{R}_0} = \Gamma_{N_0}^{\mathcal{R}_0}\frac{\eta c_T N_0}{r\sqrt{\Delta}} < 0 \tag{3.50}$$

where $N_0 \equiv s_N$ is the initial number of NK cells within the TME (e.g., at the time of tumor implantation in immunocompetent mice).

3.5 Global sensitivity analysis

In addition to the model sensitivity index derived in Section 3.4.4, we performed a global parameter sensitivity analysis with our immunocompetent model, system (3.1 – 3.4). The purpose of this computational analysis is to identify the model parameters that contribute most significantly to oncolytic virotherapy efficacy in the presence of reactive NK cells. In sampling all the parameters, we determined a plausible range for each parameter (except those readily available from the literature) from half to twice its baseline value in Table 3.1. Then following the method proposed in [182], we generated 1000 samples using Latin hypercube sampling (LHS) to compute the partial rank correlation coefficients (PRCC) and their associated p-values with respect to tumor cell population ($T_{tumor}(t) = T_u(t) + T_i(t)$) at different time points. Note that we use LHS along with PRCC because we are interested in determining which parameters have a monotonic relationship with the total tumor cell population, and also knowing that PRCC can be applied even in nonlinear monotonic relationships [183]. The PRCC varies between -1 and 1, where a negative value indicates the negative correlation between the tumor cell population and a specific parameter, and a positive value denotes the positive correlation between the tumor cell population and the specific parameter. Given 0.01 level of significance, there is a significant relationship between the tumor cell population and the specific parameter if the PRCC value is greater than 0.05 in absolute (i.e., PRCC value $> |0.05|$) and the corresponding p-values is less than 0.01 [20].

For simplicity, we assume that the NK cytotoxicity is the same against tumor cells. Thus, we set the baseline value $c = c_{T_u} = c_{T_i} = 8.68 \times 10^{-10}$ in LHS. Since the early induction of NK cell response within the TME is associated with premature OV clearance [48, 70, 95], while the later response is correlated with OV therapy enhancement [71–73], we computed the PRCCs at early time points (e.g., at $1, 5, 10$ and 15 days post-treatment with OV), and at later time points (e.g., at $30, 50, 70$ and 100 days post-injection with OV). **Fig.** 3.2 depicts the PRCC for each model parameter and at each time point.

Notably, **Fig.** 3.2 **(A)** displays the significant negative correlations between the tumor cell population and NK recruitment rate, ξ_N, environmental carrying capacity for activated NK cells, θ_N, and viral clearance rate, $\gamma = d_V$, at day 1; thus demonstrating the significance of NK cell response to infection in the early stage of OV infection. This observation is consistent with experimental studies indicating that NK cells often proliferate during early stages of viral infection [16]. The negative correlation between tumor and NK recruitment rate implies that a small change in the recruitment rate of NK cells may result in more tumor reduction. While it is conceivable that NK cells can be recruited to the TME by tumor antigens, for our modeling perspective, we assumed that NK cell recruitment is enhanced by lysis, which is immunogenic, of infected cells. This result further highlights the significance of NK antiviral response in combating tumor growth immediately upon viral infection establishment on first day of oncolytic virotherapy. Furthermore, we note that the environmental carrying capacity for activated NK cells, θ_N, is negatively correlated with tumor growth. One possible explanation for this is that if the TME allows for more infiltration of activate NK cells, this will have a negative effect on tumor growth. In a nut shell, in agreement with preclinical models [70, 95], our results **Fig.** 3.2 **(A)** show that antiviral NK cell response may inhibit OV spread and infection, if NK cells are recruited too early in oncolytic virotherapy. Thus, it seems biologically plausible that these three model parameters significantly affect the system outcome in the early stages of tumor growth.

Interestingly, in these early time points from day 10 onwards, we note that the parameter with strongest correlation with tumor cell population is the NK cell recruitment rate, ξ_N. This suggests that NK cell response induced after successful viral infection, which may force tumor to exhibit PAMPS or DAMPS [66, 69, 74], is a key parameter governing the efficacy of oncolytic virotherapy. While this result is somehow intuitive, the interpretation of this result is not obvious because NK cell recruitment rate, ξ_N, is positively correlated with tumor progression (see **Fig.** 3.2 **(A)**). For instance, one might assume that increasing the number of NK cells within the TME automatically increases tumor growth. Actually, the quantitative interpretation of this result is that increasing the NK cells within the TME may lead to tumor evasion, which we hypothesize that is due to rapid NK cell-mediated viral clearance of free viruses or few newly infected tumor cells. Moreover, this result suggests that a small change in the number of reactive NK cells within the TME can have a large impact in OV therapy. This important result further emphasizes the significance of OV-induced NK cell responses and that of designing OV which does not recruit NK cells too quickly so as to maximize the clinical potential of combining OV therapy with NK cell-based therapies. Other parameter that is significant during these early time points is the number of pre-existing NK cells, $s_N \equiv N_0$. The negative correlation between tumor cell population and s_N implies that, before infection, a small change in the number of existing NK cells that can potentially attack the OV or OV infected tumor cells, can result in more antitumoral effect. It is, however, important to note that if the number of pre-existing activated NK cells, s_N, is too large, then it reduces the basic reproductive number, $\mathcal{R}_0$, of the virus below one (see Eq. 3.47). Thus the OV infection cannot propagate within the TME. Of note, this finding highlights the undesirable effects of rapid NK cell-mediated responses which might diminish the efficacy of OV-based treatments in the early stage of viral infection.

Since the later NK cell responses may have a different impact on virotherapy compared to the early NK cell responses, we continued this investigation by performing another sensitivity analysis at $30, 50, 70$ and 100 days post-treatment with OV. **Fig.** 3.2 **(B)** depicts the PRCC for each model

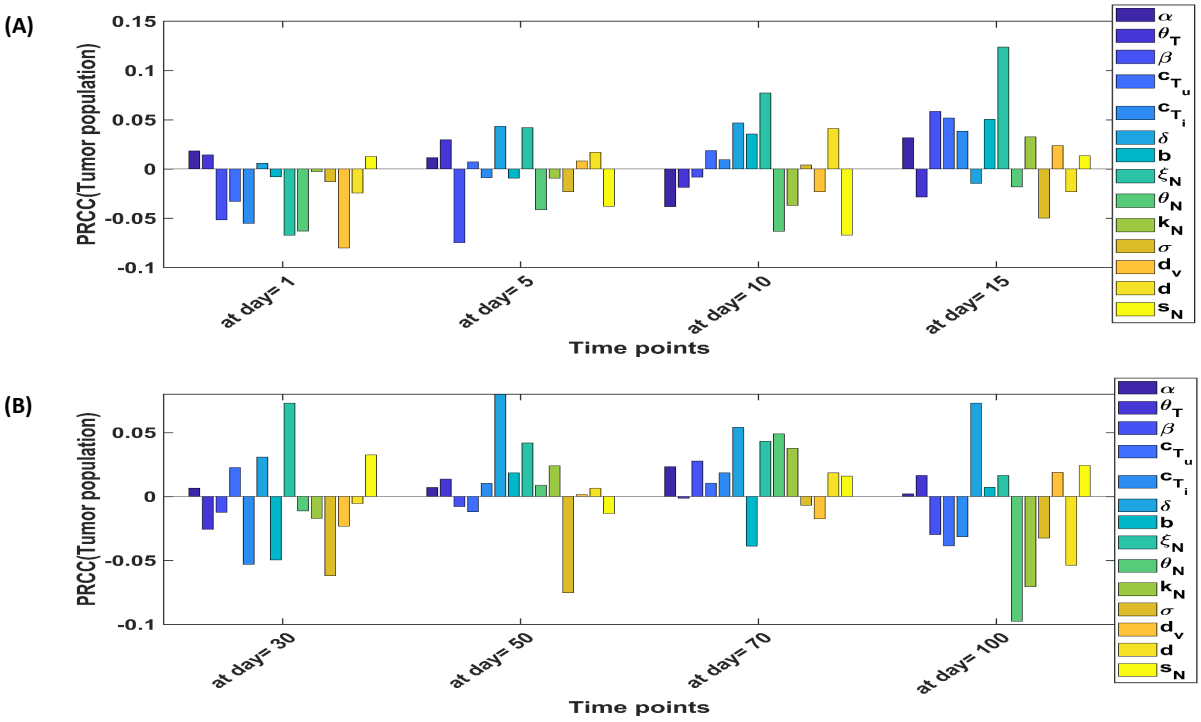

FIG. 3.2. PRCCs results: Panel **(A)** Relative sensitivity of tumor cell population on day $1, 5, 10$ and 15 days post-tumor treatment with OV. Panel **(B)** Relative sensitivity of tumor cell population on day $30, 50, 70$ and 100 days post-tumor treatment with OV. Each bar plot indicates the partial rank correlation coefficient (PRCC) between the tumor cell population and each model parameter.

parameter and at each time point. In contrast to the observation in **Fig.** 3.2 **(A)**, the influence of OV-induced NK cell responses on tumor cell population, governed by the parameter ξ_N, gains less significance in day 50 and 70 in **Fig.** 3.2 **(B)**. This is intriguing because from **Fig.** 3.2 **(A)**, NK cell recruitment rate, ξ_N, becomes increasingly significant towards the simulation end points, suggesting that this parameters is more influential as tumor grows. Furthermore, we notice that in **Fig.** 3.2 **(B)**, ξ_N is more significant at day 100. Note also that at day 100, ξ_N is again negatively correlated with tumor cell population as at day 1 in **Fig.** 3.2 **(A)**, indicating that a small change in the recruitment rate of NK cells at the late time points, may also result in great reduction in tumor cell population. Again, this observation further highlights the significance of late NK antitumoral and antiviral activities in oncolytic virotherapy. The second and the third most significant parameters are the lysis rate of infected tumor cells, δ, and the inactivation rate of NK cells by tumor cells, σ, at day 50. In addition to ξ_N and δ, at day 100, the other significant parameters are the environmental carrying capacity for activated NK cells, θ_N, and the half-saturation constant that maximizes the killing of infected tumor cells by NK cells, k_N.

In summary, our results suggest that the innate immune-related parameters regulating NK activity, are most significant either early or late time-scale of oncolytic virotherapy. This means

that the NK cell responses are most influential at either early (partly because of rapid response of NK cells to viral infections or antigens) or later (partly because of antitumoral ability of NK cells) time points of tumor treatment with OV. Rapid NK cell responses often result in premature clearance of infected cells or free OV within the TME [70, 95], while the later responses are known to enhance oncolytic virotherapy [71–73].

To investigate the antitumoral effects of OV and associated OV-induced NK cell responses, in the following section we examine the transient and long-term dynamics of our models. In particular, we focus on the variations of a few OV-related and NK cell-related parameters (identified as significant through the sensitivity analysis or based on our knowledge of biological systems), to explore different plausible treatment approaches that could yield potent reduction of a tumor or at least slow tumor growth.

3.6 Results

In this section, we outline the parameter choices and the initial conditions used in our numerical simulations. The numerical solutions of the model equations are performed using MATLAB *ode23s*. We also perform a global parameter sensitivity analysis with our immunocompetent model.

Model parameters and initial conditions

Known model parameter values and their ranges were taken from available literature, while unknown parameter ranges were estimated using values that seemed biologically reasonable. The baseline parameters used in the model simulations are given in Table 3.1. Since various mechanisms might lead to NK cell activation and recruitment, we parametrize our model based on the fact that NK cell activation/recruitment is dependent on interactions between the NK cells and infected tumor cells [72] or an ICD of infected cells [67, 162]. Thus, we adopt the activation/recruitment rate for NK cells as $\xi_N = 1 \times 10^{-5}$ day^{-1} [167] as our baseline value, but we shall vary this parameter in the numerical analysis to explore the potential effects of induced NK cell-mediated responses in oncolytic virotherapy. For the other parameters which govern the cytopathicity of OV, we also sweep parameters within their realistic biological ranges. Note that while we fix the values of most of the parameters used in our simulations, small variations in the values of OV or NK cell related parameters allow our model to capture different dynamics of the OV-tumor-NK cell interactions. Furthermore, in this study we do not consider a specific virus as our baseline state variable because we are interested in the OV-induced NK cell-mediated responses in general. We explore a plausible range of recruitment rates to capture the range of likely behavior of slow and fast replicating viruses. Notably, our model captures different aspects of slow replicating viruses, such the recombinant measles virus (MV-I98A-NIS) [184, 185], which may lead to slow recruitment of activated NK cell, and the fast replicating viruses, such the oncolytic herpes simplex virus (HSV) [95], which may lead to rapid recruitment of activated NK cells [95]. It is also known, however, that the same oncolytic virus might replicate differently in different regions [184]. Hence, we do not consider specific virus kinetics in this study, but rather

focus on the ability of OV infection in recruiting activated NK cells. For the sake of parameter estimation, we consider the virus kinetics of oncolytic vesicular stomatitis virus (VSV), which is also a fast replicating virus [75, 186], to estimate the virus lysis rate, δ, and the viral clearance rate, γ. Tumor and NK cell related kinetic parameters are taken from the experimental-mathematical models available in the literature and their sources are provided in Table 3.1. Unless otherwise stated, we assume the following initial conditions: $T_u = 1 \times 10^6$ cells, $T_i = 0$ cells, and $V = 1 \times 10^6$ pfu.

Note that in the simulations, the days ($t = 17$ and $t = 19$) at which OV is injected into the system are derived from the experiments of OV and NK cells in [42]. Even though in the experiments in [42], the NK cells were administered intratumorally following the injection of oncolytic myxoma virus (MYXV), in our simulations we consider the scenario where NK cells exist prior to viral infections, to capture the effect of endogenous NK cell response in oncolytic virotherapy. In all the simulations, we fixed the burst size of the virus to 10^3 pfu, which is in the range considered in [166]. The efficacy of oncolytic virotherapy is often defined by how fast viral infection propagates to inhibit tumor growth beyond a certain size [184]. As discussed in Section 3, when administered to immunocompetent hosts, OV infection can trigger NK cell responses [30, 42, 139], which can either enhance or inhibit therapy success.

The cytopathicity of OV, modeled as a death rate of the infected cells, is generally used as a metric to gauge the success or failure of oncolytic virotherapy [2]. In this simulation, we seek to determine the impact of a virus-induced NK cell response in virotherapy by varying the parameters related to the kill-rate of tumor cells by NK cells, c_T and c_{TV}, and virus-induced NK cell response rate, ξ_N. For simplicity, we assume that NK cells indiscriminately kill uninfected and OV-infected tumor cells at the same rate [72]. Thus, unless otherwise stated, we set $c_T = c_{TV} = 8.68 \times 10^{-10}$ (cells^{-1})(day^{-1}) in all the simulations. The major results from the model's simulations are highlighted as follows.

3.6.1 Without NK cell response

To establish a basic understanding of when and how oncolytic virotherapy can eliminate or control tumor proliferation without NK cell influence, we first compare two treatment scenarios under the assumption that tumor turnover (proliferation and death rates) is dependent on the initial tumor size. In particular, we hypothesize that oncolytic virotherapy is more efficient when applied to large tumors compared to small tumors. To test this hypothesis, we simulate two treatments with different initial tumor sizes: a small tumor size of 1×10^6 cells and large tumor size of 5×10^7 cells, in **Fig.** 3.3. Note that human tumor detection level varies between 10^7 and 10^9 [187]. Since Eftimie and Hamam [188] showed that a tumor of size 5×10^7 can exhibit growth dynamics that approach a stable steady state, we take the tumor to be large if its size is 5×10^7 cells, even though a tumor of such size might not always be clinically detectable.

Consistent with experimental studies in [29], the simulation results depicted in **Fig.** 3.3 **(A)** show that if the initial tumor size is small, oncolytic virotherapy provides little benefit because it takes a long time before infected cells are lysed by OV. For example, OV administered at day 19

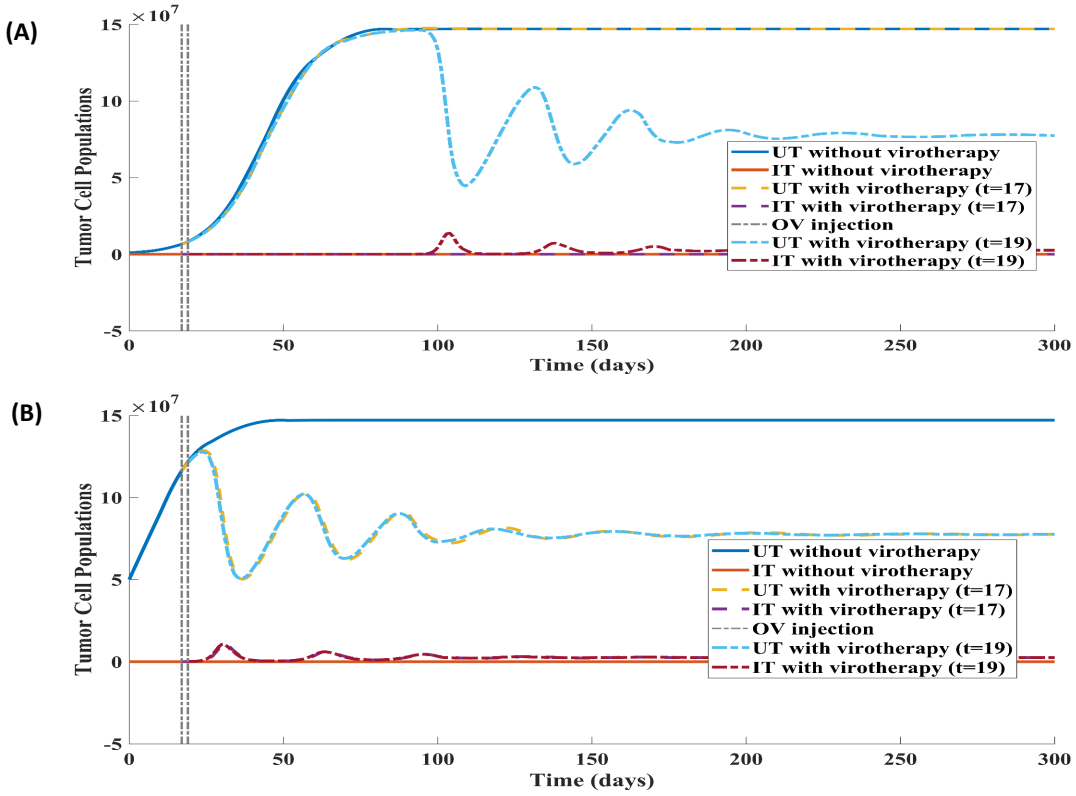

FIG. 3.3. Oncolytic virotherapy can control tumor growth in the absence of NK cell response. Here, we only vary the initial tumor size from 1×10^6 cells to 5×10^7 cells. Panel **(A)** shows simulations of tumor evolution from a small initial composition $T_{u0} = 1 \times 10^6$ cells. Vertical dashed lines indicate different times of virus injection. OV is administered as a single bolus injection of 1×10^6 pfu at days 17 and 19. Panel **(B)** indicates simulations of tumor evolution from a large initial tumor size ($T_{u0} = 5 \times 10^7$ cells). Bold lines indicate tumor progression without virotherapy and dashed lines indicate tumor progression under oncolytic virotherapy. All simulations are done with the respective baseline parameters given in Table 3.1.

greatly cytoreduced the tumor to a minimum population of 7.2054×10^7 cells, compared to OV administered at day 17, which reaches a very large size of 1.4702×10^8. To further investigate this observation, we simulate tumor evolution from a large initial size of 5×10^7 cells, shown in **Fig.** 3.3 **(B)**. The simulation results indicate that if the initial tumor size is large, oncolytic virotherapy provides rapid benefit within a short period of time, on which the tumor reaches a minimum of 4.9463×10^7 cells at day 34 before approaching a steady state population of 7.2390×10^7 cells. Since the amount of viruses injected at each time point is the same, assuming the virus replication kinetics are the same, we can say that the observed differences in tumor reduction can be due to initial tumor sizes. A possible explanation for this finding is that the higher the number of uninfected tumor cells, the higher the chances of OV infections. This in turn leads to higher virus amplification and, potentially more infected cells. Therefore, the higher the number of infected cells, the higher the cytoreduction of uninfected cells. Our finding (in **Fig.** 3.3)

is consistent with other mathematical models of tumor-virus dynamics see [151, 184, 189]. For example see **Fig.** 1 in Zurakowski and Wodarz [189], and experimental studies in [29].

Even though tumor elimination is possible under the current treatment settings, we realize that the dynamics between the tumor cell population and the virus population oscillate to a stable steady state (Coexistence Steady State ($\mathbf{SS_2}$)). Here, under the given parameters, this steady state describes a controlled but persistent infection of tumor cells by OV, which inhibit further tumor cell proliferation. Amplified by viral replication, we note that viral load at this steady state is sufficient to prevent the continued growth of tumor cells. It is at this stage of tumor progression that oncolytic virotherapy can be combined with other treatment modalities, such as immunotherapy [190], to drive the tumor burden to a desirable low level [189] or to extinction.

Comparing treated tumors in **Fig.** 3.3 **(B)** versus the ones in **Fig.** 3.3 **(A)**, we see that tumor cell population declines before reaching their carrying capacity. This suggests that tumors which are initially large can effectively be controlled by OV. In summary, OV is more effective at treating larger tumors, though OV used as a monotherapy cannot drive tumors to extinction. Interestingly, this observation is consistent with experimental models in [29, 38, 191]. In particular, it was shown that while tumors in mice treated with oncolytic measles virus (MV) were much smaller compared with untreated mice (controls) at each time point, tumors were not eliminated by MV infection [191].

3.6.2 With OV-induced NK cell surveillance

Having elucidated virotherapeutic dynamics of our submodel without NK cell response, we now perform a detailed computational analysis to study the advantages of a virus-induced NK cell surveillance. We first explore effects of viral cytopathicity by examining dynamics of weakly cytopathic versus strongly cytopathic OV in the presence of activated NK cells following OV infection of tumors. We find that NK activity enhances oncolytic virotherapy only when a weakly cytopathic OV is administered. We next investigate dynamics of NK cell recruitment in modulation of tumor growth. By comparing low and high recruitment rates of NK cells as well as the variations in NK cell cytotoxic activity, we find that while higher recruitment of NK cells to OV-infected tumor cells may attenuate oncolytic viral propagation, NK cell effector activity is also an essential factor determining the overall OV efficacy. Finally, we numerically assess how an increase or a decrease in the number of activated NK cells correlates with improved tumor growth control, and deduce that decreasing the number of activated NK cells leads to tumor evasion. These main results are further discussed in detail below.

(a) NK cell response augments oncolytic virotherapy only if viral cytopathicity is weak

In addition to understanding how OV influences the growth of tumors of different initial sizes, we are interested in exploring and characterizing virus-induced NK cell response to variations in viral cytopathicity. Here we focus on the following question: *How can we explain the signif-*

icance of viral cytopathicity in the presence of an active NK cell response? Wodarz [2] presents a computational framework for deciding when viral cytopathicity plays an important role for controlling tumor growth with non-replicating and replicating viruses. In particular, they find that using replicating viruses with low viral cytopathicity leads to greater inhibition of tumor growth. Their model predictions are only applicable to studies that have been performed *in vitro* without immune cells, or *in vivo* on immunosuppressed or immunodeficient hosts. However, infection of tumor by OV in immunocompetent hosts can stimulate NK activity [72, 192]. Now, extending this line of argument by Wodarz [2] to immunocompetent hosts, we simulate several scenarios based on different viral cytopathicity levels to investigate whether the presence of NK cells might augment or inhibit OV activity. Simulation results in **Fig.** 3.4 show that, in keeping with the same level of basal activation, virus-induced NK cytotoxicity is more beneficial when tumors are treated with weakly cytopathic viruses (i.e., a weakly cytopathic virus, $\delta = 0.04$ (as considered in [2])) than with strongly cytopathic viruses ($\delta = 0.4$ [2]). Note that, for illustrative purposes, we assumed that the cytopathicity is too weak if $\delta < 0.04$, which induces less than 4% of tumor reduction. For example, in [193], for a strong cytopathic virus, a tumor cell line was infected at a multiplicity of infection (MOI) of 10 to induce 50% cytopathic effects. In general, the cytopathicity of a virus depends on a virus type and MOI used [49, 193, 194]. One explanation is that weakly cytopathic viruses allow for more cells to be infected [2] before NK cell response is triggered. The higher the number of infected cells, the higher the cytoreduction of uninfected cells [2, 195]. More importantly, since NK cells are stimulated by infected tumor cells, then the larger the number of infected tumor cells, the higher the chance of NK cell stimulation via contact-dependent activation [72]. Consequently, there is a strong NK cell response, as depicted in **Fig.** 3.4 **(G)**, which results in more NK cytotoxicity against OV-infected cells (**Fig.** 3.4 **(C)**), free OV (**Fig.** 3.4 **(E)**), and more uninfected tumor cells (**Fig.** 3.4 **(A)**). It is important to note that a weakly cytopathic virus induces a slower OV-induced death rate (small δ) of infected cells, hence the corresponding NK cell response is not rapid (since in our model we assumed that NK cell response is enhanced by OV-infected tumor cell death), allowing for sufficient viral replication and propagation. The explanation for the observations in **Fig.** 3.4 is as follows: a weakly cytopathic virus results in a high viral load (since the antiviral NK cell response is not quickly triggered to clear OV-infected tumor cells), which consequently results in more tumor infection and increased reduction of uninfected tumor cells. On the other hand, if an OV is strongly cytopathic, then there will be a low viral load (since the antiviral NK cell response is rapidly triggered to clear OV-infected tumor cells), which consequently results in less tumor infection and a small reduction of uninfected tumor cells. These observations, interestingly, are consistent with previous experimental reports which indicate that the local interactions between the NK cells and OV-infected tumor cells resulted in more tumor cell death compared to virus infection alone [42, 72, 73] (e.g., see Fig. 3 and Fig. 4E in [72]). This suggest that NK cell response augments OV oncolysis.

We should emphasize that the activity of the strongly cytopathic virus results in fewer total infected cells. The reason for this is that the strongly cytopathic virus replicates quickly upon productive infection, which, in theory, reduces the life span of an infected cell. In other words, the shorter the life span of an infected cell, the lower the probability that it will be encountered by NK cells, reducing NK cells stimulation and recruitment. This, in turn, leads to more evasion of uninfected cells from NK cell surveillance (**Fig.** 3.4 **(B)**). One possible explanation is that rapid killing of infected cells induces a rapid NK cell response (especially NK response following OV

injected at day 19) as indicated in **Fig.** 3.4 **(H)**, and consequent tumor escape (**Figs.** 3.4 **(B)** and **(D)**) and virus persistence (**Fig.** 3.4 **(F)**). Treatment outcome depends on the different NK cell response induced by either a strong or weak viral cytopathicity.

In both **Figs.** 3.4 **(G)** and **(H)** we observe an initial growth phase of the NK cell population, followed by a decline. Note that without viral infection, a typical simulation of the NK cell response would be characterized by an initial growth phase which is followed by a retardation, after which the NK cell population reaches a relatively low stable equilibrium [5, 132] (which may correspond to a memory phase [94, 140, 196]). Based on this observation, we speculate that the long-term productive infection of tumor cells is maintained by the NK cell memory response at a later stage of the antiviral response (see **Figs.** 3.4 **(C)** and **(G)**). A future model that explicitly includes a memory population might be useful to check this hypothesis. Upon viral infection, the NK cell population expands, the extent of which depends on how weakly or strongly cytopathic the viruses are at lysing infected cells, in response to viral antigenic stimulation by infected tumor cells. It is also very important to note that if the number of effective pre-existing NK cells (s_N) is too large, then the infection will not be established [2]. In the above simulations, we assume that the pre-existing NK cell response is not sufficiently strong to inhibit the virus infection. Furthermore, it is worth noting that even though the pre-existing NK cells may remove infected cells prior to sufficient viral amplification, the weakly cytopathic viruses strongly induce activation and recruitment of NK cells, but at a slow recruitment rate (**Fig.** 3.4 **(G)**). Taken together, in accordance with previous mathematical models with inclusion of NK cell surveillance [71, 75, 132], the simulation results presented here demonstrate how useful the mathematical model is in explaining and characterizing the NK cell responses to variations in oncolytic viral cytopathicity. Notably, these findings demonstrate that NK activity could further enhance therapeutic potential of OV, and highlight the importance of comprehending a specific NK cell response which may help to maximize therapeutic benefits of OV. Of note, we observe that NK cell response induced by a weakly cytopathic OV leads to tumor elimination (see **Figs.** 3.4 **(A)** and **(C)**), whereas the NK cell response induced by a strongly cytopathic OV only the response following second injection (at day 19) is able to lead tumor eradication (see **Figs.** 3.4 **(B)** and **(D)**). It is interesting to note that these findings are in line with *in vivo* preclinical models. The *in vivo* models have shown that the administration of OV as a monotherapy rarely results in complete tumor regression of established tumors compared to combinatorial treatments [81, 82, 190, 197–199].

(b) Recruitment of NK cells modulates tumor growth

Next, we examine the impact of the NK cell antitumor effect induced by viral infections. So far we have considered viral cytopathicity as a potential mechanism by which NK cells are recruited into the TME. OV alone can, however, recruit NK cells to the TME [72, 95, 130]. To this end, various oncolytic vectors that are engineered to express immunostimulatory genes or cytokines, such as TRAIL and interleukin-12 (IL-12) [49, 200], generate robust antitumor specific NK cell responses. These cytokines or genes, however, differ greatly in their immunostimulatory potential. Some of these cytokine-expressing OV are known to recruit NK cells strongly (e.g. IL-12 [201]) while others do not (e.g., TRAIL [30, 49]). The precise mechanisms mediating NK cell recruitment to tumor sites are still poorly understood [202]. Increasing evidence from *in vivo* studies reveals that

higher recruitment of activated NK cells to the TME yielded a therapeutic effect in virotherapy [42, 203–207]. Moreover, in all these studies, it was shown that the depletion of NK cells within the TME diminished the therapeutic outcome of OV treatment. On the other hand, various experimental studies demonstrated that the depletion of activated NK cells in the TME improved oncolytic virotherapy [71, 76, 95]. Given these opposite experimental findings, it is imperative that we improve our understanding of the complex role of NK cells in oncolytic virotherapy. In the set of numerical simulations, we explore the impact of the strength of the virus-mediated NK cell responses in oncolytic virotherapy. To do so, we simulate two treatment scenarios to determine whether variations in NK cell recruitment (or proliferation) rate (ξ_N) could enhance overall oncolytic virotherapy. In the first case, we simulate a treatment scenario where there is a high recruitment of activated NK cells which are weakly cytotoxic against tumor cells (here we vary ξ_N from a baseline value in Table 3.1 to $\xi_N = 1.44 \times 10^{-4}$ and $c = c_T = c_{TV} = 8.68 \times 10^{-12}$(weaker NK cytotoxicity). In the second case, we simulate a treatment scenario where there is a high recruitment of activated NK cells which are strongly cytotoxic against tumor cells (here similarly, we vary ξ_N from the baseline value in Table 3.1 to $\xi_N = 1.44 \times 10^{-4}$ and $c = c_T = c_{TV} = 1 \times 10^{-10}$(stronger NK cytotoxicity). We should emphasize that we only vary these two parameters (ξ_N, c) because increasing evidence indicates that variations in NK cell recruitment as well as NK cytotoxicity may potentially illustrate how host immune system ally with OV against tumors [72, 95, 206, 208, 209]. Moreover, we also emphasize that the strength of the NK cell response does not only depend on NK cell recruitment (ξ_N), but also on the number of pre-existing NK cells which are ready to combat the infection upon the entry of the virus into the body (given by s_N/d) and the NK cell killing rate (given by c). Note also that if the number of pre-existing active NK cells is too high, the viral infection will not be established [132]. To account for this, in the simulations we fixed the number of NK cells that can potentially attack the virus before infection to 3.2×10^3 as in [5], and vary NK cell recruitment and effector rates as demonstrated in **Fig.** 3.5.

Interestingly, we find that the recruitment rate of NK cells and the rate at which uninfected and infected tumor cells are killed by activated NK cells strongly influence the final treatment outcome (**Fig.** 3.5). The variations of these parameters lead, as expected, to virus clearance and complete eradication of OV-infected tumor cell population. In the first case (weakly cytotoxic NK cells), there is a fast reduction of the uninfected tumor cell population, which is ultimately followed by rapid tumor growth rebound, indicating an ineffective virus-NK cell treatment (see **Figs.** 3.5 **(A)** and **(C)**). On the other hand, in the second case (strongly cytotoxic NK cells), the tumor vanishes or at least remains small upon interaction with OV and strongly cytolytic NK cells (see **Figs.** 3.5 **(B)** and **(D)**). Note that in **Fig.** 3.5 **(B)**, the uninfected tumor cell population declines sharply following viral infection and rapid killing by NK cells. However, since NK cells are stimulated by infected tumor cells, which are also susceptible to NK cell-mediated killing, there is also a swift decline in the infected tumor cell population (**Fig.** 3.5 **(D)**). Consequently, a sharp decline in the infected tumor cell population results in a subsequent drop in the NK cell population (**Fig.** 3.5 **(H)**), allowing the uninfected tumor cell population to rapidly rebound from the NK cell-mediated dormant state to carrying capacity. In the simulations, we also note that the number of weakly reactive NK cells (**Fig.** 3.5 **(G)**) reach higher peaks after the infection, but quickly declines compared with the strongly reactive NK cells with more pronounced tumor control dynamics (**Fig.** 3.5 **(H)**). This is partly because tumor evasion is depend on the virotherapy efficacy with which NK cells surge for the infection. Thus, weaker NK cell responses

can correlate with poor NK cell antitumor surveillance compared with the stronger NK cell responses. We should emphasize that the recruitment of NK cells into the TME depends on the activation of NK cells by infected tumor cells. When the NK cell activation is too fast (i.e., leading to high NK cell recruitment), the NK cell population will also decay rapidly [141], which in turn will lead to impaired NK cell-mediated killings. Together, these simulations indicate that not only high NK cell recruitment can modulate treatment efficacy, but also a small increase in the NK cell effector activity can surprisingly influence treatment success.

In a nut shell, these results suggest that while recruiting NK cells at higher rate is important for augmenting virotherapy [206, 209], it is also important to enhance the NK cell effector activity (e.g., the blockade of inhibitory NK receptor TIGIT [72]) to promote further cytoreduction of tumor cells. Surprisingly, this high NK cell recruitment within the TME leads to tumor dormancy or eradication (**Fig.** 3.5 **(B)** and **(D)**) or, perhaps as expected, maintainable lower tumor burden [210]. It is important to note that too early recruitment of activated NK cells may diminish oncolytic virotherapy efficacy.

(c) The depletion of the number of activated NK cells leads to increased overall tumor burden

Having illustrated how the success of oncolytic virotherapy correlates with NK cell infiltration following OV infection, it is essential to assess the relative killing of tumor cells by NK cells. In particular, we seek to answer the following question: "*Does OV infection of tumor lead to the preferential NK-mediated clearance of virally infected tumor cells compared to uninfected tumor cells?*" [105]. **Fig.** 3.6 displays the comparative analysis of NK activities on tumor cell dynamics under treatment with OV. NK cell antiviral activities, if invoked too early, may be detrimental to OV propagation and OV-infected tumor cells, while the later activities following OV infection of tumors may enhance NK cell-mediated antitumor surveillance.

Notably, as illustrate in **Fig.** 3.6 **(B)**, a large number of activated NK cells is able to control, or perhaps initiate clearance of, OV-infected tumor cells, compared to uninfected tumor cells **Fig.** 3.6 **(A)**. Most importantly, we realize that a decrease in the number of activated NK cells leads to an increase in tumor progression (**Fig.** 3.6 **(A)**). This simulation suggests that the effect of NK cell surveillance does not only depend on the number of pre-existing activated NK cells within the TME, but also on the subsequent recruitment of NK cells necessary to mount sufficient antitumoral activity over the entire treatment period. In particular, our findings in **Fig.** 3.6 illustrate that if activated NK cells are depleted before the end of the treatment period, then tumor may uncontrollably proliferate to a higher steady state. In general, we note that on longer time-scale, NK cell responses do not provide significant influence on tumor treatment outcome. Thus, we suggest that other immune effector cells, such as activated $CD8^+$ T cells [5, 75, 164] or cytokine-induced killer (CIK) cells [211], should be incorporated into the system to provide a longer-term immune responses that can augment oncolytic virotherapy. Taken collectively, our findings from both **Fig.** 3.5 and **Fig.** 3.6 suggest that NK activity is extremely important in determining the final outcome of OV therapy, since NK cells may augment an antitumoral activity of OV infection.

3.7 Discussion and conclusion

In this chapter, we set out to answer the question on how NK cell recruitment to the TME affects oncolytic virotherapy. NK cells play a major role in eliminating viral infections, and are known to indiscriminately attack both uninfected and OV-infected tumor cells rapidly [13, 72, 143]. This rapid clearance, however, may halt the desired spread of OV and hence diminish overall oncolytic virotherapeutic efficacy. To this end, we developed a mathematical model describing the interactions between uninfected and OV-infected tumor cells, OV, and NK cell responses.

First, we performed a global sensitivity analyses to assess which parameters are most likely to significantly impact tumor cell response to oncolytic virotherapy administered in the presence of reactive NK cells. Intriguingly, our sensitivity analysis results demonstrated that the recruitment of NK cells by OV is more important during the intermediate phase of the viral infection. It is noteworthy that although our model includes the prior existence of reactive NK cells within the TME, which may possibly clear free viral particles, the OV-induced NK cell responses (governed by the parameter ξ_N) are less influential during the early or late stages of OV infection. This finding has two important clinical implications: (a) during early time of OV infection, NK cell response should be minimized in order to allow for the virus to replicate sufficiently [58, 71, 125, 128], (b) recruiting NK cells at a very late stage of viral infection may not be effective at combating tumor burden. This result is consistent with preclinical and clinical studies which show that there is a need for time-optimization of NK-based treatments to achieve targeted therapeutic outcomes [13, 128].

From the model simulations, and in accordance with previous models [75], we find that the efficacy of oncolytic virotherapy depends on the initial tumor size and the tumor size when OV is injected into the system. As demonstrated in **Fig.** 3.3, it is important to note that a small tumor with the same OV treatment at different times responds differently. Moreover, in addition to its dependence on the initial tumor size (T_{u0}), we showed that the virotherapeutic efficacy also depends on two key aspects: (a) the rate of tumor cell death induced by oncolytic viruses (c), and (b) NK cell recruitment (or proliferation) rate in response to viral infections (ξ_N). Increasing the strength of viral cytopathicity should increase the lysis rate at which tumor cells are destroyed [2], and thereby minimize the likelihood of tumor evasion and possibly increase the chances of achieving complete tumor elimination with OV. It important to note that tumors often develop multiple strategies to evade destruction by various antitumor therapies [5, 7, 212], including oncolytic virotherapy [213]. As demonstrated by our simulations (**Fig.** 3.5), increasing viral cytopathicity also increases induction of antiviral NK cell response, which may, if induced prematurely to sufficient viral replication within infected cells, may halt further viral spread and infection. Most intriguingly, we find that the weakly cytopathic OV (i.e., OV that replicates slowly upon infection) recruit NK cells at a lower rate, and thereby allow sufficient time for viral replication and propagation. That means, the slower the lysis rate of OV-infected tumor cells, the lower the number of NK cells within the TME since NK cell recruitment is enhanced by immunogenic cell death (ICD) of infected tumor cells [67, 69, 162, 177]. If, on the other hand, an OV is strongly cytopathic (i.e., OV replicates and destroys infected tumor cells rapidly), then there will be a high influx of NK cells into the TME due to the presence of damage associated molecular patterns (DAMPs) or pathogen-associated molecular patterns (PAMPs) released during ICD of

OV-infected tumor cells [27, 66]. Previously, it has been shown that for replication-competent viruses, oncolytic virotherapy provides more antitumor effect if the virus is weakly cytopathic compared to strongly cytopathic virus [2], consistent with our simulations (**Fig.** 3.4). This implies that a weakly cytopathic OV leads to a higher virus amplification, which may potentially result in more infected tumor cells. Hence this allows OV to destroy tumor cells before NK cells are triggered to clear both OV and infected tumor cells, as well as uninfected tumor cells.

Since NK cells indiscriminately kill both uninfected and OV-infected tumor cells, they may decrease therapeutic effect of OV. Hence, an increase in the number of activated NK cell within the TME may actually exert a negative effect. In particular, we were interested in quantifying the impact of small variations in NK cell-mediated cytotoxicity (c) and the recruitment rate (ξ_N) induced by OV. In **Fig.** 3.5, we investigated whether immunovirotherapy with increased active NK cells could result in higher tumor cell lysis than oncolytic virotherapy alone (illustrated in **Fig.** 3.3). Critically, we find that elimination of tumor cells by OV, albeit incompletely, can be effectively achieved by recruiting activated NK cells at higher rates (compare **Fig.** 3.5 **(A)** to **Fig.** 3.5 **(B)** and compare **Fig.** 3.5 **(C)** to **Fig.** 3.5 **(D)**). Surprisingly, the relative impact of increasing the number of activated NK cells only leads to transient immune-mediated dormancy (**Fig.** 3.5 **(B)**), suggesting the need for inclusion of other long-term effector cells (e.g., $CD8^+$ T cells [75, 190]) in oncolytic virotherapy. To induce their cytolytic effect, NK cells expressing natural cytotoxicity receptors (such as NKp30, NKp44, and NKp46 [13, 73, 95]) need to interact with tumor cells expressing respective ligands. Normally, this interaction leads to binding of NK cell receptors with their respective ligands on tumor cells which then results in death of tumor cells [73, 93, 96, 128]. Thus, tumor evasion (as illustrated in **Fig.** 3.5) may be attributed to insufficient binding of NK cell receptors with their respective ligands on tumor cells.

Lastly, OV-induced NK cell antiviral responses provide potent killing of infected tumor cells compared to NK cell antitumoral responses (**Fig.** 3.6 **(B)**). Hence, a comparative analysis of treatment effectiveness of OV-induced NK cell and tumor-present induced NK activities should always be carefully examined before OV-NK cell therapy is applied in a clinical setting. Importantly, our numerical simulation in **Fig.** 3.6 **(A)** clearly shows that a decrease in the number of activated NK cells before the end of the OV treatment leads to tumor evasion. Overall, our simulations suggest that NK response to stimulation by OV is more efficient at reducing the infected tumor cell population than is an NK response stimulated by the presence of tumor alone.

Despite the model's utility in explaining how OV-induced NK cell responses can improve virotherapy, we acknowledge there are some limitations that may obscure the model predictions. Firstly, note that although the model simulations were not fitted to any experimental data, most of the parameter estimates used were taken from previous models that considered similar cell dynamics proposed in this study. It is therefore important to note that the variability and uncertainty in the model parameters does not limit the mathematical and computational analysis of this study, and the resulting analyses provide a simple framework for further research into combined OV-NK cell-based virotherapies. Furthermore, OV injection times considered in this model, though assumed from experiments in [42], may not be the optimal times that could yield optimal timing of NK cell recruitment. Thus, optimizing the time for OV-induced NK cell responses is needed to balance unwanted early OV clearance or premature removal of OV-infected tumor cells and the required later antitumoral NK cell responses. Despite these limitations, our mathematical

model provides useful insights into the dynamics of NK cells that may enhance the activity of OV in immunocompetent hosts. Importantly, our results suggest that although OV-induced NK cell responses play a vital role in immune surveillance (see **Fig.** 3.5), NK cells alone cannot lead to long-term tumor control, and that an additional immune surveillance arm (such as activated $CD8^+$ T cells [5, 75, 164]) is need to account for the long-term memory cell response (a key feature of adaptive immune cells such T cells and B cells [140]). We need to emphasize that while the model considered in this study is very simple, at least in its generic form, more complex dynamic interactions between OV, the tumor cells, NK cells and other immune effector cells (e.g., $CD8^+$ T cells) within the TME, will be considered in future research. Also, optimal control approaches will be devised to determine the optimal therapeutic times for OV-induced NK cell responses that provide maximal benefits in oncolytic virotherapy.

Collectively, our results illustrate the significance of understanding viral cytopathicity in the regulation of NK cell responses during oncolytic virotherapy. Furthermore, our results show not only the potential of the mathematical modeling approach for oncolytic therapy, but also provide strategies and insights into the specific mechanisms by which OV-induced NK cell responses could augment antitumoral activities of OV. These findings should foster future research aiming to enhance the understanding of interactions between OV, tumor, and OV-induced NK cell responses. This understanding may help to design and improve the NK cell-based therapies for augmenting efficient oncolytic viruses.

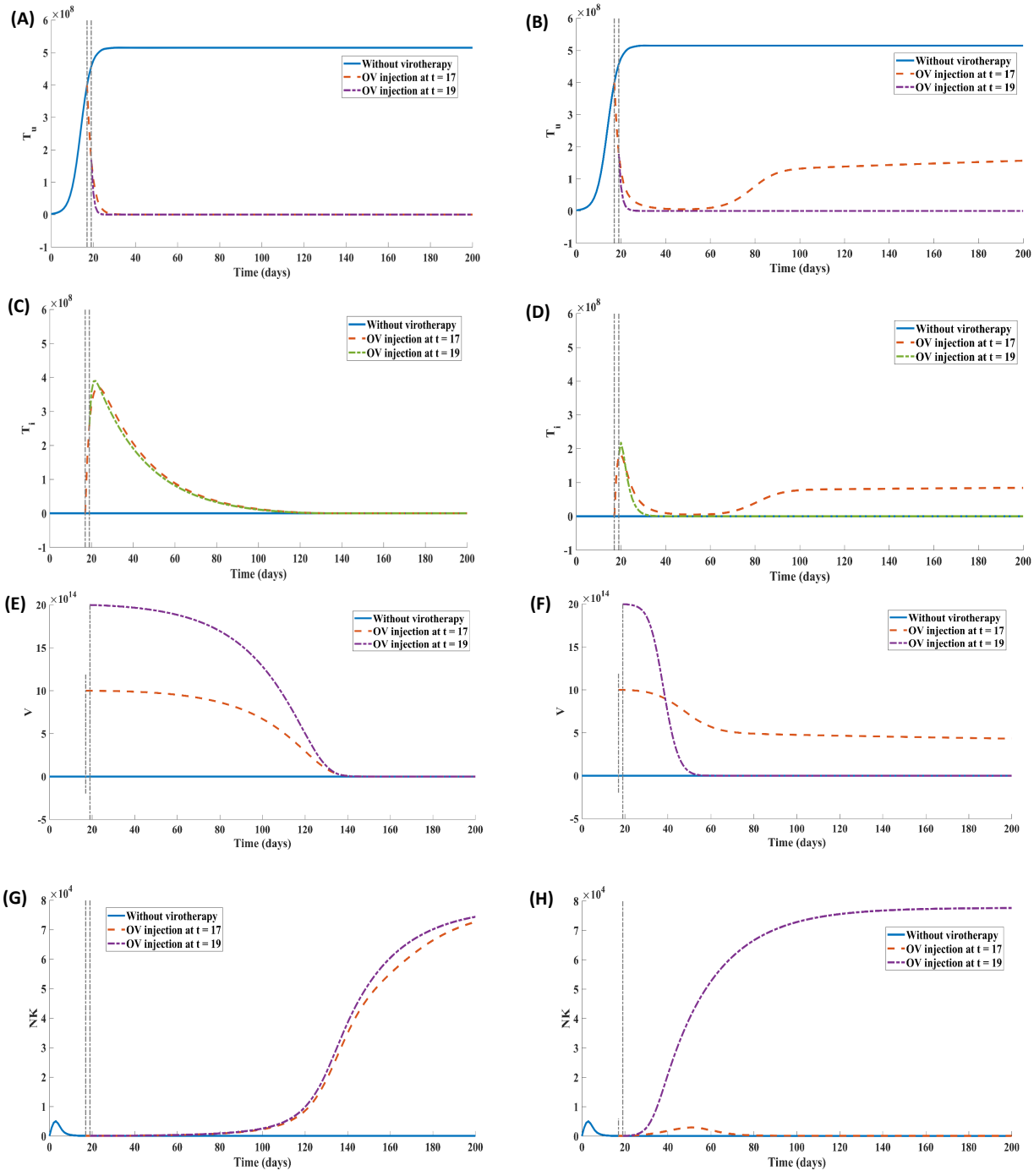

FIG. 3.4. Comparison of the impact of different manifestations of the viral cytopathicity. For simplicity, we are assuming the activation rate of NK cells ($\xi_N = 5 \times 10^{-6}$) is the same for all viruses. The left panel graphs show the number of cell or virus populations over time under the treatment with weakly cytopathic virus, and the right panel graphs indicate the treatment dynamics with strongly cytopathic viruses. The different lines represents three different instances of the model simulation with the same parameter combination. Vertical dashed lines indicate different times of virus injection. OV is administered as a single bolus injection of 1×10^6 pfu at days 17 and 19. These plots demonstrate that NK cytotoxicity synergistically enhanced oncolytic virotherapy when the weakly cytopathic viruses are used. For the weakly cytopathic virus, $\delta = 0.04$ (as in [2]). For the strongly cytopahtic virus, $\delta = 0.4$ (as in [2]). Other parameters are kept at their baseline values given in Table 3.1

.

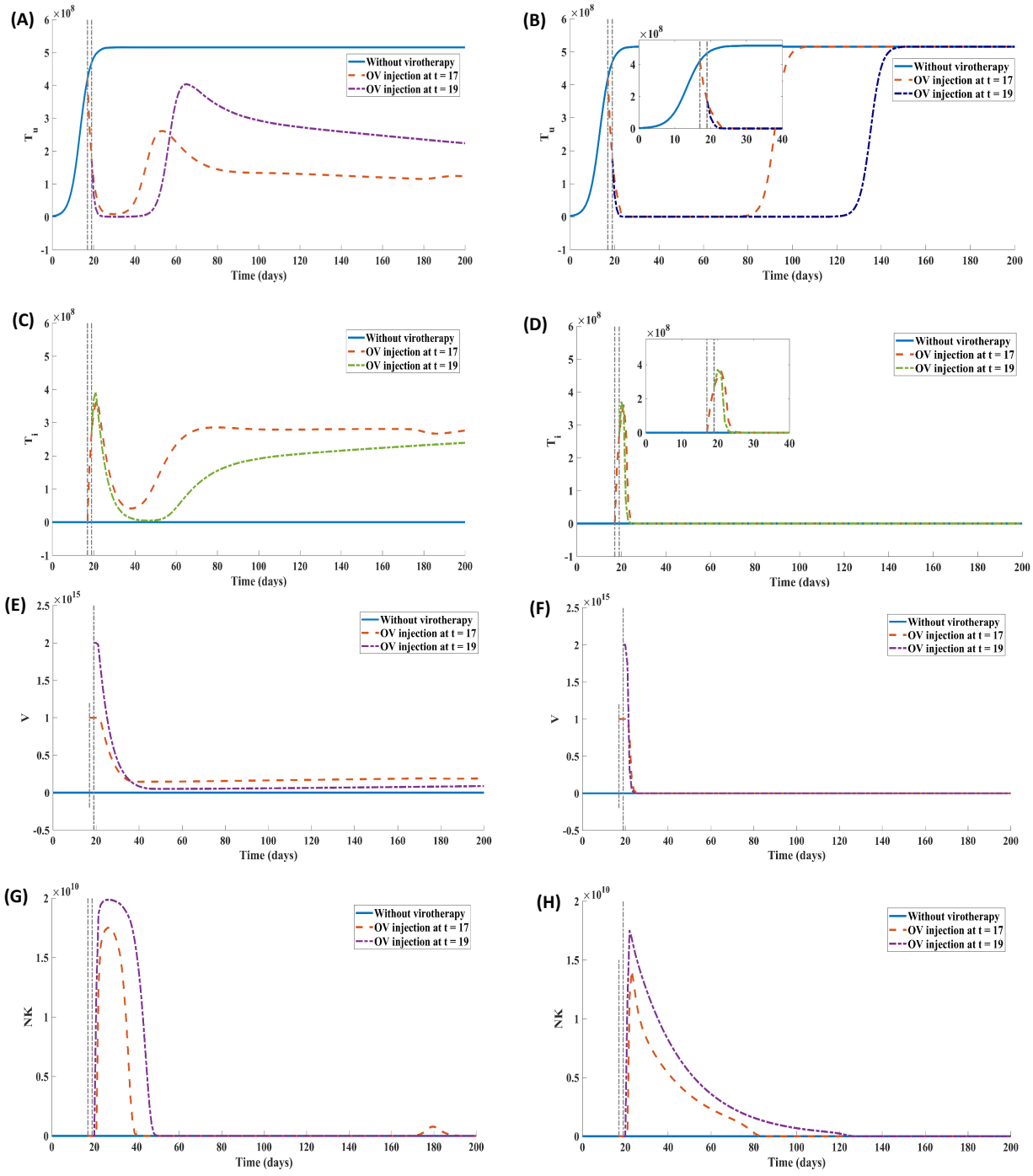

FIG. 3.5. NK cell response is an important determining factor in the success of oncolytic virotherapy. Left panel: (**(A)**,**(C)**,**(E)** and **(G)**) Simulations of our model with increased NK cell stimulation rate, but weakly cytotoxic effector activity. Right panel: (**(B)**,**(D)**,**(F)** and **(H)**) Simulations of our model with increased NK cell stimulation rate, but strongly cytotoxic effector activity. In **(B)** and **(D)**, an inset with a magnified area that shows early evolution of tumor cells is also shown. Parameters were chosen as follows: $\xi_N = 1.44 \times 10^{-4}$, $c = 8.68 \times 10^{-12}$(weak NK cytotoxicity), $c = 1 \times 10^{-10}$(stronger NK cytotoxicity). Other parameters are kept at their baseline values given in Table 3.1.

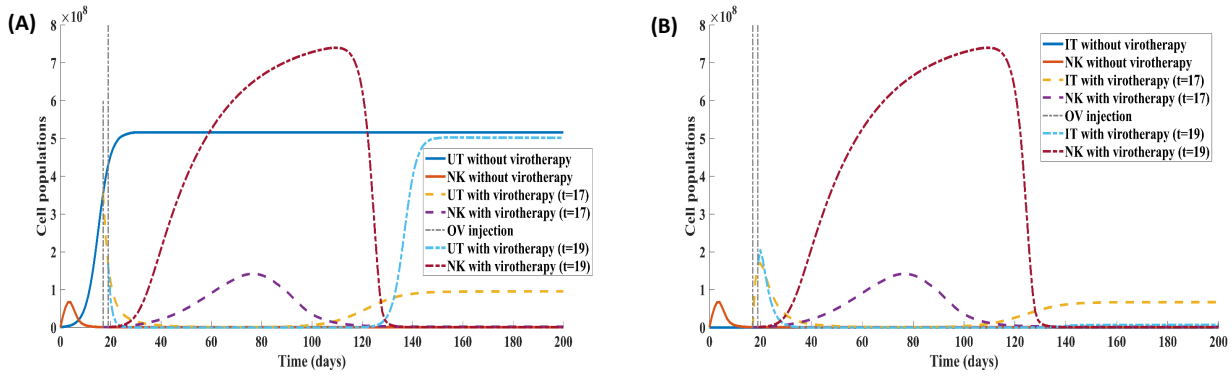

FIG. 3.6. Comparison of the impact of NK activity on tumor cell growth. Panel **(A)** shows that a decrease in the number of activated NK cells leads to an increase in tumor burden. Panel **(B)** indicates that a large number of activated NK cells has control over a virally infected tumor. These plots highlight the importance of relative contributions of NK-cell mediated antiviral and tumor clearance. Parameters were chosen as follows: $s_N = 1 \times 10^6$, $\xi_N = 1.44 \times 10^{-4}$, $c = 8.68 \times 10^{-12}$(weaker NK cytotoxicity), $c = 1 \times 10^{-10}$(stronger NK cytotoxicity). Other parameters are kept at their baseline values given in Table 3.1.

Chapter 4

Conclusions

In the present work, we have devised and formulated a novel mathematical model that describes the local dynamic interactions between tumor cells, oncolytic viruses (OV) and natural killer (NK) cells within the tumor microenvironment (TME). Initially, NK cells are assumed to be present within the TME, even when there are no tumor cells or OV. First, we enhanced our understanding of tumor-OV interactions when viral cytopathicity is varied from low to high. We then introduced an increasing influx of NK cells (due to immunogenic cell death of infected tumor cells) to the TME, to enable us to explore the possible effects of OV-induced NK cell response in terms of impediment or augmentation of oncolytic virotherapy. A complete overview of the major results of the model presented in Chapter 3 is as follows:

(a) Modeling tumor-OV interactions, in the absence of active NK cell response, demonstrated that the success of oncolytic virotherapy depends heavily on the initial tumor size and the tumor size when OV is administered into the system. Notably, it was shown Chapter 3 that small tumors (with different initial observable sizes) treated with the same OV inoculum respond differently. In accordance with previous mathematical models [75], we found that OV used as a monotherapy cannot drive tumor to extinction, but rather, it could bring tumor burden to some low level stable steady state.

(b) The role of NK cells, acting as immune surveillance effector cells against tumors, have been demonstrated in several preclinical and clinical studies. In particular, an increasing number of studies demonstrates that NK cells effectively attack tumors with low antigenicity (e.g., those with downregulated major histocompatibility complex (MHC) class I molecules) [5, 8–11, 111], and free OV and OV-infected tumors. The induction of NK cells by OV infection, within the TME, is often correlated with favorable treatment outcomes [26, 214]. Consistent with previous mathematical models [75, 166], our simulations in Chapter 3 have demonstrated that the time at which OV-induced NK cell antiviral response to OV infection is triggered can lead to detrimental results in oncolytic virotherapy if NK cells are induced to early post tumor treatment with OV. Taken together, our results suggest that NK cell recruitment to the TME must take place neither too early nor too late in the course of OV infection

to achieve therapeutic success with OV. Through both sensitivity analysis and numerical simulations, we showed that NK cell responses are can make most influence on tumor growth at either early (possibly leading to tumor escape because of rapid response of NK cells to viral infections or antigens) or later (partly because of antitumoral ability of NK cells) stages of oncolytic virotherapy. Furthermore, our model also predicts that:

(i) an NK cell response augments oncolytic virotherapy only if viral cytopathicity is weak;

(ii) the recruitment of NK cells modulates tumor growth; and

(iii) the depletion of activated NK cells within the TME enhances the probability of tumor escape in oncolytic virotherapy.

(c) Despite the contrary viewpoints that the induction of NK cells within the TME can either hinder or complement OV antitumor efficacy, our numerical simulations suggest that OV-induced NK cell response play a critical role in attaining enhanced therapeutic success with oncolytic virotherapy. Thus, our results highlights the importance of understanding and uncovering possible mechanisms that govern OV-induced NK-mediated immunity for OV-infected tumor cells, and the need for understanding of attenuated or enhanced NK cell recruitment in oncolytic virotherapy.

Limitations and future work: Despite the model's utility in explaining how OV-induced NK cell responses can improve virotherapy, we acknowledge there are some limitations that may obscure the model predictions. Firstly, note that although the model simulations were not fitted to any experimental data, most of the parameter estimates used were taken from previous models that considered similar cell dynamics proposed in this study. It is therefore important to note that the variability and uncertainty in the model parameters does not limit the mathematical and computational analysis of this study, and the resulting analyses provide a simple framework for further research into combined OV-NK cell-based virotherapies. Furthermore, OV injection times considered in this model, though assumed from experiments in [42], may not be the optimal times that could yield optimal timing of NK cell recruitment. Thus, optimizing the time for OV-induced NK cell responses is needed to balance unwanted early OV clearance or premature removal of OV-infected tumor cells and the required later antitumoral NK cell responses. Despite these limitations, our mathematical model provides useful insights into the dynamics of NK cells that may enhance the activity of OV in immunocompetent hosts. Importantly, our results suggest that although OV-induced NK cell responses play a vital role in immune surveillance (see **Fig. 5** in Chapter 3), NK cells alone cannot lead to long-term tumor control, and that an additional immune surveillance arm (such as activated $CD8^+$ T cells [5, 75, 164]) is need to account for the long-term memory cell response (a key feature of adaptive immune cells such T cells and B cells [140]). We need to emphasize that while the model considered in this study is very simple, at least in its generic form, more complex dynamic interactions between OV, the tumor cells, NK cells and other immune effector cells (e.g., $CD8^+$ T cells) within the TME, will be considered in future research. Also, optimal control approaches will be devised to determine the optimal therapeutic times for OV-induced NK cell responses that provide maximal benefits in oncolytic virotherapy.

Collectively, our findings demonstrate that treating tumors with OV is important, not only to cytoreduce tumor burden, but also to recruit stronger NK cell response that is necessary for eradicating tumors or at least control tumor growth. Moreover, our mathematical modeling framework supports the combinatorial therapies between OV and NK cells that are aimed at improving treatment approaches whether OV and NK cells work together to eliminate tumor growth and progression since there is currently an increasing need to examine NK cell responses to oncolytic virotherapy.

Bibliography

[1] Lupo KB, Matosevic S. Natural killer cells as allogeneic effectors in adoptive cancer immunotherapy. Cancers. 2019;11(6):769.

[2] Wodarz D. Computational modeling approaches to studying the dynamics of oncolytic viruses. Mathematical Biosciences and Engineering. 2013;10(3):939–957.

[3] Ventola CL. Cancer immunotherapy, part 3: challenges and future trends. Pharmacy and Therapeutics. 2017;42(8):514.

[4] Waldhauer I, Steinle A. NK cells and cancer immunosurveillance. Oncogene. 2008;27(45):5932–5943.

[5] Mahasa KJ, Ouifki R, Eladdadi A, de Pillis L. Mathematical model of tumor–immune surveillance. Journal of Theoretical Biology. 2016;404:312–330.

[6] Tham M, Abastado JP. Escape of tumor immune surveillance and metastasis. Drug Discovery Today: Disease Models. 2011;8(2):81–86.

[7] Iannello A, Thompson TW, Ardolino M, Marcus A, Raulet DH. Immunosurveillance and immunotherapy of tumors by innate immune cells. Current opinion in immunology. 2016;38:52–58.

[8] Bubenik J. MHC class I down regulation, tumour escape from immune surveillance and design of therapeutic strategies. Folia Biology (Praha). 2005;51(1):1–2.

[9] Bubenik J. MHC class I down-regulation: tumour escape from immune surveillance?(review). International journal of oncology. 2004;25(2):487–491.

[10] Haworth KB, Leddon JL, Chen C, Horwitz EM, Mackall CL, Cripe TP. Going back to class I: MHC and immunotherapies for childhood cancer. Pediatric blood and cancer. 2015;62(4):571–576.

[11] Siddle HV, Kreiss A, Tovar C, Yuen CK, Cheng Y, Belov K, et al. Reversible epigenetic down-regulation of MHC molecules by devil facial tumour disease illustrates immune escape by a contagious cancer. Proceedings of the National Academy of Sciences. 2013;110(13):5103–5108.

[12] Screpanti V, Wallin RP, Ljunggren HG, Grandien A. A central role for death receptor-mediated apoptosis in the rejection of tumors by NK cells. The Journal of Immunology. 2001;167(4):2068–2073.

[13] Ben-Shmuel A, Biber G, Barda-Saad M. Unleashing Natural Killer Cells in the Tumor Microenvironment-The Next Generation of Immunotherapy? Frontiers in Immunology. 2020;11:275.

[14] Ljunggren HG, Kärre K. In search of the 'missing self': MHC molecules and NK cell recognition. Immunology today. 1990;11:237–244.

[15] Lodoen MB, Lanier LL. Natural killer cells as an initial defense against pathogens. Current opinion in immunology. 2006;18(4):391–398.

[16] Freeman BE, Rauè HP, Hill AB, Slifka MK. Cytokine-mediated activation of NK cells during viral infection. Journal of Virology. 2015;89(15):7922–7931.

[17] Janeway CA, Travers P, Walport M, Shlomchik MJ. Immunobiology: the Immune system in Health and Disease. sixth ed. Garland Science Publishing, New York; 2005.

[18] Al-Tameemi M, Chaplain M, d'Onofrio A. Evasion of tumours from the control of the immune system: consequences of brief encounters. Biology Direct. 2012;7(1):31–31.

[19] Eladdadi A, Kim P, Mallet D, editors. Mathematical Modeling of Tumor-Immune System Dynamics. vol. 107. Springer, Proceedings in Mathematics & Statistics; 2014.

[20] Prestwich RJ, Errington F, Diaz RM, Pandha HS, Harrington KJ, Melcher AA, et al. The case of oncolytic viruses versus the immune system: waiting on the judgment of Solomon. Human gene therapy. 2009;20(10):1119–1132.

[21] Blanc KL, Mougiakakos D. Multipotent mesenchymal stromal cells and the innate immune system. Nature Reviews Immunology. 2012;12(5):383–396.

[22] Breitbach CJ, Bell JC, Hwang TH, Kirn DH, Burke J. The emerging therapeutic potential of the oncolytic immunotherapeutic Pexa-Vec (JX-594). Oncolytic Virotherapy. 2015;4:25–31.

[23] Swift SL, Stojdl DF. Big Data Offers Novel Insights for Oncolytic Virus Immunotherapy. Viruses. 2016;8(2):45.

[24] Keller BA, Bell JC. Oncolytic viruses–immunotherapeutics on the rise. Journal of Molecular Medicine. 2016;94(9):979–991.

[25] Reale A, Vitiello A, Conciatori V, Parolin C, Calistri A, Palù G. Perspectives on immunotherapy via oncolytic viruses. Infectious agents and cancer. 2019;14(1):5.

[26] Li Y, Sun R. Tumor immunotherapy: new aspects of natural killer cells. Chinese Journal of Cancer Research. 2018;30(2):173.

[27] Guo ZS, Liu Z, Bartlett DL. Oncolytic immunotherapy: dying the right way is a key to eliciting potent antitumor immunity. Frontiers in oncology. 2014;4:74.

[28] Choi IK, Strauss R, Richter M, Yun CO, Lieber A. Strategies to increase drug penetration in solid tumors. Frontiers in Oncology. 2013;3(193).

[29] Choi JW, Lee JS, Kim SW, Yun CO. Evolution of oncolytic adenovirus for cancer treatment. Advanced drug delivery reviews. 2012;64(8):720–729.

[30] Choi KJ, Zhang SN, Choi IK, Kim JS, Yun CO. Strengthening of antitumor immune memory and prevention of thymic atrophy mediated by adenovirus expressing IL-12 and GM-CSF. Gene Therapy. 2012;19:711–723.

[31] Jiang H, Gomez-Manzano C, Rivera-Molina Y, Lang FF, Conrad CA, Fueyo J. Oncolytic adenovirus research evolution: from cell-cycle checkpoints to immune checkpoints. Current opinion in virology. 2015;13:33–39.

[32] LaRocca CJ, Warner SG. Oncolytic viruses and checkpoint inhibitors: Combination therapy in clinical trials. Clinical and translational medicine. 2018;7(1):35.

[33] Shi L, Chen S, Yang L, Li Y. The role of PD-1 and PD-L1 in T-cell immune suppression in patients with hematological malignancies. Journal of hematology & oncology. 2013;6(1):74.

[34] Storey KM, Lawler SE, Jackson TL. Modeling Oncolytic Viral Therapy, Immune Checkpoint Inhibition, and the Complex Dynamics of Innate and Adaptive Immunity in Glioblastoma Treatment. Frontiers in Physiology. 2020;11:151.

[35] Hirano F, Kaneko K, Tamura H, Dong H, Wang S, Ichikawa M, et al. Blockade of B7-H1 and PD-1 by monoclonal antibodies potentiates cancer therapeutic immunity. Cancer research. 2005;65(3):1089–1096.

[36] He J, Hu Y, Hu M, Li B. Development of PD-1/PD-L1 pathway in tumor immune microenvironment and treatment for non-small cell lung cancer. Scientific reports. 2015;5(1):1–9.

[37] Rojas JJ, Sampath P, Hou W, Thorne SH. Defining Effective Combinations of Immune Checkpoint Blockade and Oncolytic Virotherapy. Clinical Cancer Research. 2015;21(24):5543–5551.

[38] Zhang Q, Liu F. Advances and potential pitfalls of oncolytic viruses expressing immunomodulatory transgene therapy for malignant gliomas. Cell Death & Disease. 2020;11(6):1–11.

[39] Ilett EJ, Prestwich RJ, Kottke T, Errington F, Thompson JM, Harrington KJ, et al. Dendritic cells and T cells deliver oncolytic reovirus for tumour killing despite pre-existing anti-viral immunity. Gene therapy. 2009;16(5):689–699.

[40] White CL, Twigger KR, Vidal L, Bono JSD, Coffey M, Heinemann L, et al. Characterization of the adaptive and innate immune response to intravenous oncolytic reovirus (Dearing type 3) during a phase I clinical trial. Gene Therapy. 2008;15(12):911–920.

[41] Angelova AL, Geletneky K, Nüesch JPF, Rommelaere J. Tumor selectivity of oncolytic parvoviruses: from in vitro and animal models to cancer patients. Frontiers in bioengineering and biotechnology. 2015;3:55.

[42] Ogbomo H, Zemp FJ, Lun X, Zhang J, Stack D, Rahman MM, et al. Myxoma Virus Infection Promotes NK Lysis of Malignant Gliomas In Vitro and In Vivo. PLoS ONE. 2013;8(6):e66825.

[43] Marchini A, Scott EM, Rommelaere J. Overcoming Barriers in Oncolytic Virotherapy with HDAC Inhibitors and Immune Checkpoint Blockade. Viruses. 2016;8(1):9.

[44] Yaacov B, Lazar I, Tayeb S, Frank S, Izhar U, Lotem M, et al. Extracellular matrix constituents interfere with Newcastle disease virus spread in solid tissue and diminish its potential oncolytic activity. Journal of general virology. 2012;93(8):1664–1672.

[45] Ayala-Breton C, Russell LOJ, Russell SJ, Peng KW. Faster replication and higher expression levels of viral glycoproteins give the vesicular stomatitis virus/measles virus hybrid VSV-FH a growth advantage over measles virus. Journal of virology. 2014;88(15):8332–8339.

[46] Msaouel P, Dispenzieri A, Galanis E. Clinical testing of engineered oncolytic measles virus strains in the treatment of cancer: an overview. Current opinion in molecular therapeutics. 2009;11(1):43.

[47] Lun X, Chan J, Zhou H, Sun B, Kelly JJ, Stechishin OO, et al. Efficacy and safety/toxicity study of recombinant vaccinia virus JX-594 in two immunocompetent animal models of glioma. Molecular Therapy. 2010;18(11):1927–1936.

[48] Kwon OJ, Kang E, Kim S, Yun CO. Viral genome DNA/lipoplexes elicit in situ oncolytic viral replication and potent antitumor efficacy via systemic delivery. Journal of Controlled Release. 2011;155(2):317–325.

[49] El-Shemi AG, Ashshi AM, Na Y, Li Y, Basalamah M, Al-Allaf FA, et al. Combined therapy with oncolytic adenoviruses encoding TRAIL and IL-12 genes markedly suppressed human hepatocellular carcinoma both in vitro and in an orthotopic transplanted mouse model. Journal of Experimental & Clinical Cancer Research. 2016;35(1):74.

[50] Kim E, Kim JH, Shin HY, Lee H, Yang JM, Kim J, et al. Ad-mTERT-Δ19, a conditional replication-competent adenovirus driven by the human telomerase promoter, selectively replicates in and elicits cytopathic effect in a cancer cell-specific manner. Human Gene Therapy. 2003;14(15):1415–1428.

[51] Varghese S, Rabkin SD. Oncolytic herpes simplex virus vectors for cancer virotherapy. Cancer gene therapy. 2002;9(12):967–978.

[52] Takasu A, Masui A, Hamada M, Imai T, Iwai S, Yura Y. Immunogenic cell death by oncolytic herpes simplex virus type 1 in squamous cell carcinoma cells. Cancer gene therapy. 2016;23(4):107–113.

[53] Chen X, Han J, Chu J, Zhang L, Zhang J, Chen C, et al. A combinational therapy of EGFR-CAR NK cells and oncolytic herpes simplex virus 1 for breast cancer brain metastases. Oncotarget. 2016;19(7):27764.

[54] Atherton MJ, Lichty BD. Evolution of oncolytic viruses: novel strategies for cancer treatment. Immunotherapy. 2013;5(11):1191–1206.

[55] Chiocca EA, Rabkin SD. Oncolytic viruses and their application to cancer immunotherapy. Cancer immunology research. 2014;2(4):295–300.

[56] Guo ZS, Thorne SH, Bartlett DL. Oncolytic virotherapy: molecular targets in tumor-selective replication and carrier cell-mediated delivery of oncolytic viruses. Biochimica et Biophysica Acta (BBA)-Reviews on Cancer. 2008;1785(2):217–231.

[57] Eissa IR, Bustos-Villalobos I, Ichinose T, Matsumura S, Naoe Y, Miyajima N, et al. The current status and future prospects of oncolytic viruses in clinical trials against melanoma, glioma, pancreatic, and breast cancers. Cancers. 2018;10(10):356.

[58] Gesundheit B, Ben-David E, Posen Y, Ellis R, Wollmann G, Schneider EM, et al. Effective Treatment of Glioblastoma Multiforme With Oncolytic Virotherapy: A Case-Series. Frontiers in oncology. 2020;10:702.

[59] Shi T, Song X, Wang Y, Liu F, Wei J. Combining Oncolytic Viruses With Cancer Immunotherapy: Establishing a New Generation of Cancer Treatment. Frontiers in Immunology. 2020;11:683.

[60] Roy DG, Bell JC, Bourgeois-Daigneault MC. Magnetic targeting of oncolytic VSV-based therapies improves infection of tumor cells in the presence of virus-specific neutralizing antibodies in vitro. Biochemical and Biophysical Research Communications. 2020;526(3):641–646.

[61] Muthana M, Rodrigues S, Chen YY, Welford A, Hughes R, Tazzyman S, et al. Macrophage delivery of an oncolytic virus abolishes tumor regrowth and metastasis after chemotherapy or irradiation. Cancer Research. 2013;73(2):490–945.

[62] Yoon AR, Hong J, Li Y, Shin HC, Lee H, Kim HS, et al. Mesenchymal stem cell-mediated delivery of an oncolytic adenovirus enhances antitumor efficacy in hepatocellular carcinoma. Cancer research. 2019;79(17):4503–4514.

[63] Mahasa KJ, de Pillis L, Ouifki R, Eladdadi A, Maini P, Yoon AR, et al. Mesenchymal stem cells used as carrier cells of oncolytic adenovirus results in enhanced oncolytic virotherapy. Scientific Reports. 2020;10(1):1–13.

[64] Kim Y, Lee HG, Dmitrieva N, Kim J, Kaur B, Friedman A. Choindroitinase ABC I-mediated enhancement of oncolytic virus spread and anti tumor efficacy: a mathematical model. PLoS ONE. 2014;9(7):e102499.

[65] Vähä-Koskela M, Hinkkanen A. Tumor restrictions to oncolytic virus. Biomedicines. 2014;2(2):163–194.

[66] Workenhe ST, Mossman KL. Oncolytic virotherapy and immunogenic cancer cell death: sharpening the sword for improved cancer treatment strategies. Molecular Therapy. 2014;22(2):251–256.

[67] Bommareddy PK, Zloza A, Rabkin SD, Kaufman HL. Oncolytic virus immunotherapy induces immunogenic cell death and overcomes STING deficiency in melanoma. OncoImmunology. 2019;8(1):e1591875.

[68] Donnelly OG, Errington-Mais F, Steele L, Hadac E, Jennings V, Scott K, et al. Measles virus causes immunogenic cell death in human melanoma. Gene therapy. 2013;20(1):7–15.

[69] van Vloten JP, Workenhe ST, Wootton SK, Mossman KL, Bridle BW. Critical interactions between immunogenic cancer cell death, oncolytic viruses, and the immune system define the rational design of combination immunotherapies. The Journal of Immunology. 2018;200(2):450–458.

[70] de Matos AL, Franco LS, McFadden G. Oncolytic viruses and the immune system: The dynamic duo. Molecular Therapy-Methods & Clinical Development. 2020;17:349–358.

[71] Kim Y, Yoo JY, Lee TJ, Liu J, Yu J, Caligiuri MA, et al. Complex role of NK cells in regulation of oncolytic virus–bortezomib therapy. PNAS. 2018;115(19):4927–4932.

[72] Leung EYL, Ennis DP, Kennedy PR, Hansell C, Dowson S, Farquharson M, et al. NK cells augment oncolytic adenovirus cytotoxicity in ovarian cancer. Molecular Therapy-Oncolytics. 2020;16:289–301.

[73] Klose C, Berchtold S, Schmidt M, Beil J, Smirnow I, Venturelli S, et al. Biological treatment of pediatric sarcomas by combined virotherapy and NK cell therapy. BMC Cancer. 2019;9:1172.

[74] Marchini A, Daeffler L, Pozdeev VI, Angelova A, Rommelaere J. Immune conversion of tumor microenvironment by oncolytic viruses: the protoparvovirus H-1PV case study. Frontiers in immunology. 2019;10:1848.

[75] Mahasa KJ, Eladdadi A, de Pillis L, Ouifki R. Oncolytic potency and reduced virus tumor-specificity in oncolytic virotherapy. A mathematical modelling approach. PLoS ONE. 2017;12(9):e0184347.

[76] Yoo JY, Jaime-Ramirez AC, Bolyard C, Dai H, Nallanagulagari T, Wojton J, et al. Bortezomib treatment sensitizes oncolytic HSV-1–treated tumors to NK cell immunotherapy. Clinical Cancer Research. 2016;22(21):5265–5276.

[77] Street SEA, Hayakawa Y, Zhan Y, Lew AM, MacGregor D, Jamieson AM, et al. Innate immune surveillance of spontaneous B cell lymphomas by natural killer cells and $\gamma\delta$ T cells. The Journal of experimental medicine. 2004;199(6):879–884.

[78] Ochsenbein AF, Klenerman P, Karrer U, Ludewig B, Pericin M, Hengartner H, et al. Immune surveillance against a solid tumor fails because of immunological ignorance. Proceedings of the National Academy of Sciences. 1999;96(5):2233–2238.

[79] Swann JB, Smyth MJ. Immune surveillance of tumors. Journal of Clinical Investigation. 2007;117(5):1137–1146.

[80] Harrington K, Freeman DJ, Kelly B, Harper J, Soria JC. Optimizing oncolytic virotherapy in cancer treatment. Nature Reviews Drug Discovery. 2019;18(9):689–706.

[81] Lemay CG, Rintoul JL, Kus A, Paterson JM, Garcia V, Falls TJ, et al. Harnessing oncolytic virus-mediated antitumor immunity in an infected cell vaccine. Molecular Therapy. 2012;20(9):1791–1799.

[82] Russell SJ, Peng KW, Bell JC. Oncolytic virotherapy. Nature biotechnology. 2012;30(7):658–670.

[83] Cassady KA, Haworth KB, Jackson J, Markert JM, Cripe TP. To Infection and Beyond: The Multi-Pronged Anti-Cancer Mechanisms of Oncolytic Viruses. Viruses. 2016;8(2):43.

[84] Lichty BD, Breitbach CJ, Stojdl DF, Bell JC. Going viral with cancer immunotherapy. Nature Reviews Cancer. 2014;14:559–567.

[85] Kaufman HL, Kohlhapp FJ, Zloza A. Oncolytic viruses: a new class of immunotherapy drugs. Nature Reviews Drug Discovery. 2015;14(9):642–662.

[86] Bartlett DL, Liu Z, Sathaiah M, Ravindranathan R, Guo Z, He Y, et al. Oncolytic viruses as therapeutic cancer vaccines. Molecular cancer. 2013;12(1):1.

[87] Wollmann G, Ozduman K, van den Pol AN. Oncolytic Virus Therapy of Glioblastoma Multiforme–Concepts and Candidates. Cancer journal (Sudbury, Mass). 2012;18(1):69.

[88] Shilpa PS, Kaul R, Bhat S, Sultana N, Pandeshwar P. Oncolytic viruses in head and neck cancer: a new ray of hope in the management protocol. Annals of medical and health sciences research. 2014;4(3):178–184.

[89] Seymour LW, Fisher KD. Oncolytic viruses: finally delivering. British journal of cancer. 2016;114:357–361.

[90] Castleton A, Dey A, Beaton B, Patel B, Aucher A, Davis DM, et al. Human mesenchymal stromal cells deliver systemic oncolytic measles virus to treat acute lymphoblastic leukemia in the presence of humoral immunity. Blood. 2014;123(9):1327–1335.

[91] Crittenden MR, Thanarajasingam U, Vile RG, Gough MJ. Intratumoral immunotherapy: using the tumour against itself. Immunology. 2005;114(1):11–22.

[92] Kim J, Hall RR, Lesniak MS, Ahmed AU. Stem Cell-Based Cell Carrier for Targeted Oncolytic Virotherapy: Translational Opportunity and Open Questions. Viruses. 2015;7(12):6200–6217.

[93] Vivier E, Tomasello E, Baratin M, Walzer T, Ugolini S. Functions of natural killer cells. Nature Immunology. 2008;9(5):503–510.

[94] Cerwenka A, Lanier LL. Natural killer cell memory in infection, inflammation and cancer. Nature reviews Immunology. 2016;16(2):112–123.

[95] Alvarez-Breckenridge CA, Yu J, Price R, Wojton J, Pradarelli J, Mao H, et al. NK cells impede glioblastoma virotherapy through NKp30 and NKp46 natural cytotoxicity receptors. Nature medicine. 2012;18(12):1827–1834.

[96] Vivier E, Ugolini S, Blaise D, Chabannon C, Brossay L. Targeting natural killer cells and natural killer T cells in cancer. Nature Reviews Immunology. 2012;12(4):239–252.

[97] Watzl C, Long EO. Exposing tumor cells to killer cell attack. Nature medicine. 2000;6(8):867–868.

[98] Gauthier L, Morel A, Anceriz N, Rossi B, Blanchard-Alvarez A, Grondin G, et al. Multifunctional Natural Killer Cell Engagers Targeting NKp46 Trigger Protective Tumor Immunity. Cell. 2019;177(7):1701–1713.

[99] Moretta A, Bottino C, Vitale M, Pende D, Cantoni C, Mingari MC, et al. Activating receptors and coreceptors involved in human natural killer cell-mediated cytolysis. Annual Review of Immunology. 2001;19(1):197–223.

[100] Long EO, Kim HS, Liu D, Peterson ME, Rajagopalan S. Controlling natural killer cell responses: integration of signals for activation and inhibition. Annual review of immunology. 2013;31:227–258.

[101] Pegram HJ, Andrews DM, Smyth MJ, Darcy PK, Kershaw MH. Activating and inhibitory receptors of natural killer cells. Immunology and cell biology. 2011;89(2):216–224.

[102] Lehmann C, Zeis M, Schmitz N, Uharek L. Impaired binding of perforin on the surface of tumor cells is a cause of target cell resistance against cytotoxic effector cells. Blood. 2000;96(2):594–600.

[103] Smyth MJ, Kelly JM, Baxter AG, Körner H, Sedgwick JD. An essential role for tumor necrosis factor in natural killer cell–mediated tumor rejection in the peritoneum. The Journal of experimental medicine. 1998;188(9):1611–1619.

[104] Sivori S, Pende D, Quatrini L, Pietra G, Chiesa MD, Vacca P, et al. NK cells and ILCs in tumor immunotherapy. Molecular Aspects of Medicine. 2020.

[105] Alvarez-Breckenridge CA, Yu J, Kaur B, Caligiuri MA, Chiocca EA. Deciphering the multifaceted relationship between oncolytic viruses and natural killer cells. Advances in virology. 2012.

[106] de Pillis LG, Radunskaya AE, Wiseman CL. A validated mathematical model of cell-mediated immune response to tumour growth. Cancer Research. 2005;65(17):7950–7958.

[107] Banerjee S, Sarkar RP. Delay-induced model for tumour-immune interaction and control of malignant tumour growth. Biological System. 2008;91(1):268–288.

[108] Kolev M. Mathematical modelling of the competition between tumors and immune system considering the role of the antibodies. Mathematical and Computer Modelling. 2003;37(11):1143–1152.

[109] Mallet DG, de Pillis LG. A cellular automata model of tumour-immune system interactions. Journal of Theoretical Biology. 2006;239(3):334–350.

[110] de Pillis LG, Eladdadi A, Radunskaya AE. Modeling cancer-immune responses to therapy. Journal of pharmacokinetics and pharmacodynamics. 2014;41(5):461–478.

[111] Walker R, Enderling H. From concept to clinic: mathematically informed immunotherapy. Current Problems in Cancer. 2016;40(1):68–83.

[112] Eftimie R, Bramson JL. Interactions between the immune system and cancer: a brief review of non-spatial mathematical models. Bulletin Mathematical Biology. 2011;73(1):2–32.

[113] Adam, John, Nicola B. A survey of models for tumor-immune system dynamics. Springer Science & Business Media; 2012.

[114] Altrock PM, Liu LL, Michor F. The Mathematics Of Cancer: Integrating Quantitative Models. Nature Review Cancer. 2015;15(12):730–745.

[115] Wodarz D, Komarova N. Towards predictive computational models of oncolytic virus therapy: basis for experimental validation and model selection. PLoS ONE. 2009;4(1):e4271.

[116] Wodarz D, Komarova NL. Dynamics of cancer: mathematical foundations of oncology. Singapore: World Scientific Publishing; 2014.

[117] Paul TJ. The replicability of oncolytic virus: defining conditions in tumor virotherapy. Mathematical biosciences and engineering. 2011;8(3):841–860.

[118] Jenner AL, Kim PS, Frascoli F. Oncolytic virotherapy for tumours following a Gompertz growth law. Journal of theoretical biology. 2019;480:129–140.

[119] Heidbuechel JPW, Abate-Daga D, Engeland CE, Enderling H. Mathematical Modeling of Oncolytic Virotherapy. In: Oncolytic Viruses, Methods in Molecular Biology. Springer, Humana, New York; 2020. p. 301–320.

[120] Wodarz D. Viruses as antitumor weapons: defining conditions for tumor remission. Cancer Research. 2001;61(8):3501–3507.

[121] Wodarz D, Komarova N. Computational biology of cancer: lecture notes and mathematical modeling. World Scientific Publishing Company, Singapour; 2005.

[122] Phan TA, Tian JP. The role of the innate immune system in oncolytic virotherapy. Computational and mathematical methods in medicine. 2017.

[123] Jenner AL, Yun CO, Yoon A, Coster ACF, Kim PS. Modelling combined virotherapy and immunotherapy: strengthening the antitumour immune response mediated by IL-12 and GM-CSF expression. Letters in Biomathematics. 2018;5(sup1):S99–S116.

[124] Choi JW, Lee YS, Yun CO, Kim SW. Polymeric oncolytic adenovirus for cancer gene therapy. Journal of Controlled Release. 2015;219:181–191.

[125] Filley AC, Dey M. Immune system, friend or foe of oncolytic virotherapy? Frontiers in oncology. 2017;7:106.

[126] Zhang J, Tai LH, Ilkow CS, Alkayyal AA, Ananth AA, de Souza CT, et al. Maraba MG1 virus enhances natural killer cell function via conventional dendritic cells to reduce postoperative metastatic disease. Molecular Therapy. 2014;22(1):1320–1332.

[127] Davola ME, Mossman KL. Oncolytic viruses: how "lytic" must they be for therapeutic efficacy? ONCOIMMUNOLOGY. 2019;8(6):e1596006.

[128] Bhat R, Rommelaere J. Emerging role of Natural killer cells in oncolytic virotherapy. ImmunoTargets and Therapy. 2015;4:65–77.

[129] Li X, Wang P, Li H, Du X, Liu M, Huang Q, et al. The efficacy of oncolytic adenovirus is mediated by T cell responses against virus and tumor in Syrian hamster model. Clinical Cancer Research. 2017;23(1):239–249.

[130] Watzl C, Sternberg-Simon M, Urlaub D, Mehr R. Understanding natural killer cell regulation by mathematical approaches. Frontiers in Immunology. 2012;3:359.

[131] Eftimie R, Eftimie G. Tumour-associated macrophages and oncolytic virotherapies: a mathematical investigation into a complex dynamics. Letters in Biomathematics. 2018;5(sup1):S6–S35.

[132] Wodarz D, Sierro S, Klenerman P. Dynamics of killer T cell inflation in viral infections. Journal of The Royal Society Interface. 2007;4(14):533–543.

[133] Prestwich RJ, Harrington KJ, Pandha HS, Vile RG, Melcher AA, Errington F. Oncolytic viruses: a novel form of immunotherapy. Expert review of anticancer therapy. 2008;8(10):1581–1588.

[134] Achard C, Boisgerault N, Delaunay T, Tangy F, Grégoire M, Fonteneau JF. Induction of immunogenic tumor cell death by attenuated oncolytic measles virus. Journal of Clinical and Cellular Immunology. 2015;6(1).

[135] Valle ASD, Anel A, Naval J, Marzo I. Immunogenic cell death and immunotherapy of multiple myeloma. Frontiers in Cell and Developmental Biology. 2019;7:50.

[136] Russell L, Peng KW, Russell SJ, Diaz RM. Oncolytic viruses: priming time for cancer immunotherapy. BioDrugs. 2019;33:485–501.

[137] Gujar S, Pol JG, Kim Y, Lee PW, Kroemer G. Antitumor benefits of antiviral immunity: an underappreciated aspect of oncolytic virotherapies. Trends in immunology. 2018;39:209–221.

[138] Gross C, Hansch D, Gastpar R, Multhoff G. Interaction of heat shock protein 70 peptide with NK cells involves the NK receptor CD94. Biological chemistry. 2003;384(2):267–279.

[139] Fionda C, Stabile H, Molfetta R, Soriani A, Bernardini G, Zingoni A, et al. Translating the anti-myeloma activity of Natural Killer cells into clinical application. Cancer Treatment Reviews. 2018;70:255–264.

[140] Paust S, von Andrian UH. Natural killer cell memory. Nature immunology. 2011;12(6):500–508.

[141] Makaryan SZ, Finley SD. Enhancing network activation in Natural Killer cells: Predictions from in silico modeling. Integrative Biology. 2020;12(5):109–121.

[142] Marcus A, Gowen BG, Thompson TW, Iannello A, Ardolino M, Deng W, et al. Recognition of tumors by the innate immune system and natural killer cells. Advances in immunology. 2014;122:91–128.

[143] Barish S, Ochs MF, Sontag ED, Gevertz JL. Evaluating optimal therapy robustness by virtual expansion of a sample population, with a case study in cancer immunotherapy. Proceedings of the National Academy of Sciences. 2017;114(31):E6277–E6286.

[144] Kim PS, Crivelli JJ, Choi IK, Yun CO, Wares JR. Quantitative impact of immunomodulation versus oncolysis with cytokine-expressing virus therapeutics. Mathematical biosciences and engineering. 2015;12(4):841–858.

[145] Bailey K, Kirk A, Naik S, Nace R, Steele MB, Suksanpaisan L, et al. Mathematical model for radial expansion and conflation of intratumoral infectious centers predicts curative oncolytic virotherapy parameters. PLoS ONE. 2013;8:e73759.

[146] Macnamara C, Eftimie R. Memory versus effector immune responses in oncolytic virotherapies. Journal of theoretical biology. 2015;377:1–9.

[147] Almuallem N, Trucu D, Eftimie R. Oncolytic viral therapies and the delicate balance between virus-macrophage-tumour interactions: A mathematical approach. Mathematical Biosciences and Engineering. 2021;18(1):764–799.

[148] Friedman A, Lai X. Combination therapy for cancer with oncolytic virus and checkpoint inhibitor: A mathematical model. PLoS One. 2018;13(2):e0192449.

[149] Paiva LR, Binny C, Ferreira SC, Martins ML. A multiscale mathematical model for oncolytic virotherapy. Cancer research. 2009;69(3):1205–1211.

[150] Wodarz D, Hofacre A, Lau JW, Sun Z, Fan H, Komarova NL. Complex spatial dynamics of oncolytic viruses in vitro: mathematical and experimental approaches. PLoS Computional Biology. 2012;8(6):e1002547.

[151] Rodriguez-Brenes IA, Hofacre A, Fan H, Wodarz D. Complex dynamics of virus spread from low infection multiplicities: Implications for the spread of oncolytic viruses. PLOS Computational Biology. 2017;13(5):e1005241.

[152] Hu W, Wang G, Huang D, Sui M, Xu Y. Cancer Immunotherapy Based on Natural Killer Cells: Current Progress and New Opportunities. Frontiers in immunology. 2019;10:1205.

[153] Liu S, Galat V, Galat Y, Kyung Y, Lee A, Wainwright D, et al. NK cell-based cancer immunotherapy: from basic biology to clinical development. Journal of Hematology & Oncology. 2021;14(1):1–17.

[154] de Pillis L, Radunskaya A. A mathematical model of immune response to tumor invasion. In: Computational Fluid and Solid Mechanics. ed. K.J. Bathe (Elsevier Science Ltd); 2003. p. 1661–1668.

[155] Breitbach CJ, Paterson JM, Lemay CG, Falls TJ, McGuire A, Parato KA, et al. Targeted inflammation during oncolytic virus therapy severely compromises tumor blood flow. Molecular Therapy. 2007;15(9):1686–1693.

[156] Iannello A, Raulet DH. Immunosurveillance of senescent cancer cells by natural killer cells. Oncoimmunology. 2014;3(2):e27616.

[157] Blue CE, Spiller OB, Blackbourn DJ. The relevance of complement to virus biology. Virology. 2004;319(2):176–184.

[158] Everts B, van der Poel HG. Replication-selective oncolytic viruses in the treatment of cancer. Cancer gene therapy. 2005;12(2):141–161.

[159] de Pillis LG, Gu W, Radunskaya AE. Mixed immunotherapy and chemotherapy of tumours: modeling, applications and biological interpretations. Journal of Theoretical Biology. 2006;238(4):841–862.

[160] Langers I, Renoux VM, Thiry M, Delvenne P, Jacobs N. Natural killer cells: role in local tumor growth and metastasis. Biologics: targets & therapy. 2012;6:73.

[161] Martin NT, Bell JC. Oncolytic Virus Combination Therapy: Killing One Bird with Two Stones. Molecular Therapy. 2018;26(6):1414–1422.

[162] Somma SD, Iannuzzi CA, Passaro C, Forte IM, Iannone R, Gigantino V, et al. The oncolytic virus $dl922-947$ triggers immunogenic cell death in mesothelioma and reduces xenograft growth. Frontiers in oncology. 2019;9:564.

[163] Tisoncik JR, Korth MJ, Simmons CP, Farrar J, Martin TR, Katze MG. Into the eye of the cytokine storm. Microbiol Mol Biol Rev. 2012;6(1):16–32.

[164] de Pillis LG, Caldwell T, Sarapata E, Williams H. Mathematical Modeling of the Regulatory T Cell Effects on Renal Cell Carcinoma Treatment. Discrete and Continuous Dynamical Systems Series. 2013;18(4):915–943.

[165] Jacobsen K, Russell L, Kaur B, Friedman A. Effects of CCN1 and Macrophage Content on Glioma Virotherapy: A Mathematical Model. Bulletin of mathematical biology. 2015;77(6):1–29.

[166] Friedman A, Tian JP, Fulci G, Chiocca EA, Wang J. Glioma virotherapy: effects of innate immune suppression and increased viral replication capacity. Cancer research. 2006;66(4):2314–2319.

[167] Guo Y, Niu B, Tian JP. Backward Hopf bifurcation in a mathematical model for oncolytic virotherapy with the infection delay and innate immune effects. Journal of Biological Dynamics. 2019;13(1):733–748.

[168] Cassidy T, Craig M. Optimal Individualized Combination Immunotherapy/Oncolytic Virotherapy Determined Through In Silico Clinical Trials Improves Late Stage Melanoma Patient Outcomes. bioRxiv. 2019:585711.

[169] Dritschel H, Waters SL, Roller A, Byrne HM. A mathematical model of cytotoxic and helper T cell interactions in a tumour microenvironment. Letters in Biomathematics. 2018;5(sup1):S36–S68.

[170] Dingli D, Cascino MD, Josić K, Russell SJ, Ž Bajzer. Mathematical modeling of cancer radiovirotherapy. Mathematical Biosciences. 2006;199(1):55–78.

[171] Diekmann O, van Giles S, Lunel S. Delay equations. Springer-Verlag: New York; 1995.

[172] Schatzman M. Numerical analysis: a mathematical introduction. Oxford University Press; 2002.

[173] Zi Z. Sensitivity analysis approaches applied to systems biology models. IET systems biology. 2011;5(6):336–346.

[174] Harris AL. Hypoxia–a key regulatory factor in tumour growth. Nature Reviews Cancer. 2002;2(1):38–47.

[175] Aghi M, Martuza RL. Oncolytic viral therapies–the clinical experience. Oncogene. 2005;24(52):7802–7816.

[176] Carr J. "Applications of Centre Manifold Theory," Applied Mathematics Sciences. 35th ed. Springer-Verlag, New York-Berlin; 1981.

[177] Workenhe ST, Simmons G, Pol JG, Lichty BD, Halford WP, Mossman KL. Immunogenic HSV-mediated oncolysis shapes the antitumor immune response and contributes to therapeutic efficacy. Molecular Therapy. 2014;22(1):123–131.

[178] Elsedawy NB, Nace RA, Russell SJ, Schulze AJ. Oncolytic activity of targeted picornaviruses formulated as synthetic infectious RNA. Molecular Therapy-Oncolytics. 2020;17:484–495.

[179] Zhang KJ, Zhang J, Wu YM, Qian J, Liua XJ, Yan LC, et al. Complete eradication of hepatomas using an oncolytic adenovirus containing AFP promoter controlling E1A and an E1B deletion to drive IL-24 expression. Cancer gene therapy. 2012;19(9):619–629.

[180] Liu W, Dai E, Liu Z, Ma C, Guo ZS, Bartlett DL. In Situ therapeutic cancer vaccination with an oncolytic virus expressing Membrane-Tethered IL-2. Molecular Therapy-Oncolytics. 2020;17:350–360.

[181] den Driessche PV, Watmough J. Reproduction numbers and sub-threshold endemic equilibria for compartmental models of disease transmission. Mathematical biosciences. 2002;180(1):29–48.

[182] Marino S, Hogue IB, Ray CJ, Kirschner DE. A methodology for performing global uncertainty and sensitivity analysis in systems biology. Journal of Theoretical Biology. 2008;254(1):178–196.

[183] Tsygvintsev A, Marino S, Kirschner DE. A mathematical model of Gene Therapy for the Treatment of Cancer, in "Mathematical Models and Methods in Biomedicine". Springer-Verlag, Berlin; 2012.

[184] Kemler I, Ennis MK, Neuhauser CM, Dingli D. In Vivo Imaging of Oncolytic Measles Virus Propagation with Single-Cell Resolution. Molecular Therapy-Oncolytics. 2019;12:68–78.

[185] Ennis MK, Hu C, Naik SK, Hallak LK, Peng KW, nd D Dingli SJR. Mutations in the stalk region of the measles virus hemagglutinin inhibit syncytium formation but not virus entry. Journal of Virology. 2010;84(20):10913–10917.

[186] Eftimie R, Eftimie G. Investigating Macrophages Plasticity Following Tumour–Immune Interactions During Oncolytic Therapies. Acta biotheoretica. 2019;67(4):321–359.

[187] Friberg S, Mattson S. On the growth rates of human malignant tumors: implications for medical decision making. Journal of surgical oncology. 1997;65(4):284–297.

[188] Eftimie R, Hamam H. Modelling and investigation of the CD4+ T cells – Macrophages paradox in melanoma immunotherapies. Journal of Theoretical Biology. 2017;420:82–104.

[189] Zurakowski R, Wodarz D. Model-driven approaches for in vitro combination therapy using ONYX-O15 replicating oncolytic adenovirus. Journal of Theoretical Biology. 2007;245(1):1–8.

[190] Gao J, Zhang W, Ehrhardt A. Expanding the Spectrum of Adenoviral Vectors for Cancer Therapy. Cancers. 2020;12(5):1139.

[191] Jung MY, Offord CP, Ennis MK, Kemler I, Neuhauser C, Dingli D. In Vivo Estimation of Oncolytic Virus Populations within Tumors. Cancer Research. 2018;78(20):5992–6000.

[192] Jost S, Altfeld M. Control of human viral infections by natural killer cells. Annual review of immunology. 2013;31:163–194.

[193] Sobol PT, Boudreau JE, Stephenson K, Wan Y, Lichty BD, Mossman KL. Adaptive antiviral immunity is a determinant of the therapeutic success of oncolytic virotherapy. Molecular Therapy. 2011;19(2):335–344.

[194] Ferreira TB, Alves PM, Gonçalves DG, Carrondo M. Effect of MOI and medium composition on adenovirus infection kinetics. In: Animal cell technology meets genomics. ed. F. Godia and Fussenegger (Springer, Dordrecht); 2005. p. 329–332.

[195] Ž Bajzer, Carr T, Josić K, Russell SJ, Dingli D. Modeling of cancer virotherapy with recombinant measles viruses. Journal of theoretical Biology. 2008;252(1):109–122.

[196] Waggoner SN, Reighard SD, Gyurova IE, Cranert SA, Mahl SE, Karmele EP, et al. Roles of natural killer cells in antiviral immunity. Current Opinion in Virology. 2016;16:15–23.

[197] Vähä-Koskela MJV, Heikkilä JE, Hinkkanen AE. Oncolytic viruses in cancer therapy. Cancer Letters. 2007;254(2):178–216.

[198] Meerani S, Yao Y. Oncolytic viruses in cancer therapy. European Journal of Scientific Research. 2010;40(1):156–171.

[199] Kim HS, Kim-Schulze S, Kim DW, Kaufman HL. Host lymphodepletion enhances the therapeutic activity of an oncolytic vaccinia virus expressing $4-1$BB ligand. Cancer Research. 2009;69(21):8516–8525.

[200] El-Shemi AG, Ashshi AM, Oh E, Jung BK, Basalamah M, Alsaegh A, et al. Efficacy of combining ING4 and TRAIL genes in cancer-targeting gene virotherapy strategy: first evidence in preclinical hepatocellular carcinoma. Gene therapy. 2018;25(1):54.

[201] Lee YS, Kim JH, Choi KJ, Choi IK, Kim H, Cho S, et al. Enhanced antitumor effect of oncolytic adenovirus expressing interleukin-12 and $B7-1$ in an immunocompetent murine model. Clinical Cancer Research. 2006;12(19):5859–5868.

[202] Navarro AG, Björklund AT, Chekenya M. Therapeutic potential and challenge of natural killer cells in treatment of solid tumors. Frontiers in Immunology. 2015;6:202.

[203] Diaz RM, Galivo F, Kottke T, Wongthida P, Qiao J, Thompson J, et al. Oncolytic immunovirotherapy for melanoma using vesicular stomatitis virus. Cancer research. 2007;67(6):2840–2848.

[204] Gujar SA, Pan D, Marcato P, Garant KA, Lee PWK. Oncolytic virus-initiated protective immunity against prostate cancer. Molecular Therapy. 2011;19(4):797–804.

[205] Samson A, Bentham MJ, Scott K, Nuovo G, Bloy A, Appleton E, et al. Oncolytic reovirus as a combined antiviral and anti-tumour agent for the treatment of liver cancer. Gut. 2018;67(3):562–573.

[206] Alkayyal AA, Tai LH, Kennedy MA, de Souza CT, Zhang J, Lefebvre C, et al. NK-cell recruitment is necessary for eradication of peritoneal carcinomatosis with an IL12-expressing Maraba virus cellular vaccine. Cancer immunology research. 2017;5(3):211–221.

[207] Miyamoto S, Inoue H, Nakamura T, Yamada M, Sakamoto C, Urata Y, et al. Coxsackievirus B3 is an oncolytic virus with immunostimulatory properties that is active against lung adenocarcinoma. Cancer research. 2012;72(10):2609–2621.

[208] Naik JD, Twelves CJ, Selby PJ, Vile RG, Chester JD. Immune recruitment and therapeutic synergy: keys to optimizing oncolytic viral therapy? Clinical Cancer Research. 2011;17(13):4214–4224.

[209] Marotel M, Hasim MS, Hagerman A, Ardolino M. The two-faces of NK cells in oncolytic virotherapy. Cytokine & Growth Factor Reviews. 2020.

[210] Gatenby RA. A change of strategy in the war on cancer. Nature. 2009;459(7246):508.

[211] Martin NT, Wrede C, Niemann J, Brooks J, Schwarzer D, Kühnel F, et al. Combined Therapy with Cytokine-Induced Killer Cells and Oncolytic Adenovirus Expressing IL-12 Induce Enhanced Antitumor Activity in Liver Tumor Model. PloS one. 2012;7(9):e44802.

[212] Farnault L, Sanchez C, Baier C, Treut TL, Costello RT. Hematological malignancies escape from NK cell innate immune surveillance: mechanisms and therapeutic implications. Clinical and Developmental Immunology. 2012;2012:1–8.

[213] Nguyen A, Ho L, Wan Y. Chemotherapy and Oncolytic Virotherapy: Advanced Tactics in the War against Cancer. Frontiers in Oncology. 2014;4:145.

[214] Seidel UJE, Schlegel P, Lang P. Natural killer cell mediated antibody-dependent cellular cytotoxicity in tumor immunotherapy with therapeutic antibodies. Frontiers in immunology. 2013;4(76). Available from: http://www.frontiersin.org/alloimmunity_and_transplantation/10.3389/fimmu.2013.00076/abstract.